

การสร้างอิมัลชันของอนุภาคนาโนทอง/ไพโรล/HRP สำหรับฟีนอลไบโอเซนเซอร์โดย
วิธีอิมัลชันโพรพอลิเมอร์ไรเซชัน

นางสาวรัชณีพัฒน์ กำแพงเพชร

วิทยานิพนธ์นี้เป็นส่วนหนึ่งของการศึกษาตามหลักสูตรปริญญาวิทยาศาสตรมหาบัณฑิต
สาขาวิชาวิศวกรรมเคมี ภาควิชาวิศวกรรมเคมี
คณะวิศวกรรมศาสตร์ จุฬาลงกรณ์มหาวิทยาลัย
ปีการศึกษา 2554

บทคัดย่อและแฟ้มข้อมูลฉบับเต็มของวิทยานิพนธ์ที่ส่งมาตั้งแต่ปีการศึกษา 2554 ที่เก็บในคลังปัญญาจุฬาฯ (CUIR)

เป็นแฟ้มข้อมูลของนิสิตเจ้าของวิทยานิพนธ์ที่ส่งผ่านทางบัณฑิตวิทยาลัย

The abstract and full text of theses from the academic year 2011 in Chulalongkorn University Intellectual Repository (CUIR)
are the thesis authors' files submitted through the Graduate School.

FABRICATION OF GOLD NANOPARTICLES/PYRROLE/HRP ELECTRODE FOR PHENOL
BIOSENSOR BY ELECTROPOLYMERIZATION

Miss Ratchaneepat Kumpangpet

A Thesis Submitted in Partial Fulfillment of the Requirements
for the Degree of Master of Engineering Program in Chemical Engineering

Department of Chemical Engineering

Faculty of Engineering

Chulalongkorn University

Academic Year 2011

Copyright of Chulalongkorn University

Thesis Title	FABRICATION OF GOLD NANOPARTICLES /PYRROLE/HRP ELECTRODE FOR PHENOL BIOSENSOR BY ELECTROPOLYMERIZATION
By	Miss Ratchaneepat Kumpangpet
Field of Study	Chemical Engineering
Thesis Advisor	Associate Professor Seeroong Prichanont, Ph.D.
Thesis Co-advisor	Chanchana Thanachayanont, Ph.D.

Accepted by the Faculty of Engineering, Chulalongkorn University in Partial Fulfillment of the Requirements for the Master's Degree

.....Dean of the Faculty of Engineering
(Associate Professor Boonsom Lerthirunwong, Dr.Ing.)

THESIS COMMITTEE

.....Chairperson
(Associate Professor Muenduen Phisalaphong, Ph.D.)

.....Thesis Advisor
(Associate Professor Seeroong Prichanont, Ph.D.)

.....Thesis Co-advisor
(Chanchana Thanachayanont, Ph.D.)

.....Examiner
(Associate Professor Bunjerd Jongsomjit, Ph.D.)

.....External Examiner
(Associate Professor Sopa Klinchan)

รัชนี้พัฒน์ กำแพงเพชร : การสร้างอิเล็กโทรดของอนุภาคนาโนทอง/ไพโรล/HRP สำหรับ
 ฟีนอลไบโอเซนเซอร์โดยวิธีอิเล็กโทรพอลิเมอร์ไรเซชัน (FABRICATION OF GOLD
 NANOPARTICLES/PYRROLE/HRP ELECTRODE FOR PHENOL BIOSENSOR BY
 ELECTROPOLYMERIZATION) อ.ที่ปรึกษาวิทยานิพนธ์หลัก : รศ. ดร. สี่รุ่ง ปรีชานนท์,
 อ.ที่ปรึกษาวิทยานิพนธ์ร่วม : ดร. ชัญชนา ธนชยานนท์, 100 หน้า.

งานวิจัยนี้ศึกษาการดัดแปลงพื้นผิวสกรีนพริ้นท์คาร์บอนอิเล็กโทรดด้วยอนุภาคนาโนทองและไพโรล
 ร่วมกับการตรึงเอนไซม์ฮอร์สแรดิชเพอร์ออกซิเดสด้วยวิธีอิเล็กโทรพอลิเมอร์ไรเซชัน สำหรับตรวจวัดสารฟี
 นอล โดยศึกษาสภาวะที่ใช้ในการดัดแปลงอิเล็กโทรดด้วยวิธีอิเล็กโทรพอลิเมอร์ไรเซชัน จากการศึกษาพบว่า
 สภาวะที่เหมาะสมที่สุดในงานวิจัยนี้คือ การใช้สารละลายทองที่มีความเข้มข้น 5 มิลลิโมลต่อลิตรและจำนวน
 รอบการดัดแปลง 10 รอบตามลำดับ ขณะที่ผลจากการศึกษาเครื่อง UV-Vis spectroscopy บ่งชี้การไม่
 เสื่อมสภาพของเอนไซม์เมื่อผสมในสารละลายที่มีไพโรลและทองคอลลอยด์ที่มีรูปร่างทรงกลมขนาด 15 ± 5
 นาโนเมตรที่ได้จากการศึกษาภาพของ TEM เมื่ออิเล็กโทรดถูกดัดแปลง SEM และ AFM จึงถูกนำมาใช้เพื่อ
 ศึกษาลักษณะทางกายภาพของฟิล์ม พบว่าฟิล์มมีลักษณะกลุ่มอนุภาคขนาดเล็กและบางส่วนเกิดเป็นแท่ง
 ขณะที่ EDX พิสูจน์การมีอนุภาคนาโนทองบนพื้นผิวอิเล็กโทรดที่ถูกดัดแปลงรวมทั้งแสดงการกระจายตัวของ
 อนุภาคนาโนทองอย่างสม่ำเสมอด้วย นอกจากนี้พบว่าการถ่ายโอนอิเล็กตรอนโดยตรงระหว่างเอนไซม์และ
 อิเล็กโทรดเกิดปฏิกิริยาแบบผันกลับชนิด surface-controlled ซึ่งมีอัตราการถ่ายโอนน้อยกว่า 0.05 s^{-1}
 และมีจลพหุศาสตร์ของเอนไซม์ไม่สอดคล้องกับทฤษฎีของ Michaelis-Menten

ฟีนอลไบโอเซนเซอร์นี้มีช่วงความเป็นเส้นตรงของฟีนอล 1-8 มิลลิโมลต่อลิตร ความไวต่อการ
 ตอบสนอง $4.585\text{ nA}/\mu\text{M}$ ($R^2 = 0.955$) ความเข้มข้นต่ำสุดที่สามารถวัดได้ $3.19\text{ มิลลิโมลต่อลิตร}$ ($n=10$),
 ($S/N=3$) และเวลาการตอบสนอง 23.5 วินาที เมื่อจัดเก็บเป็นเวลา 7 วัน มีการตอบสนองของกระแสลดลง
 เหลือ 83.37% และการผลิตซ้ำมีค่าส่วนเบี่ยงเบนมาตรฐานสัมพัทธ์ (%RSD) เท่ากับ 3.78 ($n=10$)

ภาควิชา.....วิศวกรรมเคมี.....ลายมือชื่อนิสิต.....
 สาขาวิชา.....วิศวกรรมเคมี.....ลายมือชื่อ อ. ที่ปรึกษาวิทยานิพนธ์หลัก.....
 ปีการศึกษา.....2554.....ลายมือชื่อ อ. ที่ปรึกษาวิทยานิพนธ์ร่วม.....

5270793021 : MAJOR CHEMICAL ENGINEERING

KEYWORDS: GOLD NANOPARTICLES / POLYPYRROLE/ HORSERADISH PEROXIDASE / PHENOL BIOSENSOR

RATCHANEEPAT KUMPANGPET:FABRICATION OF GOLD NANOPARTICLES /PYRROLE/HRP ELECTRODE FOR PHENOL BIOSENSOR BY ELECTROPOLYMERIZATION. ADVISOR: ASSOC. PROF. SEEROONG PRICHANONT, Ph.D., CO-ADVISOR: CHANCHANA THANACHAYANONT, Ph.D., 100 pp.

This research is the investigation of the modified screen-printed carbon electrode with gold nanoparticles (AuNPs) and polypyrrole (PPy) together with the immobilized horseradish peroxidase by electropolymerization approach for phenol detection. The optimized electropolymerization conditions were 5 mM of gold precursor concentration and 10 cycling numbers of electropolymerization, respectively. The results of UV-Vis spectroscopy indicated the non-denaturation of HRP when mixed in solutions containing pyrrole and gold precursor which were of spherical shape and an average diameter approximately 15 ± 5 nm. After that, the synthesized modified electrodes were physically characterized by SEM and AFM. AuNPs/PPy film revealed small granular particles mixed with rod-like structure. Whereas EDX results confirmed the presence and uniform distribution of AuNPs on the effective electrode surface area. Furthermore, the direct electron transfer was a typical of surface-controlled quasi-reversible process with the electron transfer rate of 0.05s^{-1} . The study of enzyme kinetic parameters, we found that the mechanism did not follow Michaelis-Menten kinetics.

The resulting biosensor performed a linear range from 1-8 μM , with sensitivity of $4.585\text{nA}/\mu\text{M}$ ($R^2= 0.955$), detection limit of $3.19 \mu\text{M}$ ($n=10$), ($S/N=3$), and fast response time of 23.5 s. this biosensor showed a storage stability of residual current was 83.37% after seven days of storage in dried form at 4°C , and reproducibility was 3.78% ($n=10$).

Department : Chemical Engineering Student's Signature :

Field of Study : ... Chemical Engineering Advisor's Signature :

Academic Year : 2011 Co-advisor's Signature :

ACKNOWLEDGEMENTS

The author would also like to acknowledge her supervisors, Associate Professor Seeroong Prichanont, for her excellent supervision, encouraging guidance, advice, discussion and helpful suggestions throughout the course of this research. Also, she is very grateful to her co-advisor, Mrs.Chanchana Thanachayanont, for material surface suggestions any techniques. While the author would also like thank to Professor Associate Professor Bunjerd Jongsomjit, for their excellent supervision and support during this period. In addition, the author would also be grateful to Associate Professor Muenduen Phisalaphong, as the chairman, Associate Professor Bunjerd Jongsomjit, Associate Professor Sopa Klinchan as the internal and external members of the thesis committee, respectively. The author thanks to the financial supports from the Higher Education Research Promotion and National Research University Project of Thailand, Office of the Higher Education Commission (FWF660I) and the Department of Chemical Engineering and the Graduate School of Chulalongkorn University are gratefully acknowledged.

Moreover, the author is grateful to Catalyst Lab, Chulalongkorn University for helps in the utilization of SEM, EDX technique. Also, she appreciates to MTEC for image analyze program.

Special thanks to Miss Lerdluck Keawimol and Master Degree students, respectively, of Associate Professor Seeroong Prichanont for suggestion, advice and information and helps. Thanks to Mr. Sirawat Saening, technicians of STREC, for many useful suggestions and helps.

Many thanks to all my family members and special friends for their patience, love, support and encouragement during the period the author have been away from home.

Most of all, the author would like to express all her colleagues in Biochemical Engineering Research Laboratory, is gratefully acknowledged for their assistance and warm collaborations.

CONTENTS

	PAGE
ABSTRACT (THAI)	iv
ABSTRACT (ENGLISH)	v
ACKNOWLEDGEMENTS	vi
CONTENTS	vii
LISTS OF TABLES	viii
LISTS OF FIGURES	iv
 CHAPTER	
I INTRODUCTION	1
1.1 Motivation	1
1.2 Objective.....	3
1.3 Scopes of the research.....	3
1.4 Expected benefits	5
 II THEORY	 6
2.1 Biosensor	6
2.2 The enzyme for phenol detection	19
2.3 Immobilized enzyme method	22
2.4 Enzyme kinetic	25
 III LITERATURE REVIEWS	 29
3.1 Synthesis of polypyrrole (PPy) based HRP biosensor.....	29
3.2 Synthesis of gold nanoparticles based HRP biosensor	35
3.3 Synthesis of gold nanoparticles and polypyrrole composite.....	39
 IV MATERIALS AND METHOD	 45

CHAPTER	PAGE
4.1 Materials	45
4.2 Apparatus	45
4.3 Preparation of Gold nanoparticles colloidal solution	45
4.4 Electropolymerization of the AuNPs/Pyrrole/HRP modified electrode ..	46
4.5 Electropolymerization of the Pyrrole/HRP modified electrode	46
4.6 Electrochemical analysis	47
4.7 Material characterization	47
V RESULTS AND DISCUSSIONS	48
5.1 Optimized electropolymerization conditions of AuNPs/PPy modified screen-printed electrode	48
5.2 Physical and chemical characterization of bare and modified screen-printed electrode	53
5.3 Electrochemical determination of phenol	63
5.4 Direct electrochemistry of HRP at AuNPs/PPy/HRP/SPE	68
5.5 Electrocatalytic activity	73
5.6 Performance factors	75
VI CONCLUSIONS AND RECOMMENDATIONS	81
REFERENCES	83
APPENDICES	91
Appendix A Preparation of PBS solutions	92
Appendix B Raw data	93
VITA	100

LISTS OF TABLES

TABLE		PAGE
1.1	Water quality standards for measurement of phenolic compounds in different countries.....	2
2.2	Comparison of immobilized enzymes method (Chibata, 1978).....	24
5.1	Optimum conditions for fabrication of AuNPs/PPY/HRP/SPE.....	52
5.2	Elemental composition for AuNPs/PPy modified SPE with various Au precursor concentrations	60
5.3	Comparison of performance factors of this research with other researches.....	80

LISTS OF FIGURES

FIGURE	PAGE
2.1 Schematic of a simple biosensor.....	7
2.2 The three modes of mass transport (Joseph Wang, 2006).....	10
2.3 A schematic cyclic voltammogram of a reversible redox process (Joseph Wang, 2006).....	14
2.4 Mechanism of the mediated electron transfer at HRP modified electrode (Rosatto et al., 1999).....	21
2.5 Mechanism of the direct electron transfer at HRP modified electrode (Rosatto et al., 1999).....	21
2.6 Classification of immobilization methods for enzymes.....	22
2.7 Immobilized enzyme www.chemic.org/ippage/e/ipdata/2004/02/file/e200402-1001.pdf	24
2.8 Dependence of reaction rate on substrate concentration for an enzyme -catalyzed reaction at constant enzyme concentration (Eggins, 1999).....	27
2.9 The Lineweaver-Burk model http://en.wikipedia.org/wiki/Enzyme_kinetics	27
5.1 Cyclic voltammogram of a SPE in a solution containing 10 mM $K_4Fe(CN)_6$ / 1mM KCl between -0.6 and 1.2V at a scan rate of 100 mV/s.....	49
5.2 Effects of Au precursor concentration and cycling number of the electropolymerization on current responses of AuNPs/PPy modified SPEs in solutions containing 10 mM $K_4Fe(CN)_6$ / 1 mM KCl at 0.58V (Symbol of A, B, C, D, E represent the concentrations of Au^{3+} at 1, 3, 5, 7, 9 mM, respectively).....	52
5.3 UV-Visible absorption bands for a) AuNPS/Py/HRP, b) HRP, c) AuNPs/Py, d) Py in PBS (pH 7.4) in wavelength range between 300 and 800 nm.....	54
5.4 a) TEM image of AuNPs, and b) the colors of colloidal AuNPs	

FIGURE	PAGE
under various concentrations of H ₂ AuCl ₄	56
5.5 SEM images of screen-printed electrodes: a) bare SPE, b) PPy-modified, c) AuNPs/PPy- modified, d) AuNPs/PPy/HRP- modified SPEs, respectively. The accelerating voltage and magnification for all images were 15 kV and 20k×, respectively	57
The accelerating voltage and magnification for all images were 15 kV and 20k×, respectively.....	57
5.6 AFM images of AuNPs/PPy/SPEs at 5 mM of Au ³⁺ concentration a) 5 cycles, and b) 20 cycles, respectively.....	58
5.7 SEM and AFM images of AuNPs/PPY/HRP/GCEs under same conditions (Yusaran, 2009).....	59
5.8 EDX for AuNPs/PPy modified SPE using 5 mM Au precursor concentrations, 0.09M Py, 10 electropolymerization cycles, and an applied voltage between 0 to 1.0V.....	61
5.9 Effect of the Au precursor concentrations on percentage of AuNPs in AuNPs/PPy modified SPE and current responses. The amperometry was tested in solution containing 10 mM K ₄ Fe(CN) ₆ / 1 mM KCl at 0.58V	61
5.10 EDX mapping for AuNPs/PPy modified SPE with various Au precursor concentrations: a) 1 mM, b) 3 mM, c) 5 mM, d) 7 mM, and e) 9 mM, respectively. From this figure, the purple points showed AuNPs in PPy film.....	62
5.11 Scheme of the ping-pong mechanism for AuNPs/PPy/HRP/SPE in 50μM H ₂ O ₂ / 50μM phenol in PBS (pH 7.4); Ph _{ox} and Ph _{ed} are the oxidized and reduced forms of phenol, respectively (Joanna Cabaj and Jadwiga (2011)).....	63
5.12 Comparison of current responses between bare SPE, PPy/SPE,	

FIGURE	PAGE
AuNPs/PPy/SPE and HRP/AuNPs/PPy/SPE in 50 μ M H ₂ O ₂ / 50 μ M phenol in PBS (pH 7.4) at -0.05V (Symbol of A, B, C, D represent Bare SPE, PPy/SPE, AuNPs/PPy/SPE, AuNPs/PPy/HRP/SPE, respectively).....	67
5.13 Comparison of current responses of AuNPs/ PPy/ HRP/SPE in different solutions (pH 7.4) at -0.05V (Symbol of A, B, C, D represent the solutions of PBS, Phenol, H ₂ O ₂ , H ₂ O ₂ /Phenol, respectively).....	67
5.14 Cyclic voltamogram of HRP/AuNPs/PPy/SPE in solution of 0.1M PBS (pH7.4) at various scan rates from 0.1-0.5 V/s.....	70
5.15 The relationship between the peak current (I _p) and the scan rate (v) for AuNPs/PPy/HRP/SPE in 0.1M PBS (pH7.4) with scan rates varied from 0.1-0.5 V/s.....	71
5.16 The relationship between the peak potential (E _p) and the natural logarithm of scan rate (lnv) for HRP/AuNPs/PPy/SPE in 0.1M PBS (pH7.4) with scan rate varied from 0.1 - 0.5 V/s.....	72
5.17 Calibration plot between the reciprocals of the steady-state current versus phenol concentration.....	74
5.18 Calibration curve of amperometric phenol response in 50 μ M H ₂ O ₂ / PBS solution (pH 7.4) at -0.05V (vs. Ag/AgCl). Inset: the linear part of the calibration curve.....	76
5.19 Amperometric current response of biosensor of 50 μ M phenol/50 μ M H ₂ O ₂ in PBS solution (pH 7.4) at -0.05V (vs. Ag/AgCl) under stirred condition...	77
5.20 Reproducibility test of ten identical biosensors in 1 μ M phenol/ 50 μ M H ₂ O ₂ /PBS (pH 7.4) at -0.05V (vs. Ag/AgCl).....	78
5.21 Storage stability of AuNPs/PPy/HRP/SPE in 50 μ M phenol/ 50 μ M H ₂ O ₂ / PBS solution (pH 7.4) at -0.05V (vs. Ag/AgCl) (Symbol of A, B, represent the storage conditions at 4°C, and 25°C).....	79

CHAPTER I

INTRODUCTION

1.1 Motivation

Phenolic compounds are well-known chemicals which were used as a disinfectant reagents and intermediate reagents utilized in many industries, especially in industries of resins and plastics, petroleum refining, dyes, chemicals, textile, food and pharmaceuticals. Phenol is one of a class of phenolic compounds which are hazardous consisting of hydroxyl groups (-OH) bonded to the aromatic hydrocarbon group such as phenol, p-Nitrophenol, o-Nitrophenol, o-Chlorophenol, 2,4-Dinitrophenol, 2,4-Dimethylphenol, 2,4-Dichlorophenol, 4-Chloro-m-cresol, 4,6-Dinitro-o-cresol 2,4,6-Trichlorophenol, Pentachlorophenol, o-Cresol, m-Cresol, p-Cresol that directly affected living beings and surrounding due to their high toxicity and stability even at low concentrations (Abdullah et al., 2006; Arecchi et al., 2010; Busca et al., 2008). Human and animals receive these substances through inhalation, ingestion, eye contact, and rapid absorption through the skin. The accumulation of these substances causes damage to the lungs, liver, kidneys, and genito-urinary systems (Abdullah et al., 2006; Busca et al., 2008). Besides, these overexposures of these compounds could lead to comas, convulsions, cyanosis and death. Therefore, phenolic compounds are strictly controlled by regulations or law of each country.

A number of phenolic compounds are listed in the European Community (EC) Directive 76/464/EEC which concerns hazardous substances discharged into the aquatic environment and in the US-EPA list of priority pollutants to protect the phenol contamination in drinking water and ground water resources. The Environmental Protection Agency specifies a water purification standard of less than 1 part per billion (ppb) of phenol in surface waters. For many countries, water quality standards are used in reference to the EC and US-EPA. For instance, in Italy, the limit for phenols in drinking and mineral waters is 0.5 $\mu\text{g/l}$ (0.5 ppb), while the limits for wastewater emissions are 0.5 mg/l (0.5 ppm) for surface waters and 1 mg/l (1 ppm) for the sewerage system (law no. 152/2006)(Busca et al., 2008). In Malaysia, the maximum level of phenolic compounds

in surface water for drinking water is in the range of 1–2 ppb ($\mu\text{g/l}$) while the acceptable limit in sewage and industrial effluents is in the range of 1–5 ppm (mg/L) (Abdullah et al., 2006).

In Thailand, in agreement with the recommendations of the US Environment Protection Agency (E.P.A.), a water purification standard of less than 5 ppb ($\mu\text{g/l}$) of phenol in surface water and the maximum level of phenolic compounds for drinking water is in the range of 1-2 ppb ($\mu\text{g/l}$) while the allowable limit in industrial effluent of less than 1 ppm (mg/l) or 10.6 μM (http://www.pcd.go.th/info_serv/reg_std_water.html). Water quality standards for phenolic compounds detection are summarized in Table 1.1.

Table 1.1: Water quality standards for measurement of phenolic compounds in different countries (Busca et al., 2008; Abdullah et al., 2006; http://www.pcd.go.th/info_serv/reg_std_water.html).

Resources	USA	EC	Malaysia	Thailand
Drinking water	1 ppb	0.5 ppb	1-2 ppb	1-2 ppb
Surface water	5 ppb	0.5 ppm	-	5 ppb
Industrial effluent	1 ppm	1 ppm	1-5 ppm	1 ppm

With the needs of sensitive and rapid phenol detection, we have developed phenol enzyme biosensors in our laboratory. The biosensor was fabricated based on glassy carbon electrodes modified with gold nanoparticles under polypyrrole film (Yusran, 2009). A satisfactory wide linear range of gold/ polypyrrole modified glassy carbon electrode in the presence of horseradish peroxidase was obtained. However, low detection limit was still not achieved (25.4 μM). These biosensors suffered from the drawback of high detection limit and instability that imply for shorter shelf life. Poor sensor stability was mainly caused by electrode fouling, enzyme inactivation and desorption from immobilization materials. Therefore, the development of good

immobilization methods and materials to improve performances of the biosensor especially in lowering the detection limit and prolonging storage stability is needed.

Electrochemical polymerization is a general method used for conductive polymer deposition because biomolecules can be added into the monomer solution for subsequent entrapment during the electrochemical oxidation process. Typically, this polymer/biomolecule layer is developed at fixed potentials or by cyclic voltammetry. The principal advantage of this method is that the resulting materials are easily prepared in a single-step procedure with controlled thickness of the polymeric layer (Andreescu et al., 2005). Therefore, this method was chosen in order to construct phenol biosensors in this study.

The aim of this study was to develop the AuNPs/PPy/HRP nanobiocomposite film for constructing a phenol biosensor. The working electrodes were fabricated in a one-step procedure by electropolymerization process of gold nanoparticles, polypyrrole and HRP. Many researches have used the immobilized enzyme on the surface of Pt, Au and glassy carbon (GC) electrodes but electropolymerization method on the surface of screen-printed carbon electrode has never been reported. Screen-printed carbon electrode is well suited for mass production and portable devices. Operational parameters such as gold precursor concentration and cycling number of electropolymerization were optimized. The performance factors were also evaluated.

1.2 Objective

To study effects of electropolymerization conditions on performances of gold nanoparticles/ polypyrrole/ HRP phenol biosensor.

1.3 Scope of the research

A conventional three electrodes system comprising platinum wire (Pt) as a counter electrode, silver/silver chloride (Ag/AgCl) as a reference electrode, and modified screen-printed carbon as a working electrode was used in this study. The AuNPs/PPy/HRP nanobiocomposite film was coated onto the surface of a screen-printed

carbon electrode by electropolymerization in a three-electrode cell. The polymerization medium contained 5 ml PBS solution (pH 7.4) containing 0.09M pyrrole, 1×10^{-3} M gold precursor solution and 250 unit/mL HRP. Electrochemical polymerization was carried out between 0.0-1.0V vs. Ag/AgCl with a scan rate of 10 mV/s. The fabricated electrode was washed and rinsed in double-distilled water to remove the unfixed enzyme before being dried at room temperature.

1.3.1 Investigation of suitable electropolymerization conditions of AuNPs/ pyrrole modified working electrode for constructing phenol biosensor using amperometric method.

1.3.1.1 Au precursor concentration (Au:Citrate, 1:34 molar ratio)

1, 3, 5, 7, 9 mM

1.3.1.2 Cycling numbers of electropolymerization

5, 10, 15, and 20 cycles

1.3.2 Physical and Chemical characterization by UV-Visible spectroscopy (UV-Vis), Scanning Electron Microscopy (SEM), Transmission Electron Microscopy (TEM), and Energy-dispersive X-ray spectroscopy (EDX).

1.3.3 Electrochemical analysis of the fabricated biosensors from item 1.3.1 were performed with amperometry technique in 50 μ M hydrogen peroxide/ 50 μ M phenol/ phosphate buffer solution (pH 7.4) at the operating potential of -0.05V.

1.3.4 Investigation of electron transfer process of modified electrode using cyclic voltammetry in 0.1M phosphate buffer (pH 7.4) at different scan rates (100, 200, 300, 400, 500 mV/s) with the potential between 0.0 and 1.0V in order to determine electron transfer rate by Laviron equation.

1.3.5 Investigation of enzyme kinetic of modified electrode using amperometry in various phenol concentrations (0.1 to 210 μ M) /50 μ M hydrogen peroxide/ phosphate buffer solution (pH 7.4) at an operating potential (-0.05V) to determine the enzyme kinetic parameters by the Lineweaver-Burk equation.

1.3.6 Determination of the performance factors of the AuNPs/PPy/HRP which are fabricated under suitable conditions.

1.3.6.1 Linear range, sensitivity, and detection limit

1.3.6.2 Response time

1.3.6.3 Reproducibility

1.3.6.4 Storage stability

1.4 Expected benefits

To obtain appropriate electropolymerization conditions for construction of AuNPs/PPy/HRP nanobiocomposite film on screen-printed carbon electrode and to improve the detection limit and stability for phenol biosensor.

CHAPTER II

THEORY

The objective of this chapter is to give an understanding of the fundamentals of biosensor and analytical electrochemistry. Moreover, this topic gives some information which relate to an enzyme such as horseradish peroxidase (HRP) together with the other methods for immobilized enzyme and enzyme kinetic.

2.1 Biosensors

Biosensors are analytical devices that combine the biological component with a transducer which are firstly discovered by Leland C. Clark. The development and progress of biosensor technology conduces to the widely uses in various field such as medicine, food, environment, process industries, security and diagnostics, etc. Biosensors composed of two major parts which are a biological substance and a transducer as shown in Fig.2.1. The first part, the biological components are responsible for recognition of the analyte that can be divided into two distinct groups i.e. catalytic and non- catalytic. The catalytic group includes enzymes, microorganisms and tissues, while the non-catalytic consists of antibodies, receptors and nucleic acid etc. Nevertheless, the biological molecules have very short lifetime in solution phase. Thus they have to be fixed in a suitable matrix by immobilization of the biological species. The second part, a transducer has a function that converts the biochemical signal to an electronic signal. Therefore, the nature of the biochemical interaction with the species of interest is essential to transducing system. Various types of transducers are available such as electrochemical (amperometric, potentiometric, and conductometric), optical, colorimetric, and acoustic etc. The amperometric and potentiometric are most common electrochemical transducers.

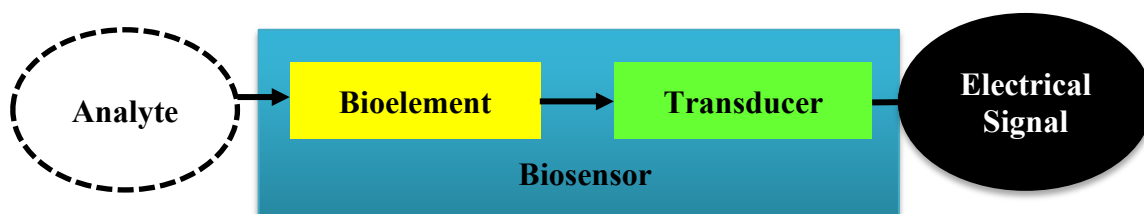


Fig. 2.1 Schematic diagram of a simple biosensor.

2.1.1 Types of Biosensors

(i) Resonant Biosensors

This biosensor composes of an acoustic wave transducer and bio-element. This device relies on the principle of the frequency change of the transducer that takes place from the change of mass when the analyte molecule is adsorbed. The output signal is measured in form of frequency wave.

(ii) Optical Biosensors

This type of biosensor is based on the principle of optical diffraction by creating a diffraction grating. This grating produces a diffraction signal when illuminated with a light source such as laser to receive the output signal which can be measured.

(iii) Thermal Biosensors

The basic principle of such biosensors is based on biochemical reaction involve the temperature change in an enzyme reaction. It combines immobilized enzyme molecules with temperature sensors. The measurement of the temperature is typically accomplished by a thermistor. Common applications of this type of biosensor include the detection of pesticides and pathogenic bacteria.

(iv) Ion-sensitive Biosensors

These biosensors operate on the principle of change of the surface electrical potential between semiconductor FET and ions. They are primarily used for pH detection.

(v) Electrochemical Biosensors

The principle for this class of biosensors is that many chemical reactions produce or consume ions or electrons which in turn cause some change in the electrical properties of the solution which can be sensed out and used as measuring parameter. Electrochemical biosensors can be classified base on the measuring electrical parameters such as: (a) *conductimetric*, (b) *amperometric* and (c) *potentiometric*.

(a) *Conductimetric*

The measured parameter is the electrical conductance / resistance of the solution. While electrochemical reactions produce ions or electrons, the overall conductivity or resistivity of the solution changes. This change is measured and calibrated to a proper scale. Conductance measurements have relatively low sensitivity. The electric field is generated using a sinusoidal voltage (AC) which helps in minimizing undesirable effects such as Faradaic processes, double layer charging and concentration polarization.

(b) *Amperometric*

This high sensitivity biosensor can detect electroactive species in biological test samples. Since the biological test samples may not be intrinsically electro-active, enzymes are needed to catalyze the production of active species. In this case, the measured parameter is current.

(c) *Potentiometric*

In this type of sensor the measured parameter is oxidation or reduction potential of an electrochemical reaction. The working principle relies on the fact that when a ramp voltage is applied to an electrode in solution, a current flow occurs because of electrochemical reactions. The voltage at which these reactions occur indicates a particular reaction and particular species.

2.1.2 A current response of an electrochemical system

A current response was determined by monitoring of electron transfers during a redox reaction of an analyte:



Where O and R are the oxidized and reduced forms of the redox couple, respectively while n is the number of electrons transferred for this reaction. Many well-known laws refer to the behavior of the redox current which relate to the effects of the applied potential. The applied potential controls the concentrations of the redox species at the electrode surface (C_O and C_R) as described by the Nernst equation:

$$\text{---} \quad \text{---} \quad \text{---} \quad \text{---} \quad (2.2)$$

Where R is the molar gas constant ($8.3144 \text{ J mol}^{-1}\text{K}^{-1}$), T is the absolute temperature (K), n is the number of electrons transferred, F is Faraday constant ($96,487 \text{ coulombs}$), and E^0 is the standard reduction potential for the redox couple. If the potential applied to the electrode is changed, the ratio $C_O(0,t)/C_R(0,t)$ at the surface will also change so as to satisfy Eq. (2.2). If the potential is made more negative the ratio becomes larger (that is, O is reduced) and, conversely, if the potential is made more positive the ratio becomes smaller (that is, R is oxidized). A change of oxidation state of the electroactive species gives current which measure directly from the rate of redox reaction. The pathway of the electrode reaction is complicated and comprises several steps so the reaction rate is determined by the slowest step. While the rate of reaction and current can be controlled either by mass transport or the rate of electron transfer which are represented in the following.

(i) Mass transport-Controlled reactions

The mass transport is a controlled reaction when this process is the slowest. Generally, mass transport can occur through three different mechanisms as shown in Fig.2.2:

- 1) Diffusion – the movement under the effect of concentration gradient which depends on distance and time according to Fick's laws.
- 2) Convection – the physical movement of solution. It arises from various causes i.e. the movement of the solution by mechanical stirring or flow of solution or vibration of electrode or density gradient, etc. this phenomena can be minimized by not stirring or quiet conditions.

- 3) Migration – the movement of charged particles in an electrical field. The rate of migration depends on the strength of the interaction between ion and the field, the charge and size of the ion. The most commonly used a neutral atom or uncharged molecule for the suppressing migration.

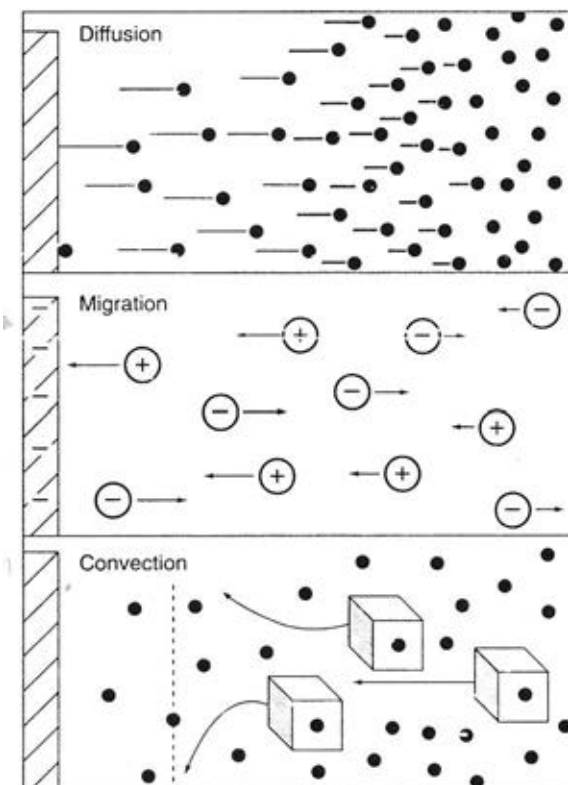


Fig. 2.2 The three modes of mass transport (Joseph Wang, 2006).

The rate of mass transport is measured in the form of flux (J ; $\text{mol cm}^{-2}\text{s}^{-1}$) which is shown according to the Nernst-Planck equation:

$$J = -D \frac{\partial C}{\partial x} - \frac{zC}{F} \frac{\partial \phi}{\partial x} + C v \quad (2.3)$$

Where D is the diffusion coefficient (cm^2s^{-1}), $\partial C(x,t)/\partial x$ is the concentration gradients, $\partial \phi(x,t)/\partial x$ is the potential gradients at x -axis and time t , z and C (mol cm^{-3}) are the charge and the concentration, respectively, $V(x, t)$ is the hydrodynamic velocity (in direction x and time t). In this equation, on the right side, the first term illustrates the diffusion rate. The second and the third terms represent the migration and the convection

of the solution, respectively. While the flux is directly proportional to the current (i) as shown below:

$$i = nFAj \quad (2.4)$$

In the diffusion controlled reaction, a current of planar electrode from a controlled potential experiment can be described with the Cottrell equation (Eq. 2.5). This equation is derived from the Fick's first law and the Fick's second law (the change in concentration with times relates to the change in flux with position):

$$i = nFA \frac{D_0^{1/2}}{\pi^{1/2}} \frac{C_0}{t^{3/2}} \quad (2.5)$$

Where A is the electrode area (cm²), r is the distance from the center of the electrode, and $(\pi D_0 t)^{1/2}$ is a diffusion layer thickness (δ). Moreover, for the spherical electrode, the current can describe as shown in equation (2.6):

$$i = nFA \frac{D_0^{1/2}}{\pi^{1/2}} \frac{C_0}{t^{3/2}} - \frac{nFA D_0 C_0}{r} \quad (2.6)$$

The first term of the equation (2.6) is a time dependent term and dominates at short time. At long time, the second term (a spherical correction term) will be more dominate than the first term, becoming time independent current. This equation can also explain a microelectrode's current.

(ii) *Electron transfer – Controlled reactions*

When the electron transfer process is the slowest step, the reaction will be controlled by the rate of electron transfer. The Butler-Volmer equation is used to describe a net current of the reaction where the net current is the difference between forward (reduction) and backward (oxidation) currents of the reaction:

$$\left\{ \left(- \frac{i_0}{\alpha} \right) - \left(\frac{i_0}{\beta} \right) \right\} \quad (2.7)$$

Where i_0 is the exchange current or the current under equilibrium state ($E=E_{eq}$), η is the over potential or the overvoltage which must be used in non-spontaneous cell reaction, and α is the transfer coefficient, generally, this value is closed to 0.5. While the value of i_0 is given by:

$$(2.8)$$

Where i_c and i_a are cathodic (reduction) and anodic (oxidation) currents, respectively, and k^0 is the standard heterogeneous rate constant (cm/s). The value of k^0 depends on the particular reactant and the electrode material used.

2.1.3 Electrochemical method

Linear sweep voltammetry and cyclic voltammetry are examples of potential-sweep experiment which the electrode potential is ramped between two limits at a particular rate. The resulting curve is known as a voltammogram and provides information on the rate of electrochemical reactions as a function of potential. From the sweep-rate dependence of the voltammetric data several quantitative properties of the charge-transfer reaction can be determined. However, cyclic voltammetry techniques are most useful.

(i) Cyclic voltammetry

Cyclic voltammetry method is applied for the study of the electrochemical behaviour of a system. In this technique current flowing between the interested electrode (whose potential is monitored with respect to a reference electrode) and a counter electrode is measured under the control of a potentiostat. The voltammogram determines the potentials at occurred different electrochemical processes. The working electrode is subjected to a triangular potential sweep, whereby the potential rises from a start value E_i to a final value E_f then returns back to the start potential at a constant potential sweep rate. The sweep rate utilized can vary from a few millivolts per second to a hundred volts per second. The measured current during this process is often normalised to the electrode surface area and referred to as the current density. The current density is then plotted

against the applied potential, and the result is referred to as a cyclic voltammogram. A peak in the measured current is shown at a potential that is characteristic of any electrode reaction taking place. The width and height of peak for a particular process depend on the sweep rate, electrolyte concentration and the electrode material. Cyclic voltammetry makes possible the explanation of the kinetics of electrochemical reactions which takes place at electrode surfaces. In a typical voltammogram, the sweep-rate dependence of the peak amplitudes, widths and potentials of the peaks observed in the voltammogram, it is possible to investigate the role of adsorption, diffusion, and heterogeneous chemical reaction mechanisms.

A schematic cyclic voltammogram of a reversible redox process (Fig.2.3) illustrates the expected response of a reversible redox couple during a single potential cyclic. Assume that only an oxidized form (O) is present at the initial state. Determining for a forward scan, a current is higher as well as increasing the potential in negative way due to the reduction of O is more increased. For this situation, the concentration of a reduced form (R) near the electrode surface is higher than concentration of O and becomes highest at the peak of the voltammogram. The peak current at the cathodic peak potential ($E_{p,c}$) is called a cathodic (reduction) peak current ($i_{p,c}$). At the switching potential or reverse scanning, R molecules are reduced back to O molecules. The peak on this side will usually have a similar shape to the cathodic peak and it is called an anodic (oxidation) peak current ($i_{p,a}$). The potential at the anodic peak current is an anodic peak potential ($E_{p,a}$).

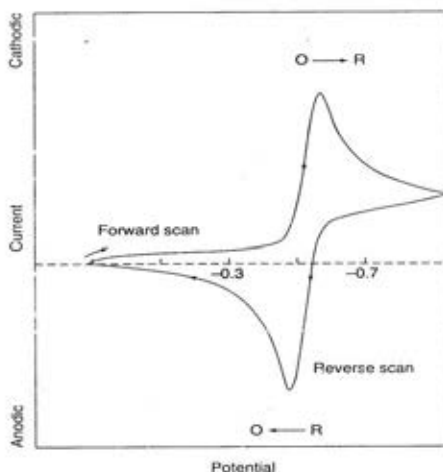


Fig. 2.3 A schematic cyclic voltammogram of a reversible redox process
(Joseph Wang, 2006).

For reversible systems at ambient temperature (25°C), the peak current is given by the Randles-Sevcik equation:

$$i_p = 0.4463 n F A C \sqrt{v} \quad (2.9)$$

Where n is the number of electrons, A is the electrode area (cm^2), C the concentration (mol/cm^3), D is the diffusion coefficient (cm^2/s), and v is the potential scan rate (V/s). Accordingly, the current is directly proportional to concentration and increases with the square root of the scan rate. Such dependence on the scan rate is indicative of electrode reaction controlled by mass transport. However, electrode reaction can be controlled by electron transfer that the current increases with the the scan rate. The standard potential (E^0) and the number of electrons transferred (n) can be determined from cathodic and anodic peak potentials:

$$E^0 = \frac{E_{pa} + E_{pc}}{2} \quad (2.10)$$

$$\Delta E_p = E_{pa} - E_{pc} \quad (2.11)$$

Where ΔE_p (also called the separation peak potential) is the difference in cathodic and anodic peak potential and the values of 0.059 V is a fast one electron process.

For irreversible systems, i.e. where the rate of the backward reaction is negligible and is described by the reaction scheme: $O + ne \rightarrow R$. ΔE_p is not independent of sweep rate. The peak potential and peak current can be described in equation 2.12 and 2.13, respectively:

$$\left(\frac{E_p}{\nu} \right) \quad / \quad / \quad / \quad (2.12)$$

$$- \left[\frac{E_p}{\nu} - \frac{RT}{\alpha n F} \left(\frac{E_p}{\nu} \right)' \right] \quad (2.13)$$

Where α is the electron transfer coefficient and n_a is the number of electrons involved in the charge transfer step.

For quasi-reversible system, the cathodic and anodic peak potential shifts by increasing the scan rate, it is possible to estimate the kinetic parameters such as the apparent heterogeneous electron transfer rate constant (k_s) according to the equation derived Laviron for diffusionless CVs. The anodic and cathodic peak potentials are linearly dependent on the \ln of scan rates (ν) when $E_p > 200/n$, which is in agreement with the Laviron theory. From a plot of E_p versus $\ln \nu$ yields two straight lines with slopes of $-RT/\alpha nF$ and $RT/(1-\alpha)nF$ for the cathodic peak and for the anodic peak, respectively, so that can be estimated α from the slope of the straight lines based on the equation and the electron transfer rate constant (k_s) can be calculated according to the following equation:

$$\left(\frac{E_p}{\nu} \right) \quad \left(\frac{E_p}{\nu} \right) \quad - \quad \frac{RT}{\alpha n F} \quad (2.14)$$

Where ν is the scan rate, α is the electron transfer coefficient, k_s is the apparent heterogeneous electron transfer rate constants, R is the gas constant, T is the absolute temperature, F the Faraday constant and n number of electrons involved in the redox couple.

(ii) *Amperometry*

The amperometry technique applied a controlled potential at the working electrode. The current responses which derive from this technique are controlled as a function of time. As the current responses are directly proportion to the concentration of the analytes according to the Cottrell equation (eq. 2.14):

$$i(t) = \frac{nFA D^{1/2} C \sqrt{kt}}{\sqrt{\pi}} \quad (2.15)$$

Several parameters such as n , F , A , D or C can be determined from this equation. By “Cottrell behavior” is termed of a constant value ($kt^{-1/2}$). However, the disadvantage of amperometry is the lack of reproducibility due to the deposition of impurities on the electrode surface. To obtain reproducible results, the electrode surface must be cleaned regularly either by polishing or performing electrochemical process.

2.1.4 Performance factors

Nowadays, biosensors are most applied for detection of analytical substances. As a new technique, one needs to establish fairly quick criteria by which its performance can be measured. As the technique is developed, these criteria have to be refined continuously as expectations are raised. This is especially true for a device containing biological material. Showing that a method will work in a laboratory is a very long way from delivering a commercial product into the hands of a medical laboratory technician. However, each biosensor is fabricated by different methods and caused different performances. Thus, methods for determining the biosensor performance factors are necessary.

(i) Selectivity

Selectivity is the key characteristic of biosensor systems. It is an ability to discriminate between different substrates and concern the range of chemical species. Selectivity of a system depends on the nature of the biological sensing element (such as enzyme) and its selectivity for the substrate. The approach for biosensor selectivity determination can be performed by measuring the biosensor response to interfering compounds, a calibration curve for each interfering compound is plotted and compared to

the analyte calibration curve under identical operating conditions. A broad range of substances refers to low selectivity sensor. On the other hand, a narrow range refers to high selectivity sensor.

(ii) Linear range and Detection Limit

The calibration of biosensor is performed by plotting the response change (such as electrode potential) vs. the analyte concentration. The linear range is the interval between the upper and lower levels of the analyte concentration that have been demonstrated to be determined with linearity. The lowest measurable concentration is called a detection limit, which is normally more than 10^{-5} M (0.01 mM). The detection limit equals to $3S_b/m$, where S_b is the standard deviation of the blank signal, and m is the slope of calibration curve.

(iii) Sensitivity

The sensitivity is located within the linear concentration range of the biosensor calibration curve which determined from the slope of the biosensor calibration curve. Sensitivity is dependent on the efficiency of signal transfer from receptor to device, and response characteristics of the device. Again, the receptor should be coupled to the device for maximum sensitivity. Receptors that are not permanently attached to the device may diffuse away from the device, causing a decrease in sensitivity with time, drift in response and a need for frequent calibration.

(iv) Reproducibility

The reproducibility is also another important factor with any analytical technique, but especially so with biosensors, where it is impossible to reproduce quality of biological and chemical substances preparation. Reproducibility is a measure of the scatter or the drift in a series of results performed over a period of time. The expected reproducibility of the biosensor should be at least ± 5 to 10 %.

(v) Response time

The response time is the amount of time required for the system to approach equilibrium. This response time can be varied for each biosensor; however, the typical value is less than 5-10 minutes.

(vi) Life time

The life time is the duration that the biological component (or enzyme) on the biosensor can perform reaction and yield reasonable response before it is deteriorate or lost its activity. There are three aspects of lifetime related to biosensor; the lifetime of the biosensor in use, the life time of the biosensor in storage and the lifetime of the biological material stored separately.

2.2 The enzyme for phenol detection

Among biological substances, it was found that horseradish peroxidase (HRP) based biosensor are very sensitive for a great numbers of phenolic compounds. For HRP based electrode can be carried out at low potential to avoid an interfering reaction by unexpected species. However, this enzyme is high cost and low stability in solution (Kafi et al., 2008). In this research, HRP was selected as a model enzyme.

2.2.1 Horseradish peroxidase (HRP)

Enzymes are proteins using as biological catalysts that catalyze chemical reactions but they different from ordinary chemical catalyst due to they have the ability to catalyze a reaction under very mild conditions in neutral aqueous solution at normal temperature and pressure. In addition to enzymes had high specificity likely, most enzymes act specifically with only one reactant (called a substrate) to produce products including they can be decrease activation energy leads to increasing the rate of reaction when compared with the absence of an enzyme. Horseradish peroxidase (HRP, EC 1.11.1.7) is a class of peroxidase enzyme. It belongs to the superfamily of heme-containing plant peroxidases which extracted from horseradish roots (*Amoracia rusticana*) and it catalyses the oxidation of various electron donor substrates (e.g. phenols, aromatic amines) with hydrogen peroxide.

HRP is one of the most widely used enzymes for detection of phenol that can be used as electron donating compound (Ruzgas et al., 1995). The research of Rosatto et al.(2006) studied in phenol biosensor based on modified carbon paste electrode by HRP immobilizing on silica gel together with titanium dioxide. They described that the HRP reaction on electrode related to mechanism of mediated and direct electron transfer.

2.2.1.1 Mechanisms of the mediated electron transfer

The mechanism when the electron donating species are involved can be represented by the equations:





The first reaction (2.16) represents an oxidation of a native peroxidase, HRP (Fe^{3+}), by the hydrogen peroxide (H_2O_2) and forming an intermediate compound I, the HRP (Fe^{5+}). Next, HRP (Fe^{5+}) is reduced by the first electron donor, (AH_2) to form an intermediate compound II, the HRP (Fe^{4+}), following the equation (2.17). The native peroxidase is then produced during the reduction of HRP (Fe^{4+}) by second electron donor in the last equation (2.18). In each step the electron donor species (AH_2), generally organic substances such as phenolic compounds, are oxidized to free radicals (AH^*) (Ruzgas et al., 1996; Rosatto et al., 1999). This mechanism can be perceived in the scheme of Fig.2.4.

Although high concentration of peroxide in the media can lead to peroxidase inactivation and some mediator molecules will pollute the electrode system or diffuse out of the enzyme layer. However, this mediated electron transfer show high sensitivity and low detection limit due to its fast electron transfer (Rosatto et al., 1999; Liu and Ju 2002). Thus, this work focuses on the mechanisms of mediated electron transfer based on HRP biosensor that phenol is used as mediator in order to measure phenolic compounds in solutions.

2.2.1.2 Mechanisms of the direct electron transfer

Direct enzyme reduction of H_2O_2 at a HRP-modified electrode can be described by the following kinetic scheme:



The enzyme immobilized on an electrode surface can be oxidized by hydrogen peroxide according to reaction (2.19) and then subsequently reduced by electrons provided by an electrode, reaction (2.21). This reaction used an electrode substitutes for

the electron donor substrates (Ruzgas et al., 1995; Lindgren et al., 1999). This mechanism can be perceived in the scheme in Fig.2.5.

The mediatorless sensor can also directly transfer electrons between enzyme itself and an electrode. This phenomenon limited the sensitivity of the biosensor for monitoring phenol due to the background current of the direct electron transfer from peroxide (Gorton et al., 1992). However, the slow electron transfer rates result in the low sensitivity and the high detection limit.

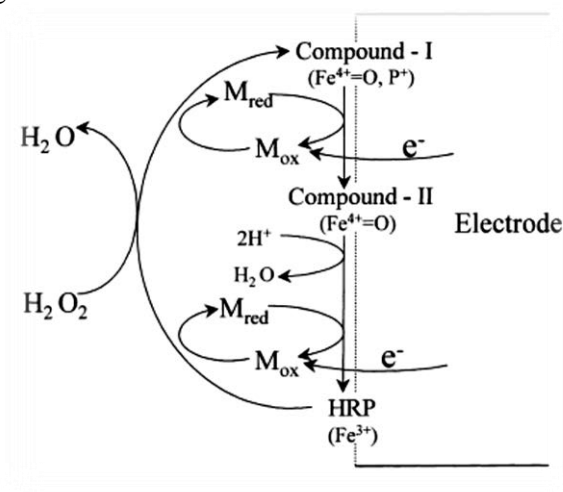


Fig. 2.4 Mechanism of mediated electron transfer at HRP modified electrode. M_{ox} and M_{red} are the oxidised and reduced forms of the mediator respectively (Rosatto et al., 1999).

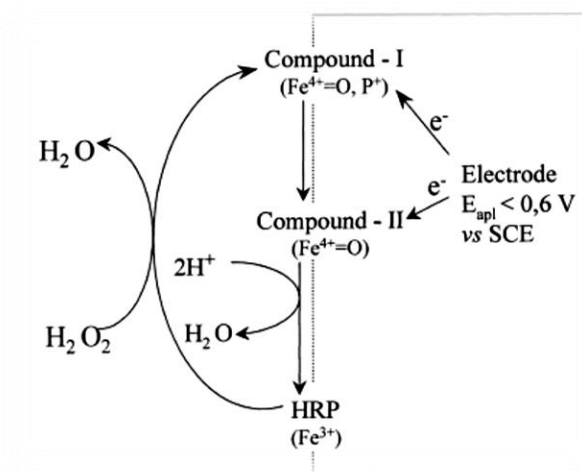


Fig. 2.5 Mechanism of the direct electron transfer between HRP and base electrode (Rosatto et al., 1999).

2.3 Immobilized enzyme method

Immobilized enzymes are defined as “enzymes physically confined or localized in a certain defined region of space with retention of their catalytic activities, and which can be used repeatedly and continuously” Immobilization of enzymes is classified into “carrier-binding”, “cross-linking” and “entrapping” types as shown in Fig.2.6 Carrier-binding is subdivided into “physical adsorption”, “ Ionic binding” and “covalent binding”

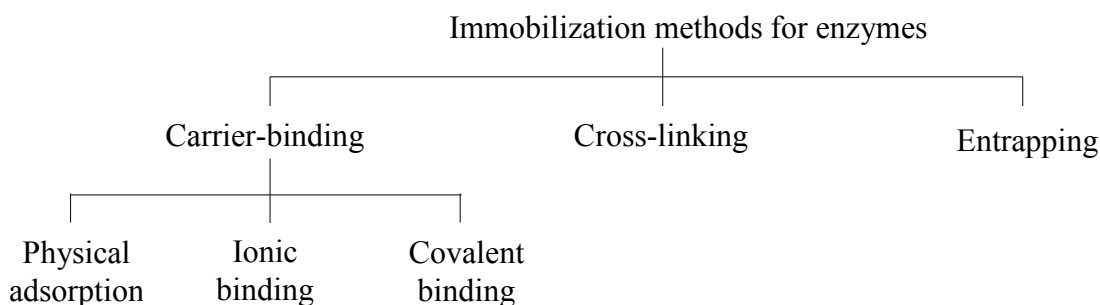


Fig. 2.6 Classification of immobilization methods for enzymes.

2.3.1 Carrier-binding Method

The carrier-binding method is the oldest immobilization method that enzymes are immobilized by binding techniques. The amount and activity of enzyme after immobilization depend on the nature of the carrier. However, particle size, surface area, molar ratio of hydrophilic to hydrophobic groups and chemical composition must be considered. As carriers for immobilized enzyme, polysaccharide derivatives such as cellulose, dextran, agarose and polyacrylamide gel are most commonly used. This method can be divided into three categories according to the binding mode of enzyme such as physical adsorption, ionic binding and covalent binding.

2.3.1.1 Physical adsorption method

The adsorption method involves the enzyme being physically adsorbed onto the backbone or support material, often a polymer matrix (i.e. polymer beads or membranes) by weak physical forces. This technique is relatively simple. Unfortunately this method is

drawback, because it can also denature the enzyme depending on the surface chemistry of the support material (Spahn and Minteer,2008).

2.3.1.2 Ionic binding method

The ionic binding method is based on the ionic binding of enzyme to water-insoluble carriers containing ion-exchange residues. As carriers for ionic binding, polysaccharides and synthetic polymers having ion-exchange residues are used. The binding of enzyme to carrier is easily carried out, and the conditions are mild in comparison with those necessary for covalent binding method. As the binding forces between enzyme and carriers are less strong than in covalent binding, leakage of enzyme from the carrier may occur in substrate solutions of high ionic strength or upon variation of pH.

2.3.1.3 Covalent binding method

The covalent binding method is based on the binding of enzymes and water-insoluble carriers by covalent bonds. The selection of conditions for immobilization by covalent binding is more difficult than in the case of physical adsorption and ionic binding. The requirement of reaction conditions for this method is complicated and not particularly mild. Therefore, covalent binding causes the conformational change and active site of enzyme resulting in major loss of its activity. However, the binding force between enzyme and carrier is strong which prevents the leakage of enzyme.

2.3.2 Cross-linking method

An enzyme may also be immobilized through the cross-linking of proteins to an insoluble support to prevent the loss of enzyme into the substrate solution. However, crosslinking or covalently binding the enzyme to the support material surface typically decreases the degree of movement of the enzyme, which can dramatically decrease the enzyme activity (Spahn and Minteer ,2008).

2.3.3 Entrapping method

The entrapment method involves confining enzyme in a material or in polymer membranes. This usually minimizes enzyme leaching and improves stabilization, but

frequently results in transport limitations of substrate to the enzyme active site. Nevertheless, this technique allows for the ability to tailor the encapsulating material to provide the optimal microenvironment for the enzyme (i.e. matching the physico-chemical environment of the enzyme and immobilization material). This can be done with a variety of materials including: polymers, sol-gels, polymer/sol-gel composites, and other inorganic materials (Spahn and Minteer, 2008). Method of preparation and characteristics of immobilized enzyme is summarized in Table 2.2.

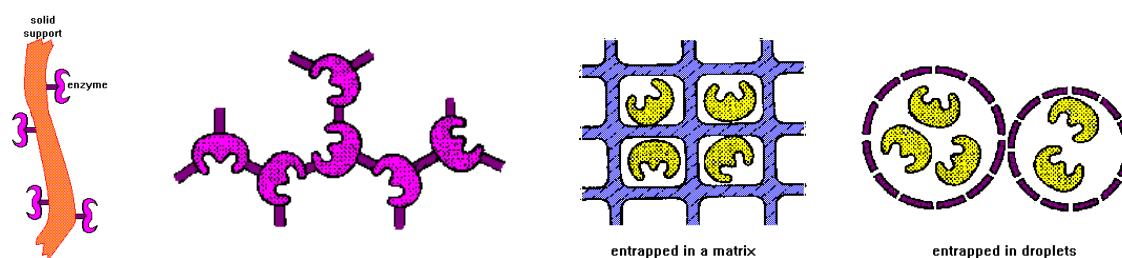


Fig. 2.7 Immobilized enzyme (www.cheric.org/ippage/e/ipdata/2004/02/file/e200402-1001.pdf)

Table 2.2 Comparison of immobilized enzymes method (Ichiro Chibata, 1978).

Characteristics	Carrier binding method			Cross-linking method	Entrapping method
	Physical adsorption	Ionic binding	Covalent binding		
Preparation	easy	easy	difficult	difficult	difficult
Enzyme activity	low	high	high	moderate	high
Substrate specificity	unchangeable	unchangeable	changeable	changeable	unchangeable
Binding force	weak	moderate	strong	strong	strong
Regeneration	possible	possible	impossible	impossible	impossible
General applicability	low	moderate	moderate	low	high
Cost of immobilization	low	low	high	moderate	low

2.4 Enzyme kinetics

An important goal of measuring enzyme kinetics is to determine the chemical mechanism of an enzyme reaction. The reaction rate was measured and the effects of changing the conditions of the reaction investigated. Particularly for the enzyme used in biosensor, the mode of action involves oxidation or reduction which can be detected electrochemically. The simple conversion of substrate (S) into product (P) catalyzed by the enzyme (E) is described below. As outlined by the hypothesis, the first step is substrate binding and the second step is the catalytic step.

A simple enzyme-catalyzed reaction:



Where E = enzyme

S = substrate

ES = enzyme-substrate complex

P = product of the enzyme-catalyzed reaction

k_1 = rate constant of the forward reaction of E+S

k_{-1} = rate of the reverse reaction where the enzyme-substrate complex, ES, falls apart to E+S

k_2 = rate constant of the forward reaction of ES forming E+P

Assumed that: (1) the dissociation rate (k_2 in Eq. 2.21) of the enzyme–substrate complex (ES) is slow compared to association (k_1) and redissociation (k_{-1}) reactions

(2) the reverse reaction (P→S) is negligible.

The formation of the product in terms of the dissociation rate (k_2) of the enzyme–substrate complex

$$v = k_2 [ES] \quad (2.22)$$

At steady state, the enzyme–substrate concentration is stable:

$$\frac{d[ES]}{dt} = 0 \quad (2.23)$$

Therefore the formation of the ES complex (association reaction) and the breakdown of the ES complex are equal.



Rearrangement of Eq. (2.24) yields

$$\frac{k_1[E] S}{k_{-1} k_2} = ES \quad (2.25)$$

Where K_M is known as the Michaelis–Menten constant equal to $(k_{-1}+k_2)/k_1$ and Eq. (2.25) can be rewritten as

$$\frac{[E] S}{K_M} = ES \quad (2.26)$$

The concentration of enzyme in Eq. (2.26) refers to the unbound enzyme. The amount of free enzyme (E) and enzyme that is bound to the substrate (ES) varies over the course of a reaction, but the total amount of enzyme (E_0) is constant such that

$$E = E_0 - ES \quad (2.27)$$

Substituting into Eq. (2.26) yields

$$\frac{([E_0]-[ES]) S}{K_M} = ES \quad (2.28)$$

Which can be rearranged to yield

$$\frac{[E_0] S}{K_M + S} = ES \quad (2.29)$$

Thus, the overall rate of reaction (rate of formation of products) is given by the Michaelis-Menton equation:

$$v = \frac{dP}{dt} = -\frac{d[S]}{dt} = k_2[ES] = \frac{k_2[E_0] S}{K_M + S} \quad (2.30)$$

From above equation can be divided two cases as shown in Fig.2.8:

- (1) $[S] \gg K_M$, a maximum rate constant V_{max} reached and $V_{max} = k_2[E_0]$
- (2) $[S] \ll K_M$, $v \propto [S]$

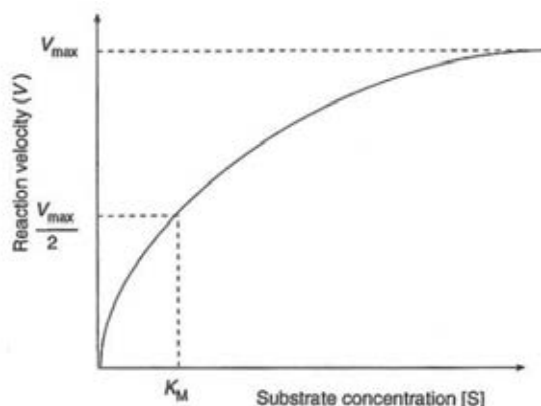


Fig. 2.8 Dependence of reaction rate on substrate concentration for an enzyme-catalyzed reaction at constant enzyme concentration (Eggs, 1999).

However, we can be estimated the Michaelis–Menten Parameters by graphical method. it is experimentally more convenient to plot the data in straight-line form which can be done by inverting the Michaelis-Menten equation:

$$\frac{1}{v} = \frac{K_M}{k_2[E_0]} \frac{1}{S} + \frac{1}{k_2[E_0]} \quad (2.31)$$

When $1/v$ is plotted against $1/[S]$, it will obtain a straight line with a slope of K_M/V_{max} and an intercept of $1/V_{max}$; hence, both K_M and V_{max} can be solved. This is called the *Lineweaver-Burk plot* as shown in Figure 2.12.

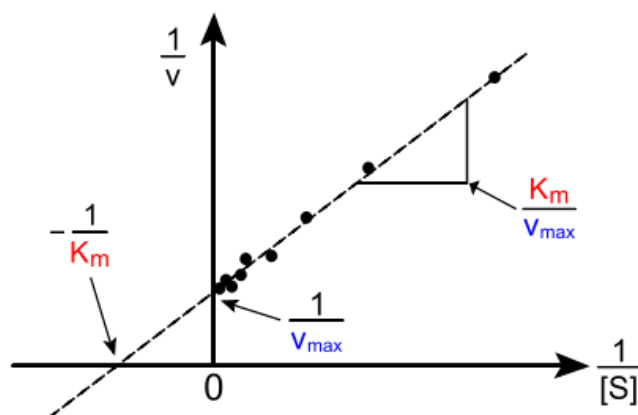


Fig. 2.9 The Lineweaver-Burk model (http://en.wikipedia.org/wiki/Enzyme_kinetics).

For this electrochemical experiment, the apparent Michaelis-Menten constants were generally used to evaluate the biological activity of immobilized enzyme and can be obtained from the electrochemical version of the Lineweaver-Burk equation:

$$\frac{1}{I_{SS}} - \frac{1}{I_{max}} = \frac{K_M^{app}}{I_{max}} \frac{1}{C} \quad (2.32)$$

Where I_{SS} is the steady state current after addition of substrate, I_{max} is the maximum current under saturated substrate condition and C is the bulk concentration of the substrate. The value of K_M^{app} and V_M^{app} can be calculated from the slope (K_M^{app}/I_{max}) and the intercept ($1/I_{max}$) for the plot of the reciprocals of the steady state current versus substrate concentration.

CHAPTER III

LITERATURE REVIEWS

An application of the enzyme based biosensors is beneficial for industrial, food and especially environmental fields. Biosensors can be used as tools to measure toxic compounds in solution. Many researches have continuously developed to overcome limited performance of biosensors through various methods and use of different materials. In this chapter, we express the importance of phenol detection including the fabrication of horseradish peroxidase (HRP) based biosensor, polypyrrole/HRP and gold nanoparticle/ polypyrrole/HRP.

3.1 Synthesis of polypyrrole (PPy) based HRP biosensor for modified electrode

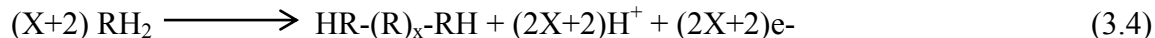
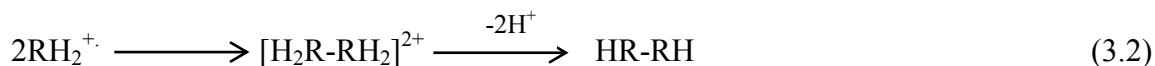
Polypyrrole (PPy) is a class of conducting polymers e.g. polypyrrole, polyaniline and polythiophene which are popularly used as the supporting matrix for enzyme immobilization and for the redox reactions to take place in biosensors (Ramanaviciene et al., 2006). It is one of the most promising supporting materials because of its ease of preparation, high conductivity, good stability in air and aqueous media, biocompatibility and biodegradation. In addition, PPy protects electrochemical biosensors from interferences (Vidal et al., 2003). It can be synthesized by chemical and electrochemical polymerization methods. The use of chemical polymerization is not as efficient when compared to electrochemical polymerization for deposition of PPy which is produced in the bulk solution, because it has a poor adherence to surface electrode. Moreover, a crucial obstacle of the deposition of this polymer is the solution containing non dissolved polymer because polypyrrole is insoluble in usual solvents. Therefore, these disadvantages might be avoided if electrochemical polymerization is applied.

3.1.1 Electropolymerization mechanism

Electrochemical polymerization approach is the most commonly used procedure to deposit conductive polymer since biomolecules can be added into the monomer solution for subsequent entrapment in a period of electrochemical oxidation process.

The polymer formation is carried out by controlled potential electrolysis of an aqueous solution containing monomers and biomolecules. The advantage of electrochemical polymerization is that films can be easily prepared in a one-step procedure and controlled thickness of the polymeric layer based on the measurement of the electrical charge passed during the electrochemical polymerization (Andreescu et al., 2005).

Electropolymerization procedure of pyrrole is similar to other conducting polymers. It composes of two reactions involving an electron transfer reaction with chemical reaction which can be best explained by reactions (3.9-3.12) (Waltman et al., 1986):



The first step (Eq.3.1) involves the transformation of pyrrole monomer, RH_2 , in the form of radical cation, $\text{RH}_2^{\cdot+}$, at the electrode surface. The second step (Eq.3.2) represents a dimerization reaction of two radical cations by deprotonation. As the dimer is more easily oxidized than the monomer, it is immediately reoxidized to form trimer (Eq.3.3) and continually formed become polymers which cover on an electrode surface. However, the polymerization reaction can be continued if only the potential used is high enough to oxidize monomer. An overall electropolymerization reaction is illustrated in (Eq.3.4).

3.1.2 Influence of variables on the characteristics of polypyrrole films

(i) Effects of an enzyme amount

ElKaoutit et al. (2009) introduced process of electro-immobilization of HRP onto PPy film by cyclic voltammetry in a potential from 0 to +1.0V. Morphology and characterization of film were investigated using atomic force microscopy (AFM).

Obviously, the presence of enzyme into the film affected the growth of PPy film that it keeps a similar ellipsoidal shape. Furthermore, the electropolymerization of HRP, onto this film, was made at a fixed potential, achieving different morphology characterized by high roughness, non-homogenous structure, and partial maintaining of the ellipsoidal particle in specific sites. This result proves the importance of the enzyme charge in the process.

(ii) *Effects of scan rate*

The scan rate is significant factor influencing the thickness and morphology of the PPy film. In the research of Shama et al. (2010) studied the synthesis and characterization of polypyrrole using cyclic voltammetry at different scan rates (5, 10, 25 and 50 mV/s). Shama's group observed that the film thickness is governed by the scan rates during electropolymerization. They found that the scan rate, 10 mV/s, was optimized and observed that the film thickness slightly decrease together with the increased scan rates. The slower scan rates gave the thicker film that provided better catalytic behavior than thinner film. Moreover, the scan rates gave the different surface morphology of film such as globular, growing buds, hook like and rod like structure that the SEM image confirm that the morphology depend on the scan rates.

(iii) *Effects of number of cycles*

The thickness of PPy film is related to the electropolymerization time scale, i.e. the number of cycles. Razola et al. (2002) found that the increased number of cycles the biosensor response gained higher up to a maximum response at three cycles and then the response decreased. Furthermore, Carquigny et al. (2008) varied the number of scans used for the electrochemical polymerization to determine the film thickness, indicate that polypyrrole film thicknesses increased linearly with the number of cycles.

3.1.3 Influence of operational parameters on biosensor responses

(i) *Effects of the enzyme concentration*

Razola and co-workers mentioned the amount of enzyme which is one of the critical parameters for the sensitivity, reproducibility and stability of the biosensor. Different concentrations of HRP in the polymerization solution were studied, namely, 0.10, 0.29, 0.48, 0.96 and 1.80 g/l. A HRP concentration of 0.48 g/l gave high response. Moreover, Tian et al. (2001) proposed the influence of enzyme concentration on the hydrogen peroxide biosensor. The use of composite solutions containing different HRP concentrations and a fixed pyrrole concentration (0.25M) for electropolymerization observed that the increasing of HRP concentration from 0.5 to 1.0 M, the sensitivity increased gradually. A rapid increment of sensitivity appeared in the range between 1.0 and 3.0 M. The biosensor exhibited an optimum response at 3.0-3.5 M HRP and then the sensitivity of the biosensor decreased slightly because the polymerization of pyrrole was hindered by HRP molecules when the HRP concentration increased. The HRP concentration, 3.0M, was selected for modified electrode to achieve the greatest sensitivity.

(ii) *Effects of pyrrole concentration*

Pyrrole concentration is an important factor affecting the growth of film. In the research of Yuan et al. (1999) referred an increased concentration of pyrrole resulted in an increased conductivity of polypyrrole film. While Li et al. (2007) proposed a disposable hydrogen peroxide amperometric biosensor. The screen-printed carbon electrodes, platinum disk and Ag/AgCl were used as working electrode, counter and reference electrodes, respectively. An enzyme electrode was fabricated by means of electrochemical polymerization which carried out potentiostatically at +1.0 V vs. Ag/AgCl to form polypyrrole together with HRP entrapped and then potassium ferrocyanide which served as electron mediator was coated onto modified screen-printed electrodes (SPE). They proposed that optimized pyrrole concentration, 0.075 M, should be high enough in order to form polymer and HRP entrapment. While Razola et al. (2002) synthesized the electropolymerization of pyrrole together with entrapped HRP

onto the platinum electrode which was previously coated by a polypyrrole layer. HRP was immobilized during electropolymerization of the monomers in lithium perchlorate (LiClO_4) using applied potential between 0.0 and +1.0 V versus Ag/AgCl at 10 mV/s. Razola and co-workers found that optimized pyrrole concentration, 0.05 M, gave the best response. They explain that lower monomer concentrations did not allow sufficient polymer formation and HRP entrapment onto the electrode surface while higher monomer concentrations generated polymer films which were not sensitive to H_2O_2 which is corresponding to Li's work (Li et al.,2007).

(iii) Effects of the electrolyte concentration

The electrolyte concentrations can be promoted the charge transfer in solution. The use of LiClO_4 is not only common supporting electrolyte for pyrrole polymerization but also no interfere with HRP activity. In the research Razola's group suggested that high response was observed at 0.1 M LiClO_4 . However, Li and co-workers utilized the LiClO_4 concentration of 0.075 M because its better catalyze effect.

(iv) Effects of the applied potential

Sulak et al. (2009) entrapped HRP with conducting polymers (PPy) through an electrochemically polymerization process onto a glassy carbon electrode previously covered with a mediator ,polyvinylferrocene (PVF) for phenol detection. This research reveals that the sensitivity response increases with the decreased potential and this low potential affected on the oxidation of some interference can be minimized. They explained that at higher values of negative potential, the enzyme molecules could be inactivated by the formation of PPy, decreasing the activity because the operational stability of HRP biosensor is greatly affected by the polarization potential. The potential was fixed at -0.2 V for the rest of the experiments since the current reached its highest value at this potential. The oxidation of some interference present in the real samples can be minimized due to the low potential.

(iii) Effects of the pH solution

The pH value of the buffer solution can be affected the enzyme activity and stability in aqueous media. Li and co-workers investigated the influence of various pH values between 5.0 and 9.0 and observed that at pH 7.0 PBS solutions obtained the maximum bioactivity and optimal sensitivity. However, Sulak and co-workers found that the pH at 6.8 of buffer solution was more optimized. Further this pH value referred previously as an optimum value for the activity of HRP in the decomposition reaction of phenol. This effect is similar to that reported in the literature for HRP biosensors.

3.2 Synthesis of gold nanoparticles based HRP biosensor

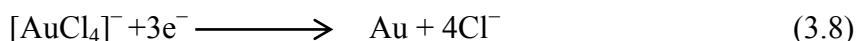
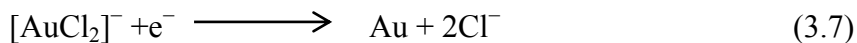
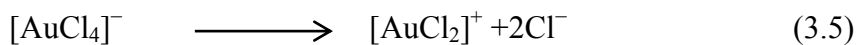
In recent years, nanomaterials i.e. carbon nanotubes, magnetic nanoparticles, quantum dots, silver and gold nanoparticles etc., have been utilized due to their unique physical and chemical characteristics such as the large surface-to-volume ratio and the increased effective surface (Miao et al., 2008). On the other hand, various methods have been applied for the immobilization of metal nanoparticles onto the surface of electrodes. Nanoparticles are dispersed onto the surface of electrodes by molecular self-assembly, covalent linking or being trapped into gel or polymer films.

In particular, gold nanoparticles (AuNPs), a well-known nanomaterial, is now being applied in analytical electrochemistry. The main advantages of gold nanoparticles provide a stable enzyme immobilization in order to retaining their bioactivity. Furthermore, gold nanoparticles allow direct electron transfer between redox enzyme and bulk electrode materials. Occasionally, the biosensor performed by utilizing non-mediator. Characteristics of gold nanoparticles such as high surface-to-volume ratio, high surface energy, ability to decrease enzyme–metal particles distance and quick electron transfer between redox enzyme and electrode surfaces (Pingarron et al., 2008). Many researches are widely used in modifying electrode i.e. Rai et al. (2005) discovered that the Au nanoparticle modified electrode could be used catalyze the oxygen reduction to hydrogen dioxide owing to the promotion of the electron transfer. Also, Majid et al. (2006) found that the deposition of Au nanoparticles onto the glassy carbon electrode (GCE) could greatly increase the sensitivity for detection of As (III). In this article, the synthesis of gold nanoparticles is very importance as well as the synthesis of polypyrrole. Gold nanoparticles can be synthesized both electrochemical and chemical methods.

3.2.1 Electrochemical method

The electrochemical technique was reported by Komsiyyska et al. (2008). They investigated the synthesis of Au nanoparticles onto GCE by electrodeposition including the mechanism involved formation and growth of them. The mechanism of formation of Au nanoparticles when the system has the $[\text{AuCl}_4^-]$ complex ions which are the active

gold species in the electrolyte solutions, was explained by reactions (Eq.3.5-3.8) (Komsiyiska et al.,2008):



This mechanism involves two charge transfer steps coupled with a chemical reaction. The first reaction (3.5) shows that tetrachloroaurate ions, $[\text{AuCl}_4]^-$, dissociate to $[\text{AuCl}_2]^+$ followed by the reduction of $[\text{AuCl}_2]^+$ at surface electrode to form $[\text{AuCl}_2]^-$. Then $[\text{AuCl}_2]^-$ receives one electron from the electrode to take place the nucleation of gold atoms. An overall deposition reaction is illustrated in the last reaction (3.8). Finally, gold atoms aggregate to form gold nanoparticles and grown up to become the bigger-sized gold nanoparticles.

3.2.2 Chemical method

However, gold nanoparticles are usually produced via chemical reduction methods, which often leads to colloidal gold and apply to modified biosensor. Gold colloids are prepared by chemical reduction of HAuCl_4 with the reducing agents which are reported in many literatures. For instance, Ishida et al. (2008) reported the use of NaBH_4 to reduce Au (III) towards a small Au^0 nanoparticles and prevent the aggregation of the small AuNPs. While sodium citrate served as reducing agent in the research of Nguyen et al. (2010) which focus on the citrate reduction of HAuCl_4 for synthesis of AuNPs to study the nucleation and growth of them. There are two steps for synthesis gold nanoparticles: (i) preparation of gold seed nanoparticles by citrate reduction reaction of HAuCl_4 ; (ii) the growth of AuNPs by seed-mediated method that gold precursors were used for seed particles. This experiment indicated that gold precursors are not only promote the nucleation of small particles but also decrease the average particle diameters. Sirajuddin et al. (2010) utilized hydroquinone as a reducing agent for a rapid synthesis of

gold nanoparticles through the addition of NaOH to a solution containing HAuCl₄ without the need for precursor seed particles. Moreover, the oxidized product of hydroquinone, benzoquinone, acts as a capping agent preventing nanoparticles aggregation.

Besides, Liu et al. (2002) synthesized AuNPs in form of a colloidal gold prior to immobilized HRP by electrochemical method to H₂O₂ detection without an electron mediator. The colloidal gold is used to retain the enzymatic activity and facilitate the direct electron transfer between HRP and electrode. In 2005, Liu and co-workers have reported colloidal gold sols used as the immobilization of enzymes and realized the role of nano-Au as an intermedator to retain the high bioactivity of HRP. HRP was entrapped a nano-Au monolayer which was supported by PAMAM dendrimer/cystamine modified gold electrode. While the apparent Michaelis-Menten constant (K_m^{app}) was evaluated to educated the affinity of enzyme and substrate. Yu et al. (2008) manipulated the adsorption of Au colloids onto Choline layer to immobilizing HRP because Au colloids increase the specific surface area and adsorb lots of enzymes including keep their bioactivities. While the Choline layer could not only fix Au colloids but also promote the direct electron transfer attributes to obtained with high selectivity and good stability. Gao et al. (2007) fabricated a hydrogen peroxide biosensor for the determination of H₂O₂. Firstly, the precursor film was electropolymerized on the glassy carbon electrode with p-aminobenzene sulfonic acid (p-ABSA) by cyclic voltammetry (CV). Then thionine (Thi) was adsorbed to the film to form a composite membrane, which yielded an interface containing amine groups to assemble gold nanoparticles (nano-Au) layer which prepared by gold colloid for immobilization of HRP. The performance factors of the resulting biosensor were studied such as the effect of pH, temperature. Besides this, the biosensor has a low determination limit, and wider response range. They observed that the peak currents increased when the nano-Au was immobilized onto the electrode. Obviously, the presence of nano-Au could promote the electron transfer. Wang et al. (2010) employed the integration of both gold nano-seeds (GNSs) and TiO₂, which provides a favorable microenvironment for the immobilized HRP. As a result, this biosensor demonstrated that

TiO₂ in the hybrid film could effectively prevent the aggregation of GNSs. They discovered that the nanocomposites exhibited advantages over TiO₂ and GNSs alone in fabricating biosensors. It means that nanoparticles based enzyme biosensors are drawback which one of the limitations is their rapid agglomeration and aggregation. For this reason, many efforts are focused on developing methods by conjugation of gold nanoparticles with other materials. In previous work, they can be incorporated in polymeric matrices to form nanocomposites with high particle distribution and high conductivity. In this case, the polymer serves as a matrix for the incorporation of NPs and for enzyme immobilization. Hence, the later article refers to the nanocomposites which combine nanoparticles and conducting polymer.

3.2.2.1 Influence of operational parameters on biosensor responses

(i) Effect of the volume of Au colloid solution

Liu et al. (2002) fabricated colloidal gold modified carbon paste electrode together with immobilized HRP to study the influence of Au colloid content for HRP-Au-CPE biosensor. They found that the current response increases gradually with increasing gold colloidal volume. This result indicated that the colloidal Au particles promote the electron transfer between HRP and electrode surface.

3.3 Synthesis of gold nanoparticles and polypyrrole composite

3.3.1 Electropolymerization method

The advantage of the electrochemical polymerization method is related to the better conducting properties and long-term stability of conductivities. Liu et al. (2006) used the electropolymerization of Py in solutions containing Au nanoparticles. First, they synthesized the Au nanoparticles of 2 nm in diameter in an aqueous solution by sonoelectrochemical technique and then Py monomers were added to prepare Au/PPy film on Au substrate. The prepared Au/PPy exhibits a morphology which is different from pure PPy and a rougher surface. While the conductivity of PPy is more increase 10 times. We can be clearly seen the advantage of electropolymerization technique when compares to other routes. However, Chen et al. (2007) have proposed the synthesis of Au nanoparticles by chemical technique in form of Au colloidal suspension in order to fabricated PPy/Au nanocomposite films. PPy/Au nanocomposite films were electrosynthesized on GCE by applying a constant current in solutions containing colloidal Au nanoparticles and Py monomer while the Au colloidal suspension prepared with chloroaurate acid using a citrate and tannic acid as reducing and protection agent, respectively. The incorporation of Au nanoparticles and PPy matrix resulted in a porous, leads to increase conductivity and better stability than only PPy alone that it was shown by scanning electron microscopy (SEM), transmission electron microscopy (TEM) and Raman spectroscopy.

To study the advantage of electropolymerization method, Wu et al. (2009) considered sol-gel compared with electropolymerization methods. Wu and co-workers synthesized Au nanoparticles though same method to obtain various sizes of Au nanoparticles by adjusting the molar ratio of sodium citrate which reduced Au^{3+} to Au^0 , to tetrachloroaurate acid. While prussian blue (PB) as the electron mediator, was pre-coated with Au nanoparticles onto surface electrode during enzyme immobilization. Electropolymerized conditions which used two scanning cycles from 0 to 1.0 V vs. Ag/AgCl with Au nanoparticles, Py and LiClO_4 solutions, gave the best performance.

The sensitivity of electropolymerization approach was much higher than others methods while the presence of PB can be reduced the operating potential from 0.7 to 0 V and avoided the interfering substances affecting noise elimination. As this research, we can be seen the useful of Au nanoparticles to amplify the output current and increase the sensitivity with itself special properties. Nevertheless, the research attempt to further study the electropolymerization method such as Chen and co-workers (2008) have studied the electrochemical deposition mechanisms of both PPy and PPy/Au composite films which relate to study the nucleation and growth of films by AFM. The Au nanoparticles were made from HAuCl_4 according to the previous reports incorporating into PPy by electropolymerization at constant potential of 1.1V in Py, Au nanoparticles and LiClO_4 . These results exhibited that PPy/Au nanocomposite films have faster reaction and growth rate than Py alone. Furthermore, another research mentioned the synthesis of PPy together with HAuCl_4 (Au^{3+}) by electropolymerization and electrodeposition method. By using Au (III) for the synthesized PPy/Au nanocomposite film has different from other works which have been more used Au nanoparticles. Qu et al. (2009) offered the synthesis of PPy- HAuCl_4 composite film by electropolymerization in solutions containing HAuCl_4 , Py and Na_2SO_4 using the potential between 0 and 0.8V at 50 mV/s for 5-10 cycles. After that, Au nanoparticles were generated by a negative voltage electrodeposition in PBS for 3-5 min to immobilized antibodies. The presence of AuNPs in PPy film enhances the immobilization of antibody and higher sensitivity. Even through, the several literatures employed HAuCl_4 as source of gold ions but can be used other source such as $\text{KAu}(\text{CN})_2$ in Rapecki's work. Rapecki et al. (2010) have prepared PPy/Au nanoparticles composites which synthesized through pulse deposition in solutions containing Py as monomer, $\text{KAu}(\text{CN})_2$ as source of gold ions, NaClO_4 as supporting electrolyte and KCN as stabilizer. They found that the oxidation of Py and reduction of gold (I) complex occur in same solution. Although the solution of gold-cyanide complexes used for this literature is neutral solution which distinguishes from the previous work using acidic solution. The potential ranges of gold deposition and PPy formation were determined by CV. The optimized potential for the electrodeposition of

PPy and Au nanoparticles applied a sequence potential of 0.75 and -1.6V. This method gives the layer smoothness and homogenous distribution of Au nanoparticles.

With the requirement of chemical compounds detection, the presence of enzyme is essential to biosensor because it contributes to the oxidation or reduction with the measured compounds at the surface electrode in order to provide biosensor response. In our laboratory will be concentrated on the fabrication of Au/PPy composite based HRP biosensor. In earlier reports, most researchers have tried to fabricate the nanocomposites of Au nanoparticles and PPy including with enzyme immobilization onto electrode surface by different methods. For instance, Liu et al. (2007) focused on electrochemical study on effect of colloidal Au on HRP in PPy layer at pre-coating electrode with Prussian blue. Colloidal Au was prepared according to the earlier reports where it was made from the solutions containing HAuCl_4 and sodium citrate. The prepared Colloidal Au solution was wine-red color. While electrode was modified with PB and then PPy/HRP was immobilized on the modified electrode using potential cycling between -0.2 V and 0.9 V in KCl solution. Subsequently, the Au Colloid was chemically deposited onto PB/PPy/HRP electrode. Earlier another work, Yusaran (2009) reported the immobilization of horseradish peroxidase onto modified glassy carbon electrodes through gold and polypyrrole to monitor phenol. In his study, the experiment was divided into two parts. First part, he synthesized the Au nanoparticles by electrodeposited onto GCE in the solutions containing $\text{HAuCl}_4 \cdot 3\text{H}_2\text{O}$ and KNO_3 which used to applied potential at -0.2V. Second part, the electropolymerization technique was utilized in the synthesized PPy/HRP onto AuNPs/GCE using potential between 0 to 1.0V at scan rate 10 mV/s. Additionally, this synthesized biosensor was interested in an effective surface area including diameter and height of rod-like nanoparticle. He also reported an excellent sensor for phenol detection had a sensitivity of 7.277 nA/ μM , a wide linear range from 3.0×10^{-5} - 2.1×10^{-4} M and fast response time (50 s) Moreover, he found that detection limit of 2.54×10^{-5} M and retained 68.34% of the initial response after three days. However, this work has the drawbacks of high detection limit and low stability. The high detection limit is a hindrance for measurement of phenol at low concentration. In

addition, low stability show that enzyme may be leached out or denatured when it was stored in several days.

3.3.2 Influence of operational parameters on morphology of film

(i) Effects of pyrrole concentration

The thickness of film influenced on the current response of enzyme biosensor. As we known, the thickness of PPy film depended on pyrrole concentration and the amount of charge passed the solution to working electrode. Li et al. (2007) discovered that the current response increased along with the nanowires thickness increased from 0 to 60 nm, and then decreased afterward. They suggested that the enhancement of the PPy nanowires thickness tend to aggregate into larger gold nanoparticles. In addition, the thick film prevented the electron transfer between substrate and electrode.

(ii) Effects of the scan rates

Qu et al. (2009) concentrated on the influence of cycling duration or scan rate on the size and distribution of AuNPs in PPy/AuNPs film. Three scan rates (25, 50, 100 mV/s) was studied and found that the size and distribution of AuNPs did not change with scan rate. However, the scan rate only affects the morphology of PPy film. The use of gold nanoparticles in PPy film enlarges effective surface area of the polymeric film. It also allows the enzyme to be more strongly adsorbed in large area with retained enzyme activity compared to the metal surface and PPy film. The electrochemically synthesized PPy/ AuNPs composite film has a rough surface with many gaps and more space which can be provided for entrapped enzyme molecules.

(iii) Effects of applied potential

Moreover, Qu's group studied the cycling potential of the constructed film. The result exhibited that the PPy showed a more roughness when cycling potential increase but not affected the size and distribution of AuNPs.

3.3.3 Influence of operational parameters on biosensor responses

(i) Effects of gold nanoparticles volume and gold concentration

Gold nanoparticles can largely enhance the rates of catalytic reaction as well as the electron transfer rate. In this research of Wu et al. (2009) have studied the effect of gold nanoparticles on sensitivity. Wu and co-workers have co-immobilized Au nanoparticles onto the electrode surface along with enzymes by electropolymerization methods. They found that the sensitivity increase initially but decreased when the added volume exceeded a certain value. They explained this phenomenon through two reasons. First, the increasing of an amount of gold nanoparticles contributed to expel the enzymes which resulted in poor sensitivity. Second, the ease of aggregation of the gold nanoparticles as the amount of gold nanoparticles increased, especially when all the particles were confined to the electrode surface which caused to decrease the catalyzing ability of gold nanoparticles. As this research, we can be seen the useful of Au nanoparticles to amplify the output current and increase the sensitivity with itself special properties. Furthermore, Yusaran (2009) and other reports exhibited that high HAuCl_4 concentration gave an increasing number and size.

(ii) *Effect of Pyrrole concentration*

Monomer concentration is an important factor affecting the growth of film. Yusaran (2009) found that optimized pyrrole concentration, 0.09M, gave the best response. When low concentration receives film which is a small nanoparticles onto electrode surface opposite to high concentration gave a rod-like particles. With a rod-like nanoparticles led to increase surface area affecting the directly sensitivity. Besides, lower monomer concentrations did not allow sufficient polymer formation and HRP entrapment while higher concentration gave film thickness resulting in the diffusion of substrate to electrode surface. it means that film thickness hinders the electron transfer.

(iii) *Effect of Scan rates*

The influence of the scan rate was studied by Liu et al. (2007). They have studied the effect of seven scan rates: 50, 45, 40, 35, 30, 25 and 20 mV/s. They found that peak current vary linearly with the scan rates and the highest scan rates showed a high signal.

(iv) *Effect of Number of cycles*

Number of cycles influences the film thickness because of the increasing electropolymerization time and very thick film. Yusaran (2009) discovered the optimized Number of cycles (10 cycles) gave a maximum response.

(v) *Effect of pH buffer solution*

pH value of the buffer solution can affect the activity of enzyme and stability in aqueous media. The effect of pH was investigated by Liu et al. (2007). They detected H₂O₂ in PBS at different pH values between 4.5 and 9.2. At optimized pH 6.2 showed the highest current response which is very close to the optimum enzymatic activity.

In this work, the gold nanoparticles/polypyrrole/HRP biosensor for the detection of phenol was reinvestigated. The procedure of synthesized AuNPs/PPy/HRP nanocomposites film was prepared two steps. The Au colloid solution was firstly prepared by chemical method using sodium citrate as a reducing agent. The AuNPs/PPy/HRP biosensors are fabricated with electropolymerization technique. Additionally, the response and performance biosensor was examined by operational parameters such as gold concentration, enzyme concentration etc. Moreover, the kinetic parameters and other parameters i.e. the detection limit, storage stability etc., will be studied for the measurement of phenol in solution.

CHAPTER IV

MATERIALS AND METHODS

4.1 Materials

1. Hydrogen tetrachloroaurate (III) ($\text{HAuCl}_4 \cdot 3\text{H}_2\text{O}$), available from Sigma–Aldrich, USA.
 2. Sodium citrate dehydrate ($\text{Na}_3\text{C}_6\text{H}_5\text{O}_7 \cdot 2\text{H}_2\text{O}$), available from RFCL limited, India.
 3. Disodium hydrogen orthophosphate (Na_2HPO_4), available from Fisher Scientific.
 4. Horseradish peroxidase (131 U/mg HRP, EC 1.11.1.7), available from Toyobo, Japan.
 5. Hydrogen peroxide (30% H_2O_2), available from E.Merck, Darmstadt.
 6. Phenol ($\text{C}_6\text{H}_5\text{OH}$), available from Carlo Erba Regent Co.
 7. Pyrrole (98% $\text{C}_4\text{H}_5\text{N}$), available from SIGMA-ALDRICH, Steinheim, Germany.
 8. Sodium chloride (NaCl), available from Asia Pacific Spacialty Chemical limited, Australia.
 9. Sodium dihydrogen orthophosphate (NaH_2PO_4), available from Fisher Scientific
- * All chemicals were of used analytical grade and without further purification.

4.2 Apparatus

Electrochemical measurements of cyclic voltammetry and amperometry was performed with an Autolab potentiostat (Metrohm, model PGSTAT101) with nova software version 1.5. The electrochemical cell consisted of a three-electrode system with a screen-printed carbon (SPE) working electrode, a platinum wire counter electrode, and a silver/silver chloride (Ag/AgCl) reference electrode.

4.3 Preparation of Gold nanoparticles colloidal solution

Gold nanoparticles (AuNPs) were prepared through the reduction of 1.0 mM HAuCl_4 using sodium citrate as a reducing agent. A 1 mM aqueous solution of HAuCl_4 was prepared by dissolving 0.012 g of $\text{HAuCl}_4 \cdot 3\text{H}_2\text{O}$ in 30 mL of de-ionised water, and

solution of sodium citrate dehydrate ($\text{Na}_3\text{C}_6\text{H}_5\text{O}_7 \cdot 2\text{H}_2\text{O}$) by dissolving 0.1 g in 10 mL deionised water. An amount of 20 ml of the HAuCl_4 solution was put in a 50 ml beaker equipped with a magnetic bar. The solution was heated to boiling point and then 2 ml of 1% by volume of citrate solution was added (Au:citrate molar ratio 1:34 mM) under stirring. The yellow color of the solution originating from hydrogen tetrachloroaurate first turns colorless. The solution remains clear for about 10 sec and then turns grayish-blue. After about 1 min a deep wine-red sol was obtained. No further change of color upon prolonged boiling will be observed. Deionised water is added dropwise to keep the volume at 22 ml. The solution was then cooled to room temperature. The prepared solution was kept in a brown bottle under 4°C until used (Mailu et al., 2010).

4.4 Electropolymerization of the AuNPs/Pyrrole/HRP modified electrode

The gold colloid, pyrrole and HRP were electropolymerized and coated onto the surface of a screen-printed carbon electrode using cyclic voltammetry. The polymerization medium contained 5 ml 0.1M PBS solution (pH 7.4) containing 0.09 M pyrrole, 1×10^{-3} M gold colloid solution and HRP. The medium was purged with N_2 for 10 minutes. Electrochemical polymerization was carried out in potential cycling between 0.0 and +1.0V vs. Ag/AgCl with scan rate 10 mV/s for 10 cycles. The fabricated electrode was washed in double-distilled water to remove the unfixed enzyme and then was dried at room temperature inside 5 minutes before tested.

4.5 Electropolymerization of the Pyrrole/HRP modified electrode

The pyrrole and HRP were electropolymerized and coated onto the surface of a screen-printed carbon electrode using cyclic voltammetry. The polymerization medium contained 5 ml 0.1M PBS solution (pH 7.4) containing 0.09 M pyrrole, 1×10^{-3} M gold colloid solution and HRP. The medium was purged with N_2 for 10 minutes. Electrochemical polymerization was carried out in potential cycling between 0.0 and +1.0V vs. Ag/AgCl with scan rate 10 mV/s for 10 cycles. The fabricated electrode was washed in double-distilled water to remove the unfixed enzyme and then was dried at room temperature inside 5 minutes before tested.

4.6 Electrochemical analysis

4.6.1 Cyclic voltammetry

The cyclic voltammogram response was studied the effect of scan rate on the response of immobilized enzyme and electron transfer rate. The modified electrode was measured in an unstirred solution by cyclic voltammetry between -1.2 to 0.6 V at 25°C in pH 7.4 0.1M PBS at scan rate in the range of 0.1, 0.2, 0.3, 0.4, and 0.5V/s.

4.6.2 Amperometry

The amperometric response of AuNPs/PPy/HRP bionanocomposite film modified screen-printed carbon electrode to phenol was measured at a fixed potential (-0.05 V). The solution of 50 μ M H₂O₂/ 50 μ M phenol in PBS (pH 7.4) was used as a substrate solution. However, this solution should be separately prepared which the solution of H₂O₂ in PBS must be prepared for day by day while the solution of phenol in PBS can be prepared like a stock solution and stored at 4°C prior to use. Before the measurement these solutions was mixed at required. Added H₂O₂ until steady state before added phenol

4.7 Material characterization

4.7.1 UV-Visible spectroscopy (UV-2450, Shimadzu, Japan) was utilized to study the conformation of HRP enzyme. While AuNPs/Py/HRP, HRP, AuNPs/Py, Py in 0.1M PBS (pH 7.4) were tested in wavelength range between 300 and 800 nm.

4.7.2 SEM-EDX (S3400N, Hitachi, Japan) was employed to investigate electrode surfaces and distribution of AuNPs in the nanocomposite film. The accelerating voltage and magnification for all images were 15 kV and 20k \times , respectively.

CHAPTER V

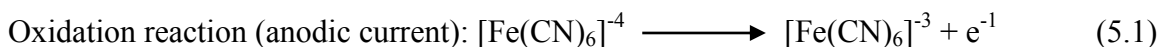
RESULTS AND DISCUSSION

This research studied the fabrication of AuNPs/PPy modified screen-printed carbon electrode for HRP based biosensors by an electropolymerization technique for phenol detection. The optimum electropolymerization conditions for fabrication of AuNPs/PPy/SPEs were firstly developed and investigated by film characterization. Next, AuNPs/PPy/HRP/SPEs were employed for the study of electrochemical behavior and performance factors in order to evaluate sensitivity, linear range, detection limit, stability, and reproducibility of this phenol biosensor.

5.1 Electropolymerization conditions for AuNPs/PPy modified SPEs

SPEs were modified with polypyrrole (PPy) which served as supporting matrix. This matrix confined enzyme and AuNPs on the electrode surface. The electrochemical formation of PPy from aqueous solution was explained in section 3.1. The oxidation of monomer in solution formed a cation radical which then reacted with another radical to form a dimer. Afterward, the propagation of dimer to oligomers continued until they generated an insoluble oligomer. The insoluble oligomer interacted with the electrode forming a polymeric film which might grow even further by incorporation of monomers in the medium. During the growth step of the polymer film, AuNPs were entrapped forming AuNPs/PPy nanocomposite film.

Before examining suitable electropolymerization conditions for biosensor fabrication, determination of suitable applied voltage for $[\text{Fe}(\text{CN})_6]^{4-}/[\text{Fe}(\text{CN})_6]^{3-}$ reaction using CV was primarily carried out in solutions containing 10 mM $\text{K}_4\text{Fe}(\text{CN})_6/$ 1mM KCl between -0.6 and 1.2V at a scan rate of 100 mV/s using a bare SPE as shown in Fig.5.1. The obtained CV was a sigmoid shape which showed characteristics of a redox reaction as shown in equations 5.1-5.2. The applied voltage at 0.58V was chosen for further amperometric studies.



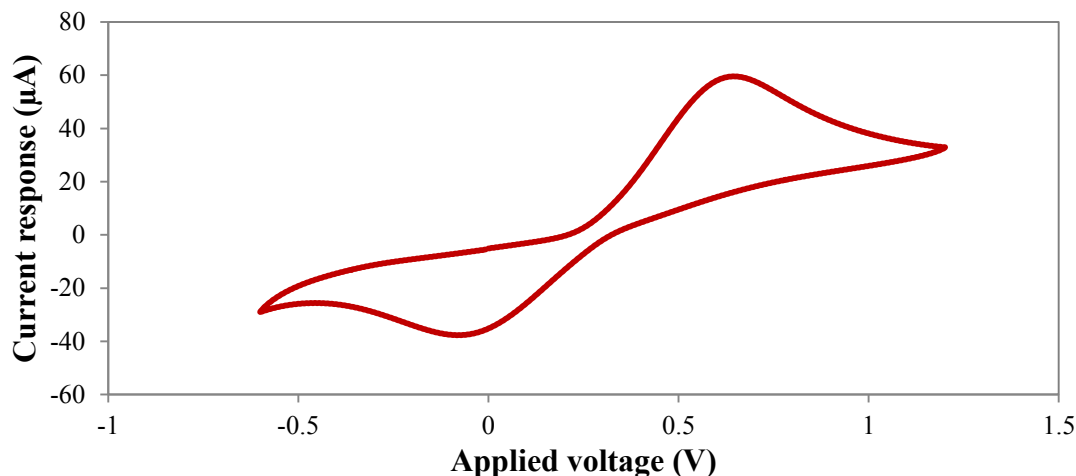


Fig. 5.1 Cyclic voltammogram of a bare SPE in a solution containing 10 mM $K_4Fe(CN)_6$ /1mM KCl between -0.6 and 1.2V at a scan rate of 100 mV/s.

1) Effects of Au precursor concentration

The synthesis of AuNPs employed an Au precursor and a suitable reducing agent which binds to AuNPs surface and helps generating high stability of colloid solution. The advantages of AuNPs are their controllable size and shape which can be experimentally adjusted using different preparation conditions. Most literature reviews concentrated on the duty of AuNPs in the direct electron transfer from redox-protein to the electrode surface without the need of additional mediators (Liu et al., 2003). Many researchers attempted to study effects of Au precursor amount after enzyme immobilization. For instance, Liu's work (Liu et al., 2002) fabricated the Au/HRP/CPE by Au colloid (Au^{3+}) content mixed with carbon powder. They found that the current gradually increased with increasing volume of Au colloid solution. However, the decreasing of current appeared at high Au colloid volume due to the increasing of resistance and double-layer capacitance of electrode surface because of the decreasing of carbon sensing sites ratio in the paste. These results are corresponded to German's group (German et al., 2010) who discovered that high concentrations of Au colloid solution gave less efficient electron transfer than at low concentrations.

However, in this part we focused on the existence of AuNPs without enzyme to study effects of Au precursor concentration and the important role of AuNPs in the $\text{Fe}^{3+}/\text{Fe}^{4+}$ reaction. AuNPs/PPy/SPEs were studied under various Au precursor (HAuCl_4) concentrations. The HAuCl_4 concentration was a key factor influencing current responses because AuNPs enhanced the electron transfer rate (Liu et al., 2003). As shown in Fig 5.2, these results exhibit that the current response increases gradually with increasing concentrations of HAuCl_4 (Au^{3+}) between 1 to 5 mM in all electropolymerization cycles, because the higher Au^{3+} concentration generated more AuNPs which promoted electron transfer. At Au^{3+} concentrations higher than 5 mM, the results were opposite. This was probably caused by the aggregation and flocculation of the formed AuNPs at high Au precursor concentrations. Therefore, the optimized Au^{3+} concentration was determined at 5 mM. Moreover, the small spherical size of AuNPs that prepared according to Turkevitch (Turkevitch et al., 1951) method with the diameter size of 15 ± 5.0 nm was obtained. It was evidenced that the AuNPs were of negative charged due to the citrate absorption during the preparation process (Liu et al., 2007). AuNPs helped facilitating electron transfer due to AuNPs played as conducting tunnel pathway of electrons between substrate as a redox couple and the electrode surface.

2) Effects of cycling number of the electropolymerization

PPy film was suitable host matrix allowing an electronic charge flowed through the polymer matrix. They provided the low resistance, and enhanced the conductivity because of their conjugated structure. Electropolymerization method was used in this study because the polymer thickness could be easily controlled, and successive polymeric layer could be generated. The generation of film layer might lead to incorporated AuNPs in the polymeric structure. This was designed to avoid AuNPs leaking out from SPE surface. The film thickness was directly affected by electropolymerization cycles because the increasing cycling number resulted in a longer time period for electropolymerization. The biosensor responses for four different electropolymerization cycles were checked by amperometry of ferri/ferrocyanide and KCl at 0.58V versus Ag/AgCl which is shown in

Fig.5.2. The results indicated that the best biosensor response was obtained with 10 cycles which dramatically increased current responses about 64.19%, 61.28%, 75.06% when compared to 5, 15 and, 20 cycles, respectively at optimized value of Au precursor concentration. At less electropolymerization cycles than 10 gave a low current response because the film thickness did not proper to adequate incorporation of AuNPs. According to the constructing of Au/PPy nanowire/GCE (Li and Lin., 2007) described that the changing of cycle number also plays an important role in an entrapment of AuNPs in polymer film. Above 10 cycles, a current dramatically diminished owing to the increasing thickness of the polymer that hindered diffusion of the substrate and electron transfer which is corresponding to the report of Pereira's work which suggested that the thin film was not proper for immobilization of reagents while thick film provoked diffusion limitations of substrate (Pereira et al., 2000; Razola et al., 2002). Behavior of other conducting polymer films is similar to PPy film namely the increasing of electropolymerization cycles increases thickness of the formed polymer film affecting an increasing biosensor response. Nevertheless, the thick film showed the poor conductivity and also reduced ability of electron transport due to it allowed the few substrates accessible to the interface of electrode (Luo et al., 2006). Moreover, the increasing of electropolymerization cycles could increasingly entrap the amount of enzyme. However, high enzyme loading might appear the poor adhesion and poor PPy polymerization yield since enzyme molecules hindered the polymerization process causing the decreasing of current (Tian et al., 2001; Razola et al., 2002). The optimize electropolymerization conditions are summarized in Table 5.1.

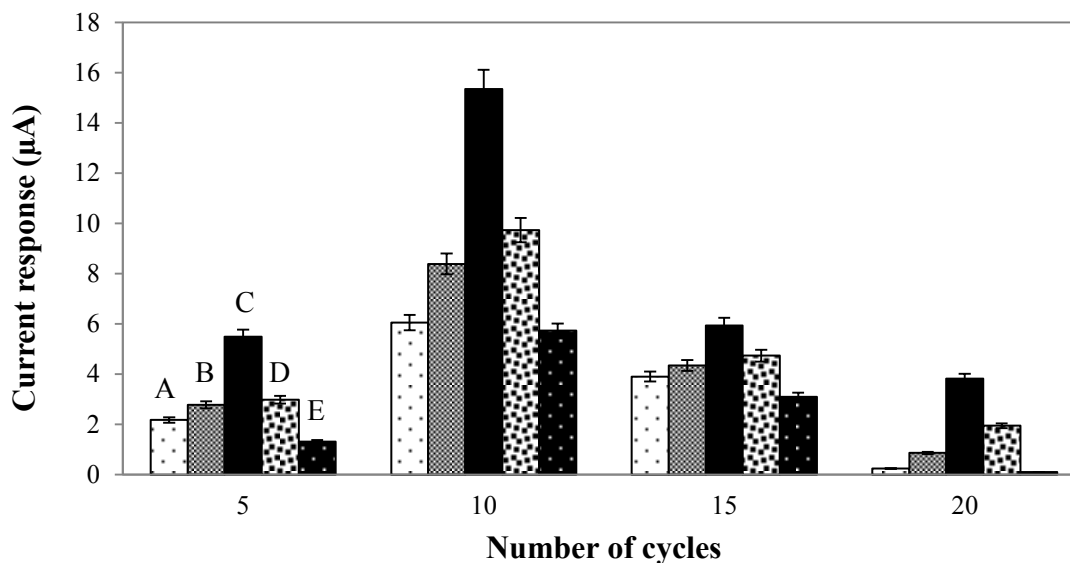


Fig. 5.2 Effects of Au precursor concentration and cycling number of the electropolymerization on current responses of AuNPs/PPy modified SPEs in solutions containing 10 mM $K_4Fe(CN)_6$ / 1 mM KCl at 0.58V (Symbol of A, B, C, D, E represent the concentrations of Au^{3+} at 1, 3, 5, 7, 9 mM, respectively).

Table 5.1 Optimum conditions for fabrication of AuNPs/PPY/HRP/SPE.

Conditions	Optimum values
Au precursor concentration	5 mM
Electropolymerization cycle	10 cycles

5.2 Physical and chemical characterization of bare and modified screen-printed electrodes

In order to deeper understand electrochemical behavior of modified electrodes, the fabricated AuNPs/PPy nanocomposites under optimum electropolymerization conditions were characterized both chemically and physically using UV-Visible spectroscopy, Transmission electron microscopy (TEM), Scanning electron microscope (SEM) and Atomic force microscopy (AFM), and Energy-dispersive X-ray spectroscopy (EDX).

5.2.1 Structural Characterization of AuNPs/Py/HRP by UV-Visible spectroscopy

UV-Vis absorption bands were used as an effective tool to study the denaturation of heme proteins. Fig.5.3 shows UV-Vis absorption spectra of pyrrole (Py), AuNPs/Py, HRP, AuNPs/Py/HRP in solutions. No characteristic absorption bands of Py are observed in a wavelength range between 300 and 800 nm while an absorption band of AuNPs is discovered at 539 nm. Furthermore, an absorption band of free HRP in PBS (pH 7.4) are observed at 402 nm which is close to the reported value by Chen et al. (2011) and Fang et al. (2011). In case of HRP in AuNPs/Py solution, the result does not show the change of absorption peak when compared to that of free enzyme. This result illustrated that the appearance of AuNPs and Py in buffer solution did not affect the structure of HRP molecules. However, the absorption peak of AuNPs/Py/HRP is still observed at 402 nm, but more increase than HRP solution due to the electrostatic interaction between HRP and AuNPs/Py (Yin et al., 2009). All results of UV-Vis absorption bands revealed that HRP retained its native structure in solutions of AuNPs/Py. Thus, AuNPs/Py should be a suitable solution for constructing AuNPs/PPy/HRP/SPE for phenol biosensor.

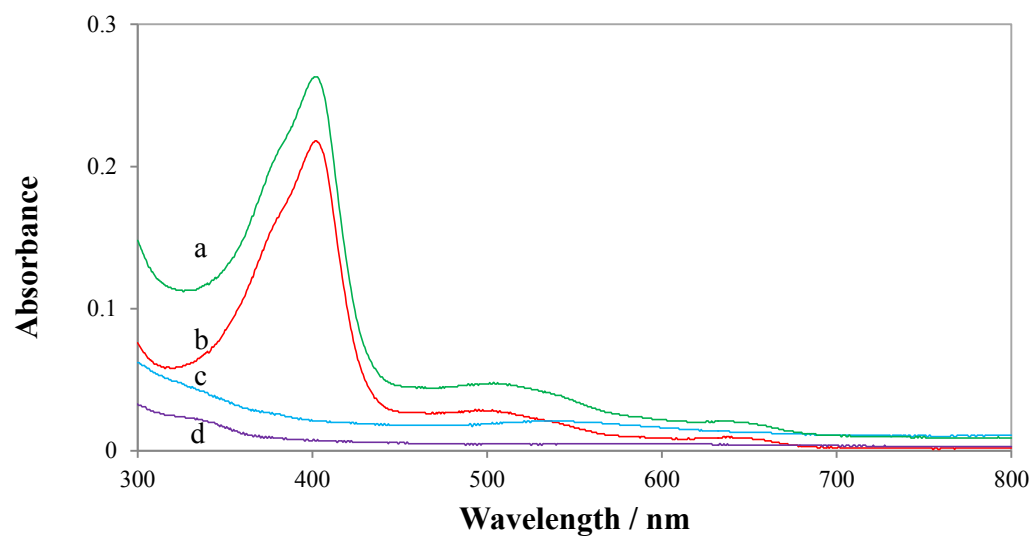
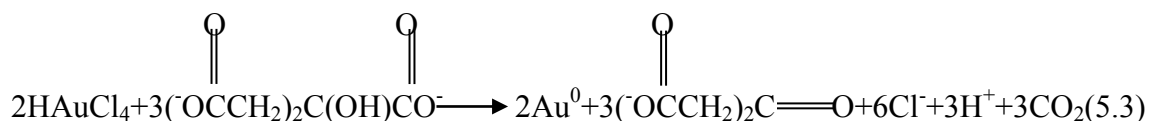


Fig. 5.3 UV-Visible absorption bands for a) AuNPs/Py/HRP, b) HRP, c) AuNPs/Py, d) Py in PBS (pH 7.4) in a wavelength range between 300 and 800 nm.

5.2.2 Characterization of AuNPs by TEM

The synthesis of AuNPs via reduction method was discovered by Turkevich in 1951. This method has been popularly used due to its simplicity, and ability to control sizes and shapes of AuNPs. The formation of AuNPs could be explained through chemical process with two steps composed of nucleation and growth of Au⁰ which depend on chemical concentration, pH, temperature, etc. Tetrachloroauric acid (HAuCl₄·3H₂O), an Au precursor, was reduced with trisodium citrate (C₆H₅O₇Na₃) which acted as both the reducing and stabilizing agents. The mechanism of nucleation was proposed by Kumar et al (2006) as shown in Eq.(5.3):



The overall stoichiometry needs three citrate molecules to reduce two Au precursor molecules which in this work we used Au:Citrate molar ratio of 1:3.8. Thus we assumed that the reaction was completed and HAuCl₄ was the limiting reagent. The above equation shows that Au precursor is reduced by citrate to form Gold atoms (Au⁰) in solution. These atoms adsorb Au⁺ to form larger aggregates of gold atoms until a nucleus is formed (German et al., 2011). The gold atoms are absorbed by the particle resulting in the growth of AuNPs.

Obviously, the initial color of HAuCl₄ was yellow then it changed from yellow to colorless, dark, and wine red, respectively after addition of citrate under the boil. However, the increased HAuCl₄ concentration affected the color change of Au colloid. It can be seen in Fig.5.4 that AuNPs achieved were relatively homogeneous in size and were of spherical shape. The average diameter of AuNPs determined by TEM was about 15±5 nm with an absorption band at 539 nm. It was similar to a mean diameter of 13±4 nm with an absorption maximum at 521.5±0.5 nm reported by Gross (Gross et al., 2008). Moreover, the citrate reduction method gave a negative surface charge which AuNPs were capped by citrate molecules as a weak base. The synthesized AuNPs in the form of

colloidal solution was then added into PBS (pH 7.4) causing the solution pH to change to pH 7.26 which was slightly higher than the isoelectric point of HRP (7.2)(Xialing and Lin, 2009). These reasons indicated that an enzyme carried a slight negative charge which could be weakly repulsed to citrate capped AuNPs.

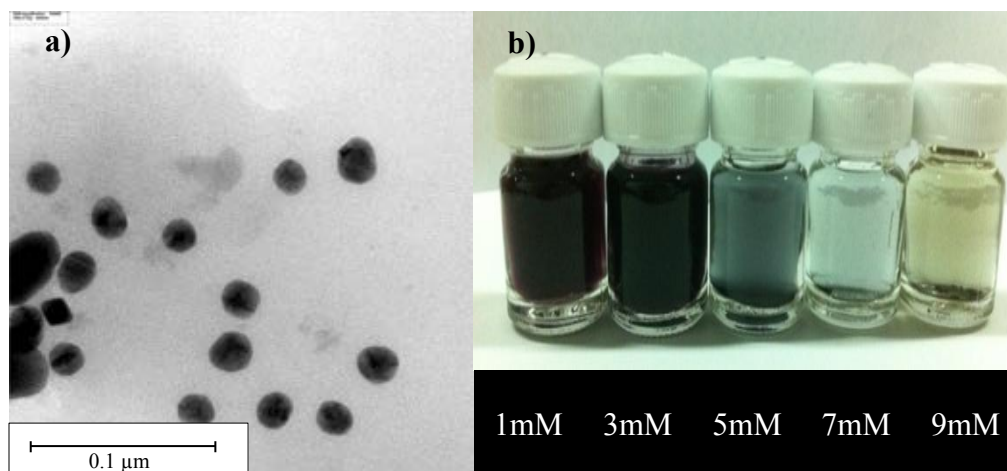


Fig. 5.4 a) TEM image of AuNPs, and b) the colors of colloidal AuNPs under various concentrations of HAuCl₄.

5.2.3 Surface characterization of various electrodes

Surfaces of bare and variously modified electrodes were characterized by SEM. Fig.5.5 (a) shows a rough typical surface of SPE. Fig.5.5 (b) shows that the growth of PPy on a bare SPE resulted in more compacted granular and some rod-like structure of PPy on SPE surfaces indicating a complete or near complete coverage of PPy on SPE. Furthermore, Fig.5.5 (c) implied that the existence of AuNPs in PPy film gave more granular like surface in comparison to AuNPs-free PPy film. However, the inclusion of HRP in the composite film as shown in Fig.5.5 (d) did not seem to change the electrode surface characteristics.

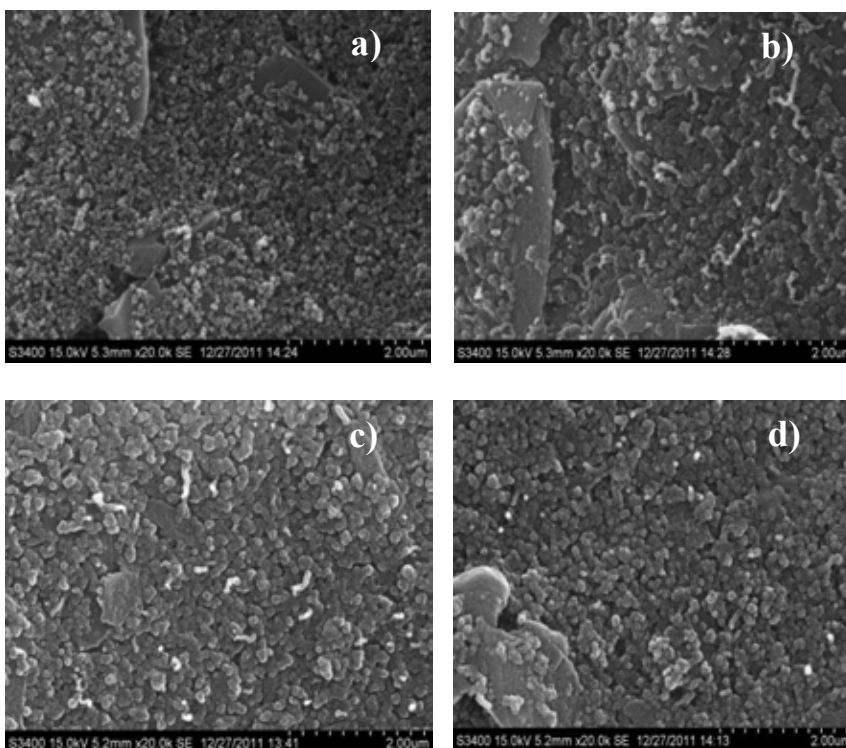


Fig. 5.5 SEM images of screen-printed electrodes: a) bare SPE, b) PPy-modified, c) AuNPs/PPy- modified, d) AuNPs/PPy/HRP-modified SPEs, respectively. The accelerating voltage and magnification for all images were 15 kV and 20k \times , respectively.

From the SEM results, we concluded that HRP did not affect the film features. Therefore, HRP needed not be included in an AFM analysis. Fig. 5.6 shows the AFM

images of AuNPs/PPy/SPE with two different electropolymerization cycles under fixed electropolymerization conditions. The AFM images demonstrate the surface roughness by two and three-dimensions of two samples. The minimum and maximum electropolymerization cycles were selected in the comparison namely 5, and 20 cycles. Fig.5.7 (a) shows AFM images in 2-D and 3-D of the 5-cycle sample. The AuNPs were observed to be uniformly distributed throughout the electrode surface without clusters or agglomerates. Fig. 5.7 (b) shows that the 20-cycle sample was rougher than the 5-cycle sample because the electropolymerization cycle increased which caused the growth of film and surface roughness.

The surface roughness is expressed as a root-mean-square (RMS) roughness value and can be obtained from the AFM measurement. In general, this value depends on the size and height variation of area. The measured RMS roughnesses of 5- and 20- cycle samples were 245.69 and 619.74 nm, respectively for the AuNPs/PPy/SPE in $5 \times 5 \mu\text{m}^2$ of the measured area. An increasing in electropolymerization cycle number led to an increased roughness.

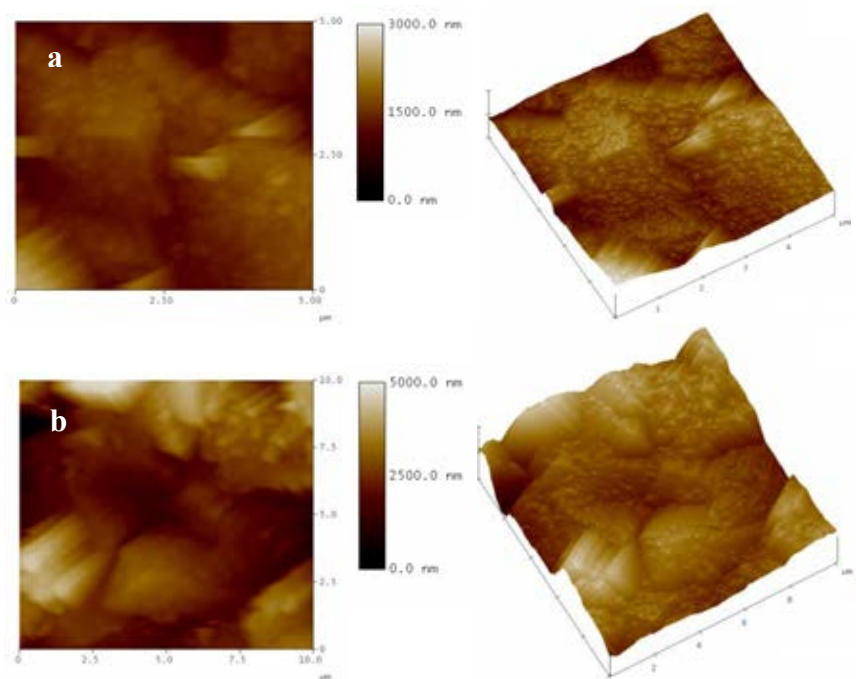


Fig. 5.6 AFM images of AuNPs/PPy/SPEs at 5 mM of Au^{3+} concentration a) 5 cycles, and b) 20 cycles of electropolymerization, respectively.

The investigation of AuNPs/PPy modified electrode of this work was similar to the previous work of Yusran's (2009) under the same electropolymerization conditions which were 0.09M pyrrole concentration, 250 unit/ml of HRP, a scan rate at 10 mV/s, 10 electropolymerization cycles, and applied potential range of 0.0-1.0V. However, this work chose different electrode type from Yusran's work which used a glassy carbon electrode. SEM and TEM images of his showed a rod-like structure of the formation of PPy on GCE surface. While this work used screen-printed carbon electrode as a working electrode because it is cheap, easy to prepare, convenient to used, and disposable. Film characterization of our work differs from his work in view of the obtained film feature. Different surface was postulated to be due to the different electrode type. Our work obtained more compacted granular and some rod-like structure of PPy on SPE surfaces which had a rough surface. These results confirmed that the formation of PPy film on different electrode types gave the distinguish film feature.

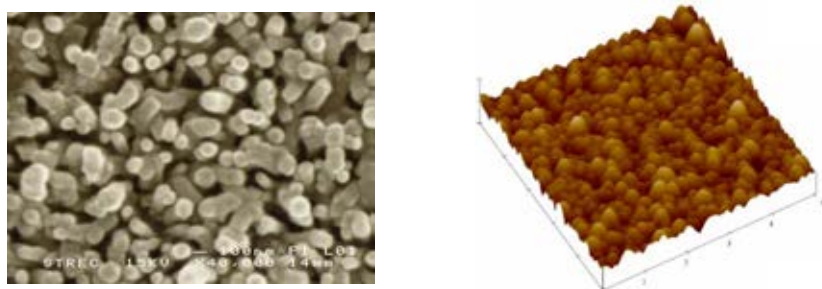


Fig. 5.7 SEM and AFM images of AuNPs/PPY/HRP/GCEs under same conditions (Yusran, 2009).

5.2.4 Elemental analysis by EDX

Energy dispersive X-ray spectroscopy (EDX) was used to investigate the elemental compositions and gold distribution in AuNPs/PPy/SPEs using different Au precursor concentrations. The obtained AuNPs/PPy/SPE showed many elemental compositions such as carbon, nitrogen, oxygen, sodium, gold, and chloride, this observation clearly indicated percentages of AuNPs on modified SPE which are presented as Table 5.2 and Fig.5.8. Moreover, a different in gold percentage with different Au precursor concentration is observed i.e. 3.71%, 3.96%, 5.89%, 4.6%, 2.33%, respectively for 1, 3, 5, 7 and 9 mM of Au precursor concentration. Fig. 5.9 illustrates the relationship between the percentages of AuNPs on current responses. This result exhibited that the percentages of AuNPs were proportional to current response which clearly demonstrated influential factor of Au precursor concentration. However, we found that at high Au precursor concentration, low percentage of AuNPs was obtained which was probably because most of AuNPs aggregated and flocculated in gold colloidal solution which was not included in electropolymerization procedure for electrode modification. Fig. 5.10 shows the uniform distribution of small AuNPs entrapped in PPy film on SPE.

Table 5.2: Elemental composition of (% wt/wt) AuNPs/PPy modified SPE with various Au precursor concentrations.

Defined as: C= Carbon, N= Nitrogen, O= Oxygen, Na= Sodium, Au= AuNP, Cl= Chloride.

Element	The percentage by weight of Au precursor concentration (mM)				
	1	3	5	7	9
C	82.18	81.54	79.48	81.41	82.66
N	05.19	04.73	03.02	04.88	06.39
O	03.71	03.61	05.29	04.38	05.12
Na	00.07	00.14	00.11	00.13	00.27
Au	03.88	03.96	05.89	04.60	03.24
Cl	04.97	06.02	06.21	04.60	02.33

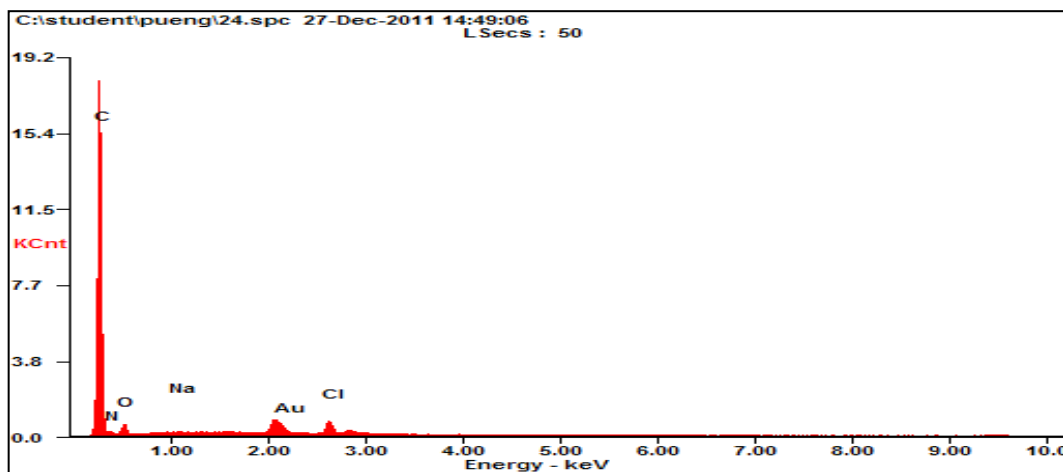


Fig. 5.8 EDX for AuNPs/PPy modified SPE using 5 mM Au precursor concentrations, 0.09M Py, 10 electropolymerization cycles, and an applied voltage between 0 to 1.0V.

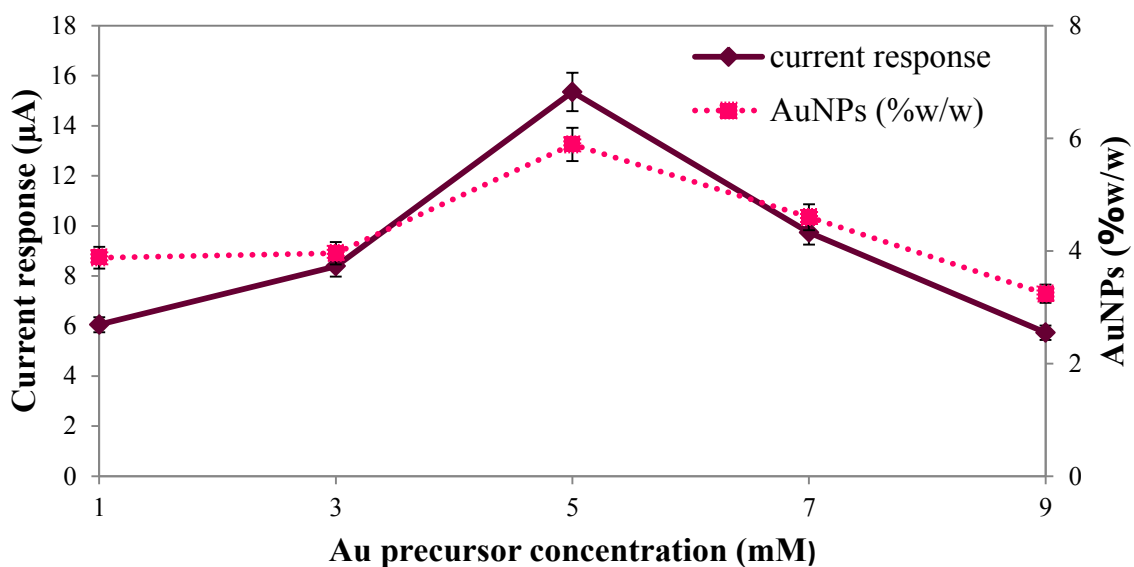


Fig. 5.9 Effect of the Au precursor concentrations on percentage of AuNPs in AuNPs/PPy modified SPE and current responses. The amperometry was tested in solution containing 10 mM $K_4Fe(CN)_6$ / 1 mM KCl at 0.58V.

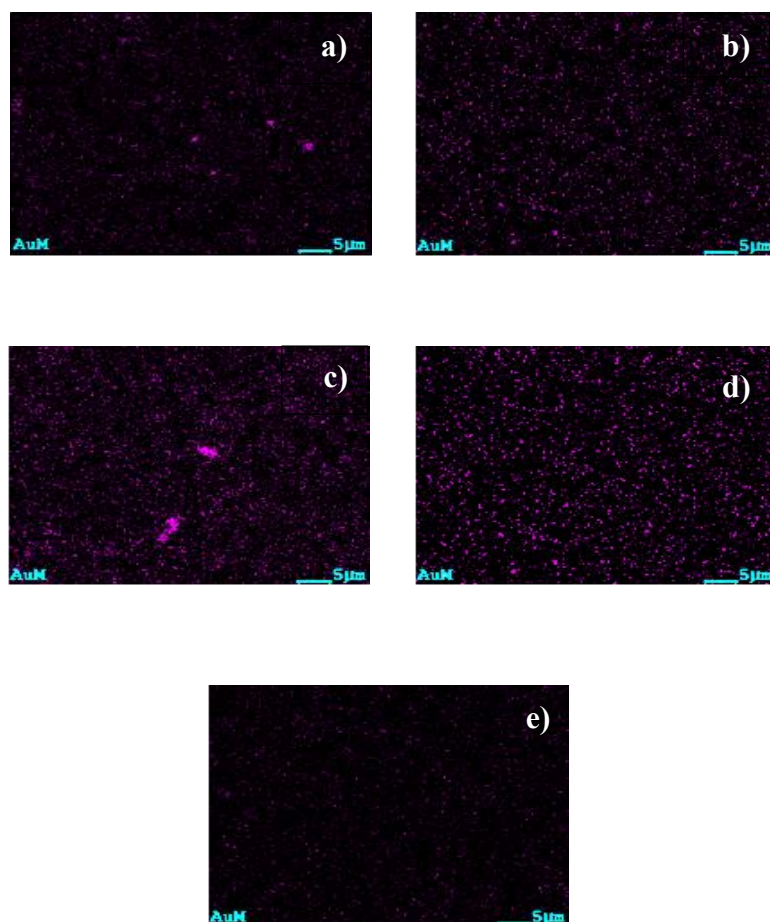


Fig. 5.10 EDX mapping for AuNPs/PPy modified SPE with various Au precursor concentrations: a) 1 mM, b) 3 mM, c) 5 mM, d) 7 mM, and e) 9 mM, respectively. From this figure, the purple points showed AuNPs in PPy film.

5.3 Electrochemical determination of phenol

Before discussing the influence of modified electrode and solution types, we need to know a reaction mechanism. Several researchers (Ruzgas et al., 1999; Gorton et al., 1999) attempted to explain the response of the HRP biosensors to phenolic compounds based on “double displacement or ping-pong mechanism” by two substrates such as a H_2O_2 and a phenolic compound as shown in Fig.5.11. HRP molecules are first oxidized by H_2O_2 followed by twice reduction by phenol which acts as a mediator. Phenol is converted to free radical products in last reaction that they are electroactives and can be reduced on the electrode surface. The phenol concentration in solution is proportional to the reduction current as long as the concentration of H_2O_2 is still not limiting. However, the presence of a high H_2O_2 concentration causes inhibition of the HRP activity. These facts cause difficulties in the practical use of HRP based biosensor for phenol detection (Joanna Cabaj and Jadwiga (2011)).

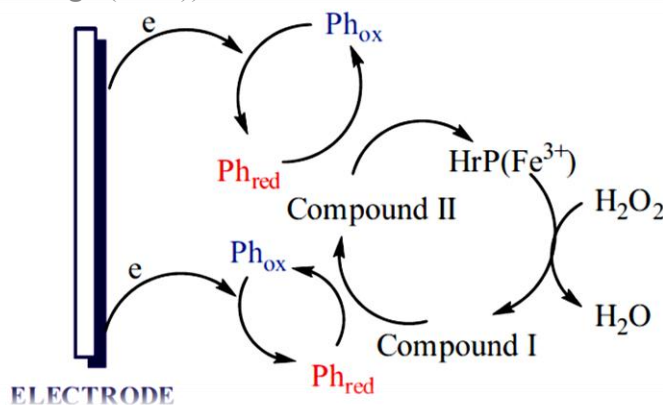
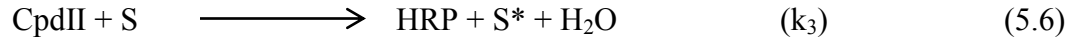
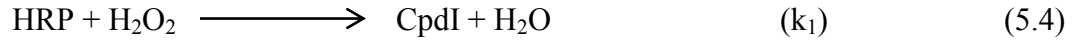


Fig. 5.11 Scheme of the ping-pong mechanism for AuNPs/PPy/HRP/SPE in $50\mu\text{M}$ H_2O_2 / $50\mu\text{M}$ phenol in PBS (pH 7.4); Ph_{ox} and Ph_{ed} are the oxidized and reduced forms of phenol, respectively (Joanna Cabaj and Jadwiga (2011)).

In general, the measured current combines both the mass transfer limited current (I_{lim}) and the enzyme kinetic limited current (I_{kin}). Many reports investigated the reaction which was controlled by enzyme kinetic limited current according to Gorton’s group (Gorton et al., 1999):

For the mediated electron transfer of HRP cycle can be expressed as follows (Gorton et al., 1999):



The total surface concentration of HRP can be calculated as:

$$\Gamma = \Gamma_{\text{HRP}} + \Gamma_{\text{CI}} + \Gamma_{\text{CII}} \quad (5.8)$$

The rate of the peroxidase reaction cycle is according to Eq. (5.9-5.12):

$$v = -\frac{d[\text{S}]}{dt} = k_2[\text{S}]\Gamma_{\text{CI}} + k_3[\text{S}]\Gamma_{\text{CII}} \quad (5.9)$$

$$\frac{d\Gamma_{\text{CI}}}{dt} = k_1[\text{H}_2\text{O}_2]\Gamma_{\text{HRP}} - k_2[\text{S}]\Gamma_{\text{CI}} \quad (5.10)$$

$$\frac{d\Gamma_{\text{CII}}}{dt} = k_2[\text{S}]\Gamma_{\text{CI}} - k_3[\text{S}]\Gamma_{\text{CII}} \quad (5.11)$$

$$\frac{d\Gamma_{\text{HRP}}}{dt} = k_3[\text{S}]\Gamma_{\text{CII}} - k_1[\text{H}_2\text{O}_2]\Gamma_{\text{HRP}} \quad (5.12)$$

The surface concentrations of HRP, CpdI, CpdII are constant at steady state:

$$\frac{d\Gamma_{\text{CI}}}{dt} = \frac{d\Gamma_{\text{CII}}}{dt} = \frac{d\Gamma_{\text{HRP}}}{dt} = 0 \quad (5.13)$$

$$k_1[\text{H}_2\text{O}_2]\Gamma_{\text{HRP}} = k_2[\text{S}]\Gamma_{\text{CI}} \quad (5.14)$$

$$k_2[\text{S}]\Gamma_{\text{CI}} = k_3[\text{S}]\Gamma_{\text{CII}} \quad (5.15)$$

$$k_3[\text{S}]\Gamma_{\text{CII}} = k_1[\text{H}_2\text{O}_2]\Gamma_{\text{HRP}} \quad (5.16)$$

Thus, the relationship of total surface concentration of HRP and Eq. (5.14-5.16) results in the following expression:

$$\Gamma_{\text{CI}} = \frac{k_1 k_3 \Gamma [\text{H}_2\text{O}_2]}{k_1 k_2 [\text{H}_2\text{O}_2] + k_1 k_3 [\text{H}_2\text{O}_2] + k_2 k_3 [\text{S}]} \quad (5.17)$$

$$\Gamma_{CII} = \frac{k_1 k_2 \Gamma [H_2O_2]}{k_1 k_2 [H_2O_2] + k_1 k_3 [H_2O_2] + k_2 k_3 [S]} \quad (5.18)$$

The substitution of Γ_{CI} and Γ_{CII} into Eq. (5.9) expresses in the following equation:

$$\frac{2\Gamma}{v} = \frac{1}{k_1 [H_2O_2]} + \frac{k_2 k_3}{k_2 k_3 [S]} \quad (5.19)$$

Assuming that $k_2 \gg k_3$ because Eq. (5.6) is rate limiting step, the expression for I_{kin} of mediated electron transfer is obtained:

$$\frac{2\Gamma}{v} = \frac{1}{k_1 [H_2O_2]} + \frac{1}{k_3 [S]} \quad (5.20)$$

$$I_{kin} = nFAv \quad (5.21)$$

$$\frac{1}{I_{kin}} = \frac{1}{2nFA\Gamma} \left(\frac{1}{k_1 [H_2O_2]} + \frac{1}{k_3 [S]} \right) \quad (5.22)$$

Where I_{kin} represent the enzyme kinetic limited current, n is number of electron per each electron donor molecule, F is Faraday constant (96,584 C/mol), A is the real surface area of electrode, and Γ is the total surface concentration of HRP (mol/cm²).

From Eq. 5.23 shows the two-substrate enzyme kinetics depending on both the concentration of A and B substrates by plotting between the reciprocal of current and concentration of substrate A at fixed the concentration of B. It relates to the Michaelis-Menten constants in form of bellowed equation (http://chemwiki.ucdavis.edu/Biological_Chemistry/Catalysts/Enzymatic_Kinetics/Ping-pong_mechanisms):

$$\frac{1}{I} = \frac{K_m^A}{I_{max}} \left(\frac{1}{A} \right) + \left(1 + \frac{K_m^B}{[B]} \right) \left(\frac{1}{I_{max}} \right) \quad (5.23)$$

Although AuNPs/PPy/SPE without enzyme was already tested in ferri/ferrocyanide which acted as a redox couple in the past section, AuNPs/PPy/HRP/SPE was still not tested with the target substrate, phenol. To expel this suspicious point, it was proved in the phenol solution. Type of modified electrodes affected the current responses which were examined in $50\mu\text{M H}_2\text{O}_2 / 50\mu\text{M phenol}$ in PBS (pH 7.4) by amperometric method at a potential of -0.05V as shown in Fig. 5.12. The results demonstrated that the modified electrode with PPy gave the current response which is higher than that of the bare SPE. However, the current response is not higher than the incorporation of AuNPs in PPy film. Therefore, the use of conductive polymer like PPy and metal nanoparticles like AuNPs enhanced biosensor efficiency. Moreover, the presence of HRP which was immobilized in AuNPs/PPy modified SPE gave current derive from enzyme catalytic.

While effects of solution type related to direct current response were determined via amperometric approach of AuNPs/PPy/HRP/SPE in different solution such as PBS, $50\mu\text{M H}_2\text{O}_2$ in PBS, $50\mu\text{M phenol}$ in PBS, and $50\mu\text{M H}_2\text{O}_2 / 50\mu\text{M phenol}$ in PBS (same pH 7.4) at -0.05V as shown in Fig. 5.13. The use of applied potential was -0.05V because of inactivated enzyme molecules when more negative potential is employed (Rosatto et al., 1999; Rosatto et al., 2002; Mello et al., 2003; Korkut et al., 2009). The results illustrated that the current responses in PBS were the lowest value indicating that HRP/AuNPs/PPy/SPE was not electroactive. Whereas modified electrode was examined in phenol and H_2O_2 , respectively, we discovered that the little current responses increased when compared with PBS solution. AuNPs gave the effective electron transfer between enzyme and electrode for direct electron transfer reaction while this work proved that AuNPs helped the electron transfer between mediator as phenol and electrode for mediated electron transfer.

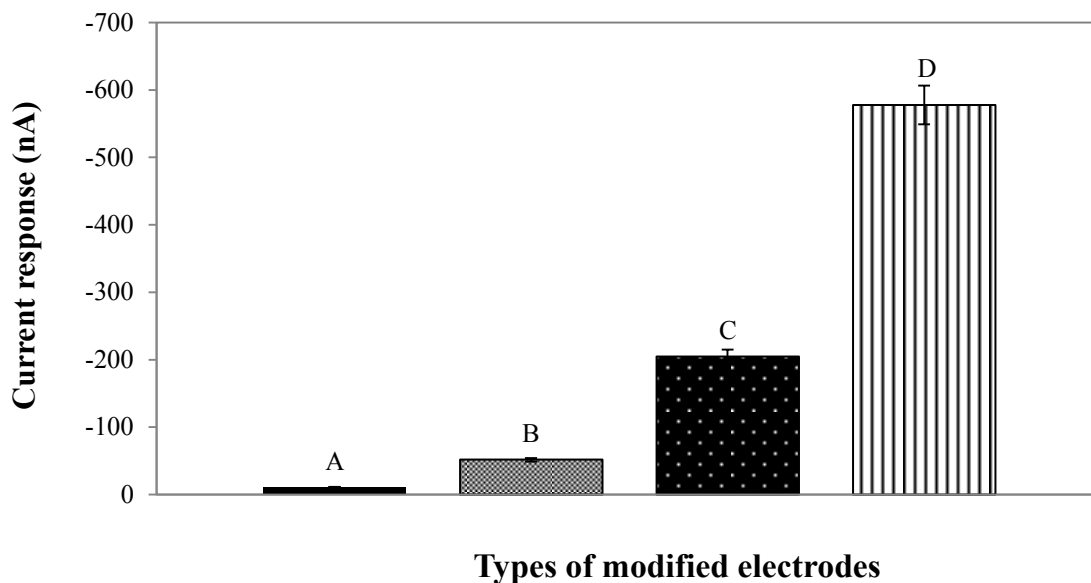


Fig. 5.12 Comparison of current responses between bare SPE, PPy/SPE, AuNPs/PPy/SPE and HRP/AuNPs/PPy/SPE in $50\mu\text{M H}_2\text{O}_2$ / $50\mu\text{M}$ phenol in PBS (pH 7.4) at -0.05V (Symbol of A, B, C, D represent Bare SPE, PPy/SPE, AuNPs/PPy/SPE, AuNPs/PPy/HRP/SPE, respectively).

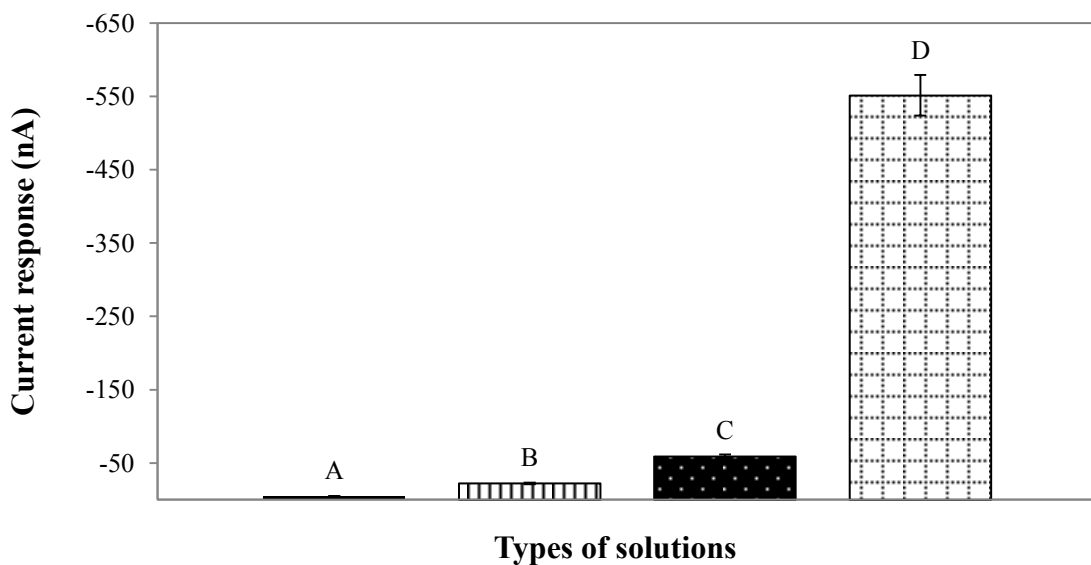


Fig. 5.13 Comparison of current responses of AuNPs/PPy/HRP/SPE in different solutions (pH 7.4) at -0.05V (Symbol of A, B, C, D represent the solutions of PBS, Phenol, H_2O_2 , H_2O_2 /Phenol, respectively).

5.4 Direct electrochemistry of HRP at AuNPs/PPy/HRP/SPE

Modification of HRP onto a bare electrode achieved the low current responses due to two reasons which were the denaturation and loss of electroactivity of HRP molecules, and the slow electron exchange between enzyme active site and electrode surface. Since the active sites of HRP are deeply embedded in a protein shell, resulting in the long distance between the active sites and electrode surface (Zhao et al., 2008; Yin et al., 2009; Teng et al., 2009). Thus, the aim of direct electrochemistry research of this enzyme was to design appropriate electrode surface providing fast electron transfer pathway. An ideal promoter should provide a suitable interface between protein and electrode surface to facilitate electron transfer, and eliminate the denaturation of HRP molecules on the electrode surfaces.

The study of direct electron transfer was checked through cyclic voltammograms of HRP/AuNPs/PPy modified SPE in 0.1M PBS (pH7.4) between a scan rate of 0.1-0.5 Vs⁻¹ as shown in Fig.5.14 to investigate the electron transfer process between the electrode and immobilized HRP without any mediators (Teng et al.,2009). Moreover, we focused on the enzyme concentration at electrode surface. The surface concentration of HRP (Γ^*) in HRP/AuNPs/PPy modified SPE can be estimated using Brown-Anson equation (2000):

$$I_p = \frac{n^2 F^2 \Gamma^* A v}{4RT} \quad (5.24)$$

Where I_p represents the cathodic peak current, n is the number of electron, F is the faraday constant (96,584 C/mol), A is the surface area of electrode, v is the scan rate (V/s), R is the gas constant (8.314 J/molK), and T is the absolute temperature (298K). From the reduction peak of HRP/AuNPs/PPy/SPE, the surface coverage of HRP, Γ^* was calculated at 2.488×10^{-9} mol/cm² which was larger than a fully packed monolayer of HRP (5.0×10^{-11} mol/cm²)(Xiao et al.,2000). However, this value was likely to be more than the actual value since only the planar electrode area was used for calculations without considering enhanced surface area due to the rough electrode surfaces. However, this

obtained biosensor might demonstrate the multiple layer coverage of HRP indicating that HRP molecules could be more adsorbed on the electrode surface area thus higher current responses could be executed. Nevertheless, the multiple layers of HRP might obstruct the mediated electron transfer.

The cyclic voltammograms of HRP/AuNPs/PPy/SPE in 0.1M PBS (pH7.4) from 0.1-0.5 V/s is depicted in Fig.5.14. It can be seen that scan rate affected the current responses of immobilized HRP. Also, it is observed that the increasing scan rate, the oxidation peak shifts to more positive potentials, whereas the reduction peak shifts to more negative potentials. The anodic and cathodic peak currents (i_{pa} and i_{pc}) are proportional to the scan rate. Thus, the electrode reaction was typical a surface-controlled and was of quasi-reversible process.

The formal potential ($E^{0'}$) of the Fe^{III}/Fe^{II} redox couple calculated from the average potentials in the scan rate range from 0.1 to 0.5 V/s is expressed according to Eq.(5.25):

$$E^{0'} = \frac{E_{pa} + E_{pc}}{2} \quad (5.25)$$

Where E_{pa} and E_{pc} are the anodic and cathodic peak potentials, respectively. The formal potential of this work was -0.21 V similar to the HRP/AuNPs/SF/GCE of Xu et al. (2003) which was determined at -0.22V of native HRP in solution than the formal potential of -0.338V for the HRP immobilized on a colloidal gold modified SPE (Yin et al., 2009; Xu et al., 2003), suggesting that most HRP molecules retained their native enzyme structure after entrapment in nanocomposite matrix. The peak to peak separation values (ΔE_p) was determined using the following equation:

$$\Delta E_p = E_{pa} - E_{pc} \quad (5.26)$$

These results in Fig.5.14 show that the peak to peak separation increases with scan rate. The peak to peak separation was calculated to be 0.398V, which was similar to that obtained from HRP/nano-Au/GCE (0.32V) and HRP/AuNPs/SF/GCE (0.3V)(Zheng

and Lin,2008; Yin et al.,2009). Furthermore, this large peak to peak separation value indicated the improper orientation of immobilized enzyme molecules which corresponded to HRP/Au colloid-cysteamine modified gold electrode and HRP/AuNPs/SF modified GCE (Xiao et al., 2000; Yin et al., 2009). Even though the electron transfer of large peak to peak separation was inferior to case of small peak to peak separation, but it was superior to the absence of AuNPs as previously illustrated in section 5.3.

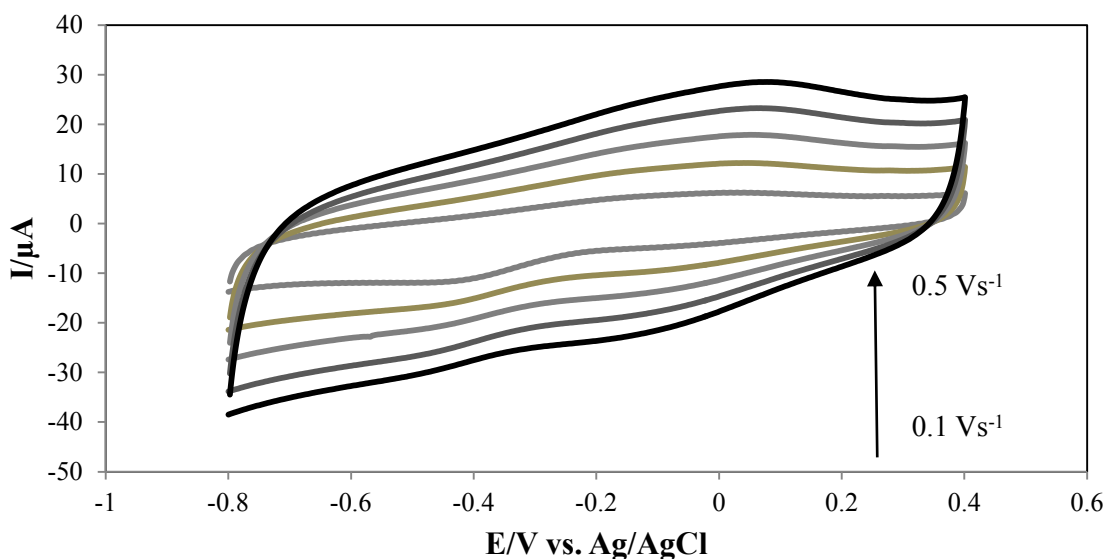


Fig. 5.14 Cyclic voltammogram of HRP/AuNPs/PPy/SPE in solution of 0.1M PBS (pH7.4) at various scan rates from 0.1-0.5 V/s.

The relationship of redox peak current with the scan rate is described in Fig.5.15. The linear regression equation were $i_{pa} = 0.0558v + 0.846$ (μA , mV/s , $R=0.9993$), $i_{pc} = -0.0483v - 6.2061$ (μA , mV/s , $R=0.9988$). The relationship between the peak potential (E_p) and the natural logarithm of scan rate ($\ln v$) for HRP/AuNPs/PPy/SPE in 0.1M PBS (pH 7.4) is shown in Fig.5.16. The cathodic peak potential (E_{pc}) decreased linearly with $\ln v$ which expressed the linear regression equation of $E_{pc} = -0.0563\ln v - 0.1356$ (μA , mV/s , $R= 0.8933$) in the range from 0.1-0.5 V/s following Laviron model (Eq.5.27):

$$E_p = E^{0'} + \frac{RT}{\alpha nF} - \frac{RT}{\alpha nF} \ln v \quad (5.27)$$

Where α is the cathodic electron transfer coefficient, n is the electron number, F is Faraday constant (96,584 C/mol), R is the gas constant (8.314 J/molK), and T is the absolute temperature (298K). Also, αn was estimated to be 0.46 (Given $0.3 < \alpha < 0.7$ in general) which could be concluded that $n=1$ and $\alpha=0.46$. Therefore, the reaction between HRP and SPE was a single electron transfer process.

The apparent heterogeneous electron transfer rate (k_s) can be estimated with Laviron equation as shown in Eq.5.28:

$$\log k_s = \alpha \log(1 - \alpha) + (1 - \alpha) \log \alpha - \log \frac{RT}{nFv} - \frac{\alpha(1-\alpha)nF\Delta E_p}{2.3RT} \quad (5.28)$$

Unfortunately, the k_s was calculated to be 0.05 s^{-1} of AuNPs/PPy/HRP/SPE which this value was much less than $0.75 \pm 0.04 \text{ s}^{-1}$ of AuNPs/HRP/SPE (Xu et al., 2003). They made the colloidal gold modified screen-printed carbon ink before printed on silver conducting tracks to drop HRP solution. Thus the scaffold for the immobilization of HRP of their work was better than this work. However, the presence of the small colloidal AuNPs can function as electron conduction pathways which facilitated the electron transfer between the active area of HRP and electrode surface area (Liu and Ju, 2002; Xu et al., 2003; Yin et al., 2009).

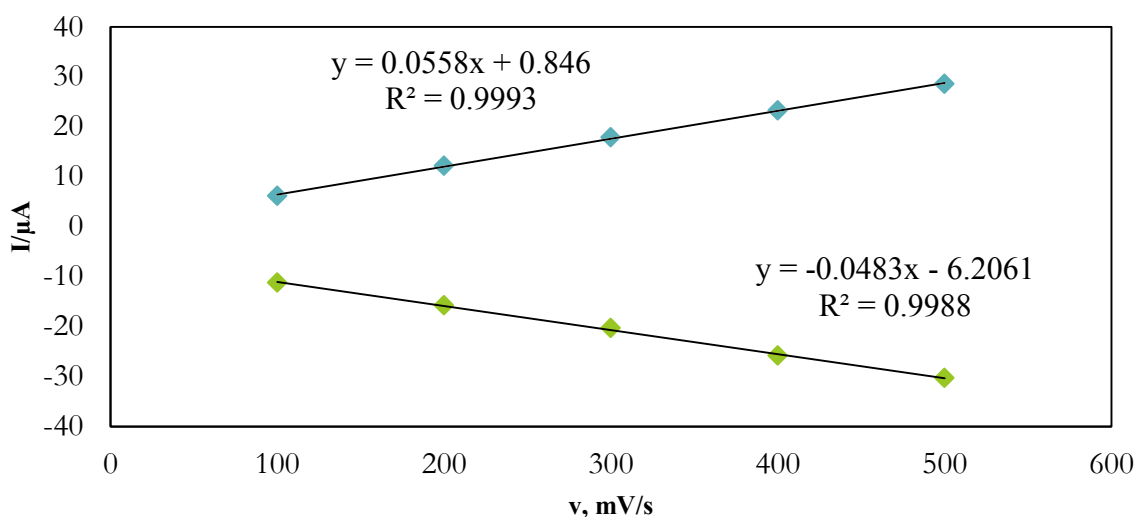


Fig. 5.15 The relationship between the peak current (I_p) and the scan rate (v) for AuNPs/PPy/HRP/SPE in 0.1M PBS (pH7.4) with scan rates varied from 0.1-0.5 V/s.

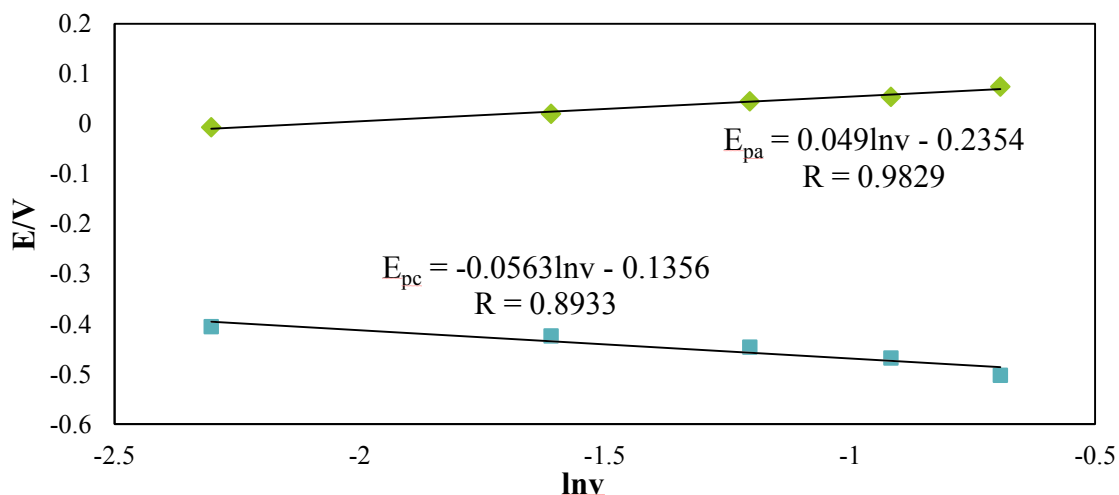


Fig. 5.16 The relationship between the peak potential (E_p) and the natural logarithm of scan rate ($\ln v$) for HRP/AuNPs/PPy/SPE in 0.1M PBS (pH7.4) with scan rate varied from 0.1 - 0.5 V/s.

The fabrication of AuNPs/PPy/HRP/SPE using electropolymerization method gave the advantage of the immobilization of much active enzyme due to the increasing of the electropolymerization cycles allowed more HRP molecules to be immobilized on underlying electrode. From these results, we concluded that AuNPs helped to promote the electron transfer and AuNPs/PPy composite material was suitable for HRP immobilization and fabrication of phenol biosensor. Although direct electron transfer of the obtained biosensor was not target mechanism in this study but the fabrication conditions could be applied for mediated electron transfer. These results showed the decreasing of direct electron transfer which greatly implied the enhancement of mediated electron transfer. In the following, therefore, we will discuss an enzyme kinetic to study the reaction between HRP and substrate like phenol.

5.5 Electrocatalytic activity

The rate of reaction can be controlled by substrate mass-transfer or by enzyme reaction depending on substrate concentration in solution. As a result, the kinetics of the reaction divides into two regions. The first region is the region of diffusion limitation at low substrate concentration. The second region is the region representing reaction by enzyme, which exhibits normal Michaelis-Menten kinetics (Vakurov et al., 2004). From Fig.5.17 shows that our results did not show Michaelis-Menten mechanism. It was most possible that substrate and/or electron transfer governed the reaction rate.

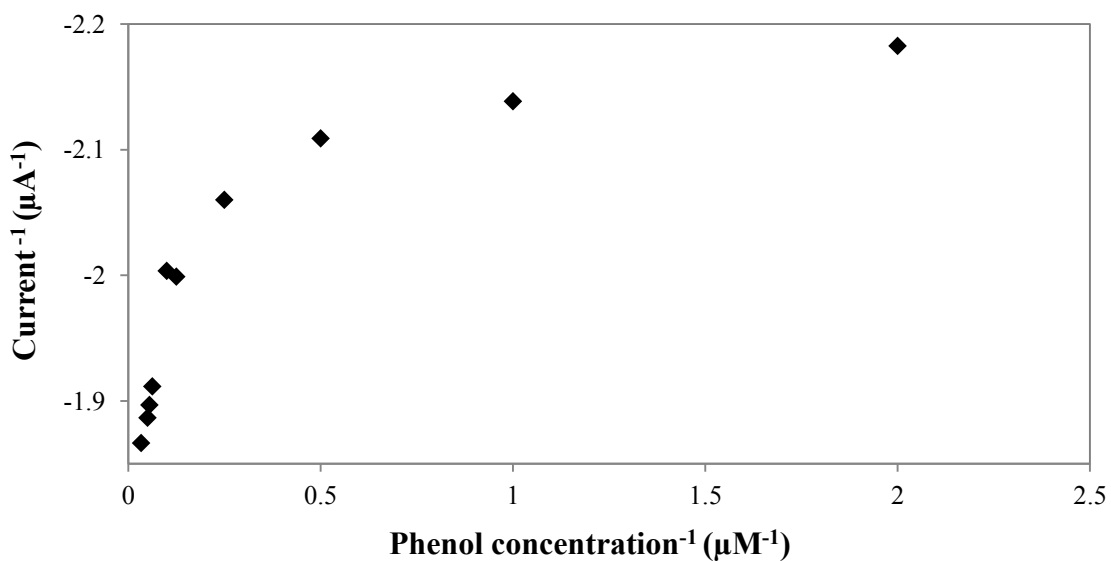


Fig. 5.17 Calibration plot between the reciprocals of the steady-state current versus phenol concentration.

5.6 Performance factors

5.6.1 Linear range

Fig.5.18 illustrates the calibration curve of the phenol biosensor. The phenol solution was prepared in the solution of H_2O_2 / PBS (pH 7.4). Obviously, the increasing of phenol concentrations showed the range of linearity at first. However, the current response is not linear when the concentration of phenol increased at fixed H_2O_2 concentration. The concentration of H_2O_2 is one of the important factors that affected the response of biosensor (Rosatto et al., 1999; Rosatto et al., 2002; Mello et al., 2003; Korkut et al., 2009; Kafi and Chen, 2009). The low H_2O_2 concentration might bring to the low response current of biosensor and higher H_2O_2 concentration might effects to direct electron transfer and activity inhibition of HRP. The proposed biosensor displayed a linear response to phenol concentration ranges from 1 μM to 8 μM ($R^2=0.984$) as shown in Fig.5.18. This biosensor performed narrower linear range than those of 2 to 12 μM at HRP/Poly(GMA-co-MTM)/PPy/Au, 0.5 to 10 μM at PVF/PPy/GCE (Korkut et al., 2009; Sulak et al., 2009).

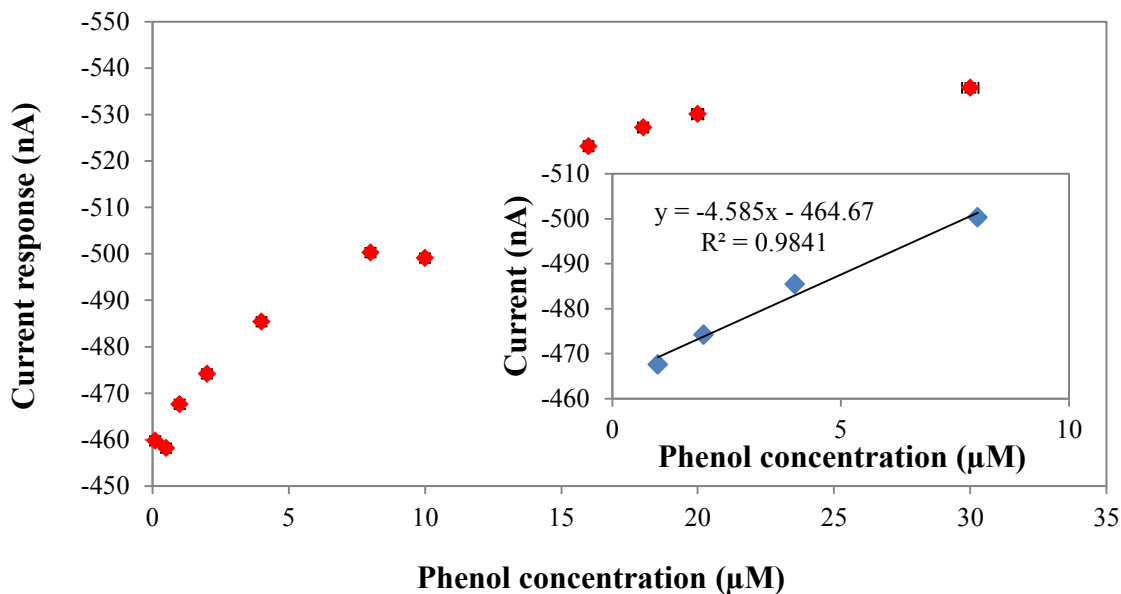


Fig.5.18 Calibration curve of amperometric phenol response in 50 μM H_2O_2 / PBS solution (pH 7.4) at -0.05V (vs. Ag/AgCl). Inset: the linear part of the calibration curve.

5.6.2 Sensitivity

The slope of linear regression was calculated to be $4.585 \text{ nA}\mu\text{M}^{-1}$ as exhibited in Table 5.3. A sensitivity was superior than $1 \text{ nA}\mu\text{M}^{-1}$ of CNT/PPy/Au and $0.7 \text{ nA}\mu\text{M}^{-1}$ of Poly(GMA-co-MTM)/PPy/CNT/Au for HRP biosensor (Korkut et al.,2008; Ozoner et al., 2010).

5.6.3 Detection limit

A detection limit was $3.19 \mu\text{M}$ when the signal to noise ratio of 3, calculated according to the following equation:

$$3S_b/m \quad (5.5)$$

where S_b is the standard deviation of the blank signal ($n=10$) and m is the slope of the linear calibration curve (Ardakani et al.,2008; Sulak et al., 2009). This value did not exceed $10.6 \mu\text{M}$ for the restricted legislation of industrial ministry.

5.6.4 Response time

Response time is a time necessary to reach 95% of the steady-state current. The response time for this biosensor was found within 23.5 s as shown in Fig.5.19 which was much lower than previously reported 5 min for Polyvinylferrocene (PVF)/PPy/HRP modified GC electrode (Sulak et al.,2009) and 50 s for immobilized HRP with pyrrole after electrodeposit of gold (Yusran's thesis, 2009). This result showed a short response time achieving the advantages.

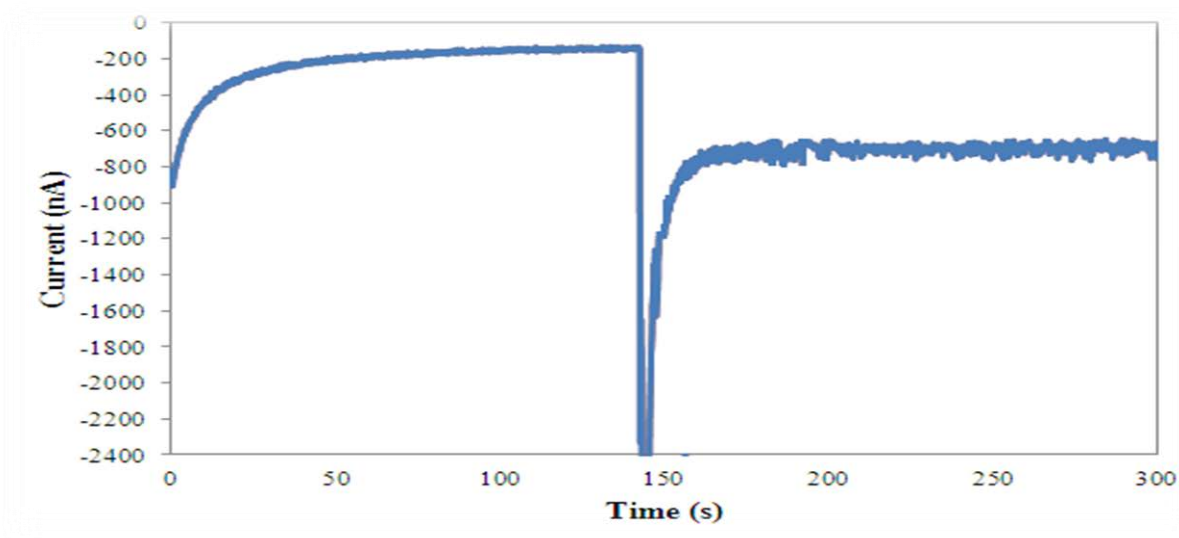


Fig. 5.19 Amperometric current response of biosensor of 50 μ M phenol/50 μ M H₂O₂ in PBS solution (pH 7.4) at -0.05V (vs. Ag/AgCl) under stirred condition.

5.6.5 Reproducibility

The reproducibility of ten identical biosensors for the phenol detection was evaluated under the same experimental conditions as shown in Fig.5.20. The relative standard deviation (RSD) of the biosensor responses to 1 μ M phenol/ 50 μ M H₂O₂ in 0.1M PBS (pH 7.4) at -0.05V, prepared independently, shows an allowable reproducibility with a RSD of 3.78% (n=10) which exhibited good reproducibility. Thus this method is rapid, easy, and of high reproducibility.

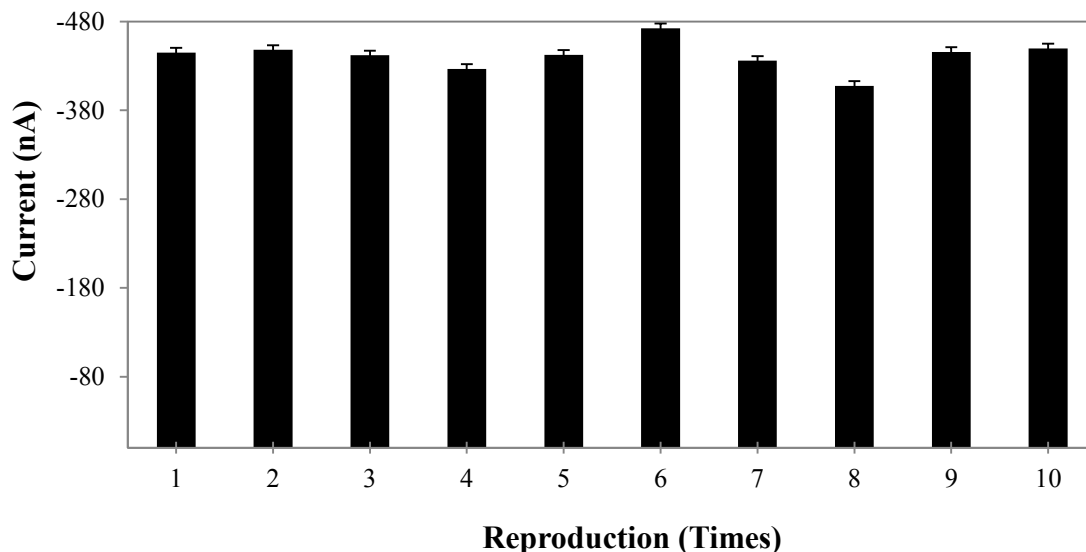


Fig. 5.20 Reproducibility test of ten identical biosensors in 1 μM phenol/50 μM H_2O_2 /PBS (pH 7.4) at -0.05V (vs. Ag/AgCl).

5.6.4 Storage stability

To examine the storage stability of AuNPs/PPy/HRP modified SPE, amperometric approach was selected. The current responses of the enzyme electrode dramatically decreased after dried storing for one month because of enzyme deactivation. The stability of fabricated biosensor was tested over a period of 30 days, which was carried on in the solution containing in 50 μM phenol/50 μM H_2O_2 / PBS solution (pH 7.4) at -0.05V (vs. Ag/AgCl) as shown in Fig. 5.21. Each electrode was synthesized and kept in two conditions like 4°C and 25 °C before it was measured. After that, it was disposed which defined as a disposable electrode. This biosensor retained 83.37 % residual activity in the first seven days of storage. After 14 and 30 days of storage, the residual currents were approximately 60.52% and 47.38 %, respectively when stored at 4°C. While storage at 25°C, we found that 7 days retained current response about 61.75%. Meanwhile, the residual currents were 56.43 %, and 31.43 % after 14 and 30 days storage, respectively. Therefore, we should be keep modified electrode at 4°C.

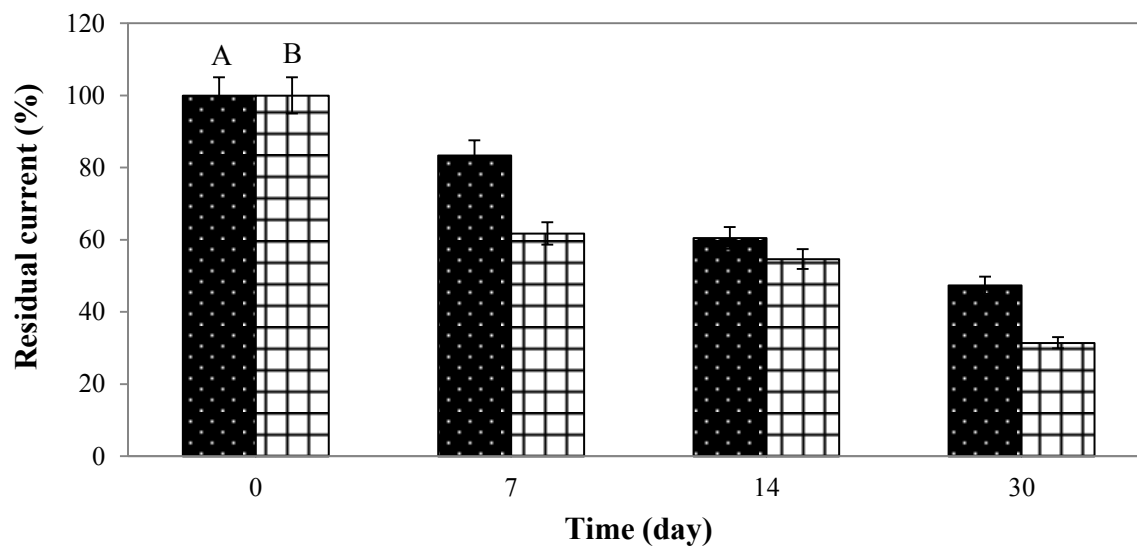


Fig. 5.21 Storage stability of AuNPs/PPy/HRP/SPE in 50µM phenol/50µM H₂O₂ / PBS solution (pH 7.4) at -0.05V (vs. Ag/AgCl) (Symbol of A, B, represent the storage conditions at 4°C, and 25°C).

5.6.6 Comparisons with other researches

At this point, some performance factors such as linear ranges, sensitivity, detection limit, and response time were compared to these of other researches.

Table 5.3 Comparisons of performance factors of phenol biosensors obtained in this research with other researches.

Modified electrode	Detection limit	Linear range	sensitivity	Response time
HRP+DNA/silica-titanium cross linked with glutaraldehyde in carbon SPE Mello et al. (2003)	0.7 μM	1-50 μM	181 nA μM^{-1} cm^{-2}	-
CNT/ PPy/ HRP/ Au Korkut et al.(2008)	3.52 μM	16-44 μM	1 nA μM^{-1}	2 s
Poly(GMA-co-MTM)/ polypyrrole/HRP/GCE Korkut et al.(2009)	0.3 μM	2-12 μM	90 nA μM^{-1}	3 s
PVF/ PPy/ HRP/ GCE Sulak et al.(2009)	0.17 μM	0.5-10 μM	29.91 nA μM^{-1}	5 min
Poly(GMA-co-MTM)/ polypyrrole/CNT/HRP/Au S.K. Ozoner et al.(2010)	0.73 μM	1.6-72 μM	0.7 nA μM^{-1}	3.8 s
Gold/ PPy/ HRP/ GCE Yusaran thesis (2009)	25.4 μM	30-210 μM	7.277 nA μM^{-1}	50 s
PPY/HRP /GCE Panjai thesis (2009)	4.55 μM	2-100 μM	0.1053 nA μM^{-1}	150 s
AuNPs/PPy/HRP/SPE This work	3.19 μM	1-8 μM ,	4.585 nA μM^{-1}	23.5 s

CHAPTER VI

CONCLUSIONS AND RECOMMENDATIONS

6.1 Conclusions

AuNPs/PPy/HRP modified screen-printed electrodes were successfully achieved using electropolymerization method. Firstly, AuNPs were synthesized by citrate reducing method, and then HRP and AuNPs could be entrapped with the electropolymerization of pyrrole under optimized conditions for phenol detection.

6.1.1 The optimum of electropolymerization conditions of AuNPs/PPy/SPEs were determined as follows:

The appropriate fabrication conditions for AuNPs/PPy were concentration of Au precursor was 5 mM, and electropolymerization cycle was 10 cycles.

6.1.2 Physical and chemical characterization of bare and modified screen-printed electrodes:

UV-Visible spectroscopy exhibited AuNPs/Py in PBS solution (pH 7.4) suitable for the constructing HRP biosensor. The synthesized AuNPs was of spherical shape and with the average size of 15 ± 5 nm. SEM images revealed the globular and rod-like structure while AFM images indicated the high roughness. In addition, the presence and uniform distributions of AuNPs in PPy film was confirmed by EDX.

6.1.3 Electrochemical determination of phenol

6.1.4 Direct electrochemistry of HRP at AuNPs/PPy/HRP/SPE

The surface concentration of HRP in AuNPs/PPy/HRP/SPE was found to be 2.488×10^{-9} mol/cm², and the electron transfer rate was calculated to be 0.05s^{-1} .

6.1.5 Reaction kinetics

Michaelis-Menten kinetic was not observed most likely due to influential substrate or electron transfer limitation.

6.1.6 Performance factors

1) *Linear range:* The response current of the AuNPs/PPy/HRP/SPE was linear in the range of 1-8 μM phenol.

- 2) *Sensitivity*: It was found to be 4.585 nA/ μM .
- 3) *Detection limit*: The value of 3.19 μM phenol was obtained.
- 4) *Response time*: A response time was observed within 23.5 s.
- 5) *Reproducibility*: The R.S.D. of the ten biosensors current responses was 3.78% (n=10).
- 6) *Storage stability*:, It was found that the current response decreased 16.63%, 39.48%, and 52.62%, respectively, after 7, 14, and 30 days storage when keep at 4°C. While the current response decreased 38.25%, 45.37%, and 68.57%, respectively, after 7, 14, and 30 days storage when keep at room temperature.

6.2 Recommendations for future studies

6.2.1 The pH of supporting electrolyte should be investigated and studied for improving electropolymerization of AuNPs/PPy/HRP modified screen-printed electrode due to addition supporting electrolyte might also affect the enzyme and biosensor efficiency.

6.2.2 To improve sensitivity of phenol biosensor, other conducting polymers may be investigated.

6.2.3 Other phenolic compounds should also be tested with this biosensor.

References

- Abdullaha, J., Ahmad M., Karuppiah, N., Henga, L. Y., Sidek, H. Immobilization of tyrosinase in chitosan film for an optical detection of phenol. Sensors and Actuators B: Chemical 114(2006): 604-609.
- Andreescu, D., Andreescu, S., Sadik, O. A., Gorton, L. Chapter 7 New materials for biosensors, biochips and molecular bioelectronics. Comprehensive Analytical Chemistry, Elsevier. 44(2005): 285-327.
- Arecchi, A., Scampicchio M., Drusch S., Mannino S. Nanofibrous membrane based tyrosinase-biosensor for the detection of phenolic compounds. Analytica Chimica Acta 659(2010): 133-136.
- Busca, G., Berardinelli, S., Resini C., Arrighi, L. Technologies for the removal of phenol from fluid streams: A short review of recent developments. Journal of Hazardous Materials 160(2008): 265-288.
- C. G. Zoski, Handbook of Electrochemistry 2007.
- Carquigny, S., Segut, O., Lakard, B., Lallemand, F., Fievet P. Effect of electrolyte solvent on the morphology of polypyrrole films: Application to the use of polypyrrole in pH sensors. Synthetic Metals 158(2008): 453-461.
- Chen, W., Li, C. M., Yu, L., Lu Z., Zhou Q. In situ AFM study of electrochemical synthesis of polypyrrole/Au nanocomposite. Electrochemistry Communications 10(2008): 1340-1343.
- Chen, W., Li, C. M., Chen P., Sun C. Q. Electrosynthesis and characterization of polypyrrole/Au nanocomposite. Electrochimica Acta 52(2007): 2845-2849.
- Chen, Z., Xi, F., Yang, S., Wu Q., Lin X. Development of a bienzyme system based on sugar-lectin biospecific interactions for amperometric determination of phenols and aromatic amines. Sensors and Actuators B: Chemical 130(2008): 900-907.
- Chen, Ch-Ch., Gu Y. Enhancing the sensitivity and stability of HRP/PANI/Pt electrode by implanted bovine serum albumin. Biosensors and Bioelectronics 23(2008): 765-770.
- Cheng, J, Yu, SM, Zuo, P. Horseradish peroxidase immobilized on aluminum-

- pillared interlayered clay for the catalytic oxidation of phenolic wastewater. water research 40(2006): 283-290.
- Dai, X., Compton, R. G. Direct Electrodeposition of gold nanoparticles onto indium tinoxide film coated glass: application to the detection of arsenic(III). ANALYTICAL SCIENCES 22(2006): 567-570.
- Dai, X., Nekrassova, O., Hyde, M. E., Compton, R. G. Anodic stripping voltammetry of arsenic(III) using gold nanoparticle-modified electrodes. Anal. Chem. 76(2004): 5924-5929.
- Du, Y., Luo, X-L., Xu, J-J., Chen, H-Y. A simple method to fabricate a chitosan- gold nanoparticles film and its application in glucose biosensor Bioelectrochemistry 70(2007): 342-347.
- Eggs, B. R., Biosensors: An Introduction. John Wiley & Sons Ltd, chichester, 1999.
- Ekanayake, E. M. I. M., Preethichandra, D. M. G., Kaneto, K. Bi-functional amperometric biosensor for low concentration hydrogen peroxide measurements using polypyrrole immobilizing matrix. Sensors and Actuators B: Chemical 132 (2008): 166-171.
- ElKaoutit, M., N-R., I., Dominguez, M., Hernandez-Artiga, M. P., Bellido-Milla, D., Cisnerosa, J. A third-generation hydrogen peroxide biosensor based on horseradish peroxidase (HRP) enzyme immobilized in a nafion-sonogel-carbon composite. Electrochimica Acta 53(2008): 7131-7137.
- ElKaoutit, M., Naggar, A. H., Naranjo-Rodrigueza, I., Dominguezc, M., José, Luis, Hidalgo-Hidalgo, de Cisnerosa. Electrochemical AFM investigation of horseradish peroxidase enzyme electro-immobilization with polypyrrole conducting polymer. Synthetic Metals 159(2009): 541-545.
- Fang, Z.-H., Lu, L.-M. Zhang, X-B., Li, H-B., Yang, B., Shen, G-L., Yu, R-Q. A Third-Generation Hydrogen Peroxide Biosensor Based on Horseradish Peroxidase Immobilized in Carbon Nanotubes/ SBA-15 Film. Electroanalysis 23(2011): 2415-2420.
- Feng, D., Wang, F., Chen, Z. Electrochemical glucose sensor based on one-step

- construction of gold nanoparticle–chitosan composite film. Sensors and Actuators B 138(2009): 539–544.
- Gao, F., Yuan, R., Chai, Y., Chen, S., Cao S., Tang, M. Amperometric hydrogen peroxide biosensor based on the immobilization of HRP on nano-Au/Thi/poly (p-aminobenzene sulfonic acid)-modified glassy carbon electrode. Journal of Biochemical and Biophysical Methods 70(2007): 407-413.
- German, N., Ramanavicius, A., Voronovic, J., Oztekin, Y., Ramanaviciene, A. The effect of colloidal solutions of gold nanoparticles on the performance of a glucose oxidase modified carbon electrode. Microchimica Acta 172(2011): 185-191.
- Gorton, L., Lindgren, A., Larsson, T., Munteanu, F. D., Ruzgas T., Gazaryan, I. Direct electron transfer between heme-containing enzymes and electrodes as basis for third generation biosensors. Analytica Chimica Acta 400(1999): 91-108.
- Gross, S., Schubert, U., Hüsing N., Laine, R. M. Colloidal Dispersion of Gold Nanoparticles Materials Syntheses. Springer Vienna (2008): 155-161.
- Ichiro Chibata, Immobilized Enzyme 1978.
- Ishida, T., Kuroda, K., Kinoshita, N., Minagawa, W., Haruta, M. Direct deposition of gold nanoparticles onto polymer beads and glucose oxidation with H₂O₂. Journal of Colloid and Interface Science 323(2008): 105-111.
- Joanna Cabaj and Jadwiga (2011). Hybrid Film Biosensor for Phenolic Compounds Detection, Environmental Biosensors, Prof. Vernon Somerset (Ed.), ISBN: 978-953-307-486-3, InTech, Available from: <http://www.intechopen.com/books/environmental-biosensors/hybrid-film-biosensor-for-phenolic-compounds-detection>.
- Kafi, A. K. M., Lee, D.-Y., Park, S.-H., Kwon, Y.-S. Potential application of hemoglobin as an alternative to peroxidase in a phenol biosensor. Thin Solid Films 516 (2008): 2816-2821.
- Kafi, A. K. M., Wu, G., Chen, A. A novel hydrogen peroxide biosensor based on the immobilization of horseradish peroxidase onto Au-modified titanium dioxide nanotube arrays. Biosensors and Bioelectronics 24(2008): 566-571.

- Kang, X., Wang, J., Tang, Z., Wub, H., Linb, Y. Direct electrochemistry and electrocatalysis of horseradish peroxidase immobilized in hybrid organic–inorganic film of chitosan/sol–gel/carbon nanotubes. Talanta 78(2009): 120–125.
- Komsiyska, L, Staikov, G. Electrocrystallization of Au nanoparticles on glassy carbon from HClO₄ solution containing [AuCl₄]⁻. Electrochimica Acta 54(2008): 168–172.
- Kong, Y-T, Boopathi, M., Shim, Y-B. Direct electrochemistry of horseradish Peroxidase bonded on a conducting polymer modified glassy carbon electrode. Biosensors and Bioelectronics 19(2003): 227-232.
- Korkut, S., Keskinler, B., Erhan, E. An amperometric biosensor based on multiwalled carbon nanotube-poly(pyrrole)- horseradish peroxidase nanobiocomposit film for determination of phenol derivatives. Talanta 76(2008): 1147–1152.
- Kumar, S., Gandhi, K. S., Kumar, R. Modeling of Formation of Gold Nanoparticles by Citrate Method. Industrial & Engineering Chemistry Research 46(2006): 3128-3136.
- Li, F., Chen, W., Tang, C., S H. Development of hydrogen peroxide biosensor based On in situ covalent immobilization of horseradish peroxidase by one-pot polysaccharide-incorporated sol-gel process. Talanta 77(2009): 1304–1308.
- Li, G., Wang, Y., Xu, H. A hydrogen peroxide sensor prepared by electropolymerization of pyrrole based on screen-printed carbon paste electrodes. Sensors 7(2007): 239-250.
- Li, J., Lin, X., Electrocatalytic oxidation of hydrazine and hydroxylamine at gold nanoparticle—polypyrrole nanowire modified glassy carbon electrode. Sensors and Actuators B 126 (2007): 527–535.
- Li, W, Yuan, R., Chai, Y., Zhou, L., Chen, S., Li, N. Immobilization of horseradish peroxidase on chitosan/silica sol–gel hybrid membranes for the preparation of hydrogen peroxide biosensor. Biochem. Biophys. Methods 70(2008): 830–837.

- Liu, S.-Q. Ju H.-X. Renewable reagentless hydrogen peroxide sensor based on direct electron transfer of horseradish peroxidase immobilized on colloidal gold-modified electrode. Analytical Biochemistry 307(2002): 110-116.
- Liu, S., Yu, J., Ju, H. Renewable phenol biosensor based on a tyrosinase-colloidal gold modified carbon paste electrode. Journal of Electroanalytical Chemistry 540(2003): 61-67.
- Liu, Sh-f., Li, X-H., Li, Y-C., Li, Y-F., Li, J-R., Jiang, L. The influence of gold nanoparticle modified electrode on the structure of mercaptopropionic acid self-assembly monolayer. Electrochimica Acta 51(2005): 427-431.
- Liu, Sh-f., Li, Y-f., Li, J-r., Jiang, L. Enhancement of DNA immobilization and hybridization on gold electrode modified by nanogold aggregates. Biosensors and Bioelectronics 21(2005): 789-795.
- Liu, Sh-f., Wang, L., Zhao, F. Influence of gold nanoparticle modified electrode on the mediation reduction of ferricyanide by methylene blue. Journal of Electroanalytical Chemistry 602 (2007): 55–60.
- Lui, Y-Ch, Yang, K-H. Catalytic electroxidation pathway for electropolymerization of polypyrrole in solutions containing gold nanoparticles. Electrochimica Acta 51 (2006): 5376–5382.
- Luo, X., Killard, A. J., Morrin, A. Smyth M. R. Enhancement of a conducting polymer-based biosensor using carbon nanotube-doped polyaniline. Analytica Chimica Acta 575 (2006): 39-44.
- Mello, L. D., Sotomayor, M. D. P. T., Kubota, L. T. HRP-based amperometric biosensor for the polyphenols determination in vegetables extract. Sensors and Actuators B: Chemical 96(2003): 636-645.
- Nguyen, D. T., Kim, D.-J., Kim, K.-S. Controlled synthesis and biomolecular probe application of gold nanoparticles. Micron 42(2010): 207-227.
- Nguyen, D. T., Kim, D.-J., So, M. G., Kim, K.-S. Experimental measurements of gold nanoparticle nucleation and growth by citrate reduction of H₂AuCl₄." Advanced Powder Technology 21(2009): 111-118.

- Ozoner, S. K., Erhan E., Yilmaz ,F., Celik, A., Keskinler, B., Newly synthesized poly (glycidylmethacrylate-co-3-thienylmethylmethacrylate)-based electrode designs for phenol biosensors. Talanta 81(2009): 81-87.
- Pereira, A. C., Fertoni, F. L., Neto, G. D. O., Kubota, L. T., Yamanaka, H. Reagentless biosensor for isocitrate using one step modified Pt-Ir microelectrode. Talanta 53(2001): 801-806.
- Periasamy, A. P., Chang Y.-J., Chen, S.-M. Amperometric and Impedimetric H₂O₂ Biosensor Based on Horseradish Peroxidase Covalently Immobilized at Ruthenium Oxide Nanoparticles Modified Electrode. International Journal Electrochemistry Science 6(2011): 2688 – 2709.
- Pingarron, J. M., Yanez-Sedeno P.,Gonzalez-Cortes, A. Gold nanoparticle-based electrochemical biosensors. Electrochimica Acta 53(2008): 5848-5866.
- Qu, L., Xia, S., Bian, C., Sun, J., Han, J. A micro-potentiometric hemoglobin immunosensor based on electropolymerized polypyrrole-gold nanoparticles composite. Biosensors and Bioelectronics 24(2009): 3419-3424.
- Rajesh, S. S., Pandey, W., Takashima, Kaneto, K. Simultaneous co-immobilization of enzyme and a redox mediator in polypyrrole film for the fabrication of an amperometric phenol biosensor. Current Applied Physics 5(2005): 184-188.
- Ramanaviciene, A., Schuhmann, W., Ramanavicius, A. AFM study of conducting polymer polypyrrole nanoparticles formed by redox enzyme - glucose oxidase - initiated polymerisation. Colloids and Surfaces B: Biointerfaces 48(2006): 159-166.
- Rapecki, T., Donten, M., Stojek, Z. Electrodeposition of polypyrrole-Au nanoparticles composite from one solution containing gold salt and monomer." Electrochemistry Communications 12(2010): 624-627.
- Razola, S. S., Ruiz, B. L., Diez, N. M., Mark, H. B., Jr, Kauffmann, J-M. Hydrogen peroxide sensitive amperometric biosensor based on horseradish peroxidase entrapped in a polypyrrole electrode. Biosensors and Bioelectronics 17(2002) 921-928.

- Rosatto, S. S., Sotomayor, P. T., Kubota, L. T., Gushikem, Y. SiO₂/Nb₂O₅ sol-gel as a support for HRP immobilization in biosensor preparation for phenol detection. Electrochimica Acta 47(2002): 4451-4458.
- Rosatto, S. S., Kubota, L. T., Neto, G. D. O. Biosensor for phenol based on the direct electron transfer blocking of peroxidase immobilising on silica-titanium. Analytica Chimica Acta 390(1999): 65-72.
- Ruzgas, T., Emnéus, J., Gorton, L. Marko-Varka, G. The development of a peroxidase biosensor for monitoring phenol and related aromatic compounds. Analytica Chimica Acta 311(1995): 245-253.
- Ruzgas, T., Csöregi, E., Emnéus, J., Gorton, L., Marko-Varka, G. Review Peroxidase-modified electrodes: Fundamentals and application. Analytica Chimica Acta 330(1996): 123-138.
- Ruzgas, T., Gorton, L., Emneus, J., Marko-Varga, G. Kinetic models of horseradish peroxidase action on a graphite electrode. Journal of Electroanalytical Chemistry 391(1995): 41-49.
- Shi, A. W., Qu, F. L., Yang, M. H., Shen, G. L., Yu, R. Q. Amperometric H₂O₂ biosensor based on poly-thionine nanowire/HRP/nano-Au-modified glassy carbon electrode. Sensors and Actuators B 129 (2008): 779–783.
- Teng, Y. J., Zuo, S. H., Lan, M. B. Direct electron transfer of Horseradish peroxidase on porous structure of screen-printed electrode. Biosensors and Bioelectronics 24 (2009): 1353-1357.
- Tian, F., Xu, B., Zhu, L., Zhu, G. Hydrogen peroxide biosensor with enzyme entrapped within electrodeposited polypyrrole based on mediated sol-gel derived composite carbon electrode. Analytica Chimica Acta 443(2001): 9–16.
- Tong, Z., Yuan, R., Chai, Y., Xie Y., Chen S. A novel and simple biomolecules immobilization method: Electro-deposition ZrO₂ doped with HRP for fabrication of hydrogen peroxide biosensor. Journal of Biotechnology 128(2007): 567-575.

- Topcu Sulak, M., Erhan, E., Keskinler, B. Amperometric Phenol Biosensor Based on Horseradish Peroxidase Entrapped PVF and PPy Composite Film Coated GC Electrode. Applied Biochemistry and Biotechnology 160(2010): 856-867.
- Turkevitch, J., P. C.Stevenson, P. C., Hillier, J. Nucleation and Growth Process in the Synthesis of Colloidal Gold. Discuss.Faraday Society 11(1951): 55-75.
- Umana, M. and Waller, J. Protein-Modified Electrodes. The Glucose Oxidase/Polypyrrole System. Anal. Chem. 58 (1986): 2979-2983.
- Vidal, J. C., Mndez, S., Castillo, J. R. In situ preparation of a cholesterol biosensor: entrapment of cholesterol oxidase in an overoxidized polypyrrole film electrodeposited in a flow system: Determination of total cholesterol in serum. Analytica Chimica Acta 385(1999): 213-222.
- Wang, J, Wang, L, Di, J., Tu, Y. Electrodeposition of gold nanoparticles on indium/tin oxide electrode for fabrication of a disposable hydrogen peroxide biosensor. Talanta 77(2009): 1454-1459.
- Wang, P., Li, S., Kan, J. A hydrogen peroxide biosensor based on polyaniline/FTO. Sensors and Actuators B 137(2009): 662–668.
- Wang, Y., Deng, J., Di, J., Tu Y. Electrodeposition of large size gold nanoparticles on indium tin oxide glass and application as refractive index sensor. Electrochemistry Communications 11(2009): 1034–1037.
- Wu, S., Zhao, H., Ju, H., Shi, C., Zhao, J. Electrodeposition of silver–DNA hybrid nanoparticles for electrochemical sensing of hydrogen peroxide and glucose. Electrochemistry Communications 8(2006): 1197–1203.
- Xi, F., Liu, L., Chen, Z., Lin, X. One-step construction of reagentless biosensor based on chitosan-carbon nanotubes-nile blue-horseradish peroxidase biocomposite formed by electrodeposition. Talanta 78(2009): 1077–1082.
- Xu, J-Z, Zhang, Y., Li, G-X, Zhu, J-J. An electrochemical biosensor constructed by nanosized silver particles doped sol–gel film. Materials Science and Engineering C 24(2004): 833–836.
- Xu, Q., Mao, C., Liu, N.-N., Zhu, J.-J., Sheng, J. Direct electrochemistry of

- horseradish peroxidase based on biocompatible carboxymethyl chitosan-gold nanoparticle nanocomposite. Biosensors and Bioelectronics 22(2006): 768-773.
- Yang, Y. and Sh. Mu. Bioelectrochemical responses of the polyaniline horseradish peroxidase electrodes. Journal of Electroanalytical Chemistry 432(1997): 71-78.
- Yang, Y., G. Yang, A new hydrogen peroxide biosensor based on gold nanoelectrode ensembles/ multiwalled carbon nanotubes/ chitosan film-modified electrode. Colloids and Surfaces A: Physicochem. Eng. Aspects 340(2009): 50-55.
- Yin, H., Zhou, Y., Ai, S., Han, R., Tang, T., Zhu, L. Electrochemical behavior of bisphenol A at glassy carbon electrode modified with gold nanoparticles, silk fibroin, and PAMAM dendrimers. Microchimica Acta 170(2010): 99-105.
- Yusran Daoa. Gold nanoparticles/polypyrrole modified electrode for phenol biosensor. Master's Thesis, Department of Chemical Engineering Engineering, Chulalongkorn University, 2009.
- Zhao, X., Mai, Z., Kanga, X., Zou, X. Direct electrochemistry and electrocatalysis of horseradish peroxidase based on clay chitosan-gold nanoparticle nanocomposite. Biosensors and Bioelectronics 23(2008): 1032-1038.
- Zeng, X., Li, X., Xing, L., Liu, X., Luo, Sh. Electrodeposition of chitosan-ionic liquid-glucose oxidase biocomposite onto nano-gold electrode for amperometric glucose sensing. Biosensors and Bioelectronics 24 (2009): 2898-2903.
- Zoski, C.G. Handbook of Electrochemistry. Elsevier, (2009).

APPENDICES

Appendix A

Preparation of PBS solutions

Preparation of buffer solution for modified SPEs

The stock of phosphate buffer (PBS, pH 7.4) of $5.28 \times 10^{-2} \text{M}$ disodium hydrogen orthophosphate, $1.3 \times 10^{-2} \text{M}$ sodium dihydrogen orthophosphate, and then $5.1 \times 10^{-3} \text{M}$ sodium chloride were prepared using distilled water and stored under 4°C .

Preparation of buffer solution for substrates detection

The stock of phosphate buffer (0.1M PBS, pH 7.4) of disodium hydrogen orthophosphate and sodium dihydrogen orthophosphate were prepared using distilled water and stored under 4°C .

$$\text{Molecular weight of Na}_2\text{HPO}_4 \cdot 12\text{H}_2\text{O} = 358.14 \text{ g/g mole}$$

$$\text{Molecular weight of NaH}_2\text{PO}_4 \cdot 2\text{H}_2\text{O} = 156.03 \text{ g/g mole}$$

Calculation method:

$$\text{Na}_2\text{HPO}_4 \cdot 12\text{H}_2\text{O}: \frac{\text{weight of Na}_2\text{HPO}_4 \cdot 12\text{H}_2\text{O}}{358.14} = \frac{0.1 \times A}{1000}$$

$$\text{weight of Na}_2\text{HPO}_4 \cdot 12\text{H}_2\text{O} = x \text{ (g)}$$

$$\text{NaH}_2\text{PO}_4 \cdot 2\text{H}_2\text{O}: \frac{\text{weight of NaH}_2\text{PO}_4 \cdot 2\text{H}_2\text{O}}{156.03} = \frac{0.1 \times A}{1000}$$

$$\text{weight of NaH}_2\text{PO}_4 \cdot 2\text{H}_2\text{O} = y \text{ (g)}$$

where A is volume of distilled water, x and y are the weight of $\text{Na}_2\text{HPO}_4 \cdot 12\text{H}_2\text{O}$, and $\text{NaH}_2\text{PO}_4 \cdot 2\text{H}_2\text{O}$, respectively. The solution of $\text{NaH}_2\text{PO}_4 \cdot 2\text{H}_2\text{O}$ was added the solution of $\text{Na}_2\text{HPO}_4 \cdot 12\text{H}_2\text{O}$ by tuning of pH meter until pH 7.4.

Appendix B

Raw Data

Cyclic voltammetry data were a large number of approximately 6,000 to 10,000 values including UV-Visible spectroscopy data for one graph. Therefore, the data of cyclic voltammogram were not shown.

Follows tables showed the response currents which got from steady state responses of amperometry techniques in solution containing 10 mM $K_4Fe(CN)_6$ / 1 mM KCl at 0.58 V. These data were information from finding of optimum electropolymerization conditions.

Table A.1 Amperometric current responses (at 0.58 V) of AuNPs/PPy/SPE at different Au precursor concentration at 5 cycles.

Au precursor Conc. (mM)	I (μ A)
1	2.176
3	2.781
5	5.497
7	2.985
9	1.315

Table A.2 Amperometric current responses (at 0.58 V) of AuNPs/PPy/SPE at different Au precursor concentration at 10 cycles.

Au precursor Conc. (mM)	I (μ A)
1	6.054
3	8.388
5	15.349
7	9.733
9	5.732

Table A.3 Amperometric current responses (at 0.58 V) of AuNPs/PPy/SPE at different Au precursor concentration at 15 cycles.

Au precursor Conc. (mM)	I (μA)
1	3.904
3	4.341
5	5.943
7	4.738
9	3.104

Table A.4 Amperometric current responses (at 0.58 V) of AuNPs/PPy/SPE at different Au precursor concentration at 20 cycles.

Au precursor Conc. (mM)	I (μA)
1	0.247
3	0.866
5	3.828
7	1.948
9	0.102

Table A.5 The percentage of AuNPs in AuNPs/PPy/SPE and current response at different Au precursor concentration under electropolymerization cycles number (10 cycles).

Au precursor Conc. (mM)	AuNPs (%w/w)	I (μ A)
1	3.88	6.054
3	3.96	8.388
5	5.89	15.349
7	4.6	9.733
9	3.24	5.732

Table A.6 Amperometric current response (at -0.05V) of an optimum AuNPs/PPy/HRP/SPE using different electrode.

Type	I ₁ (nA)	I ₂ (nA)	I ₃ (nA)	I _{avg} (nA)	SD	%RSD
Bare	-11.383	-10.882	-10.501	-10.922	0.442358	-4.05016
PPy	-54.139	-53.387	-47.752	-51.7593	3.490762	-6.74422
AuNPs/PPy	-199.62	-215.259	-199.361	-204.747	9.104869	-4.44689
AuNPs/PPy/HRP	-588.054	-594.974	-550.08	-577.703	24.17086	-4.18396

Table A.7 Amperometric current response (at -0.05V) of an optimum AuNPs/PPy/HRP/SPE using different solution.

Solution	I ₁ (nA)	I ₂ (nA)	I ₃ (nA)	I _{avg} (nA)	SD	%RSD
PBS	-3.384	-4.208	-5.792	-4.46133	1.223826	-27.4318
PHENOL	-22.7316	-21.821	-22.109	-22.2205	0.465433	-2.09461
H ₂ O ₂	-57.9865	-60.34	-58.326	-58.8842	1.272165	-2.16045
PHENOL/H ₂ O ₂	-550.08	-545.822	-558.743	-551.548	6.584456	-1.19381

Table A.8 The anodic and cathodic of potential and current peaks of AuNPs/PPy/HRP/SPE at different scan rate under electropolymerization conditions.

Scan rate (V/s)	E_{pa} (V)	E_{pc} (V)	I_{pa} (μ A)	I_{pc} (μ A)
0.1	-0.007	-0.407	6.155	-11.221
0.2	0.02	-0.424	12.17	-15.775
0.3	0.045	-0.446	17.862	-20.297
0.4	0.054	-0.46	23.242	-25.824
0.5	0.074	-0.49	28.528	-30.338

Table A.9 The relationship between the peak potential (E_p) and the natural logarithm of scan rate ($\ln v$) for AuNPs/PPy/HRP/SPE in 0.1M PBS (pH7.4) at different scan rate under electropolymerization conditions.

Scan rate (V/s)	E_{pa} (V)	E_{pc} (V)	$\ln v$
0.1	-0.007	-0.407	-2.30259
0.2	0.02	-0.424	-1.60944
0.3	0.045	-0.446	-1.20397
0.4	0.054	-0.46	-0.91629
0.5	0.074	-0.49	-0.69315

Table A.10 Amperometric current response (at -0.05V) of a phenol calibration curve of a AuNPs/PPy/HRP/SPE in 50 μM H_2O_2 /PBS solution.

Phenol concentration (μM)	I (nA)
0.1	-459.776
0.5	-458.14
1	-467.597
2	-474.167
4	-485.407
8	-500.271
10	-499.101
16	-523.16
18	-527.2
20	-530.069
30	-535.743
50	-551.978
70	-571.997
90	-596.807
110	-600.62
130	-607.123
150	-635.795
170	-677.497
190	-722.266
210	-724.82

Table A.11 Amperometric current response (at -0.05V) for reproducibility using of AuNPs/PPy/HRP/SPE in 1 μ M Phenol/50 μ M H₂O₂/PBS solution.

No.	I(nA)
1	-444.952
2	-448.108
3	-441.97
4	-426.672
5	-442.443
6	-472.315
7	-435.794
8	-407.449
9	-445.786
10	-449.687
avg	-441.518
SD	16.6784912
RSD (%)	3.77753712

Table A.12 Amperometric current response (at -0.05V) for storage stability of a AuNPs/PPy/HRP/SPE in 50 μ M phenol/ 50 μ M H₂O₂/PBS under 4°C.

Days	I ₁ (nA)	I ₂ (nA)	I ₃ (nA)	I _{avg} (nA)	%Residual current
0	-526.53	-526.113	-522.8	-525.148	100
7	-438.201	-439.36	-435.88	-437.814	83.37
14	-319.662	-318.777	-315.055	-317.831	60.52
30	-248.377	-248.834	-249.191	-248.801	47.38

Table A.13 Amperometric current response (at -0.05V) for storage stability of a AuNPs/PPy/HRP/SPE in 50 μM phenol/ 50 μM H_2O_2 /PBS under 25°C.

Days	I₁ (nA)	I₂(nA)	I₃ (nA)	I_{avg} (nA)	%Residual current
0	-523.371	-525.424	-523.732	-524.176	100
7	-329.032	-320.447	-321.558	-323.679	61.75
14	-285.17	-288.079	-285.889	-286.379	54.63
30	-169.112	-162.761	-162.447	-164.773	31.43

VITA

Miss Ratcahneepat Kumpangpet was born in Chachoengsao, Thailand on April 12, 1987. She finished her secondary school from Benchama Rat Rungsaruit in March, 2005. After that, she studied in the major of Chemical Engineering in Faculty of Engineering at King Mongkut's University of Technology North Bangkok. She continued her further study for master's degree in Chemical Engineering at Chulalongkorn University in the Biochemical Engineering Research Group and achieved her Master's degree in April, 2012.

Ratchaneepat Kumpangpet, Chanchana Thanachayanont, Bunjerd Jongsomjit, and Seeroong Prichanont. “**Fabrication of Gold nanoparticles/Polypyrrole/HRP electrode for phenol biosensor by electropolymerization**” Extended Abstract for Conference at Nakhon Ratchasima, Thailand with the name of —German-Thai Symposium on Nanoscience and Nanotechnology (GTSNN2011); Green Nanotechnology for the future, 13-16 September 2011.

Ratchaneepat Kumpangpet, Chanchana Thanachayanont, Bunjerd Jongsomjit, and Seeroong Prichanont. “**Electropolymerization of AuNPs/PPy/HRP modified screen-printed carbon electrode for phenol detection**” Extended Abstract for Conference at Bangkok, Thailand with the name of — The 4th AUN/SEED-Net Regional Conference on Biotechnology: EMERGING BIOTECHNOLOGY FOR GREEN ENGINEERING, 26-27 January 2012.

